National Academy

SCIENCE LETTERS

Amino terminal

Glycine rich loop
DFG

Activation loop

Catalytic loop

Carboxy terminal

The National Academy of Sciences, India
(Registered under Act XXI of 1860)
Founded 1930

COUNCIL FOR 2004

President
1. Prof. Jai Pal Mittal, Ph.D.(Notre Dame), F.N.A., F.A.Sc., F.N.A.Sc., F.T.W.A.S., Mumbai.

Two Past Presidents (including the Immediate Past President)
2. Prof. S.K. Joshi, D.Phil., D.Sc.(h.c.), F.N.A., F.A.Sc., F.N.A.Sc., F.T.W.A.S., New Delhi.
3. Dr. V.P. Sharma, D.Phil.,D.Sc.,F.A.M.S.,F.E.S.I., F.I.S.C.D., F.N.A., F.A.Sc., F.N.A.Sc., F.R.A.S., New Delhi.

Vice-Presidents
4. Dr. P.K. Seth, Ph.D., F.N.A., F.N.A.Sc., Lucknow.
5. Prof. M. Vijayan, Ph.D., F.N.A., F.A.Sc., F.N.A.Sc., F.T.W.A.S., Bangalore.

Treasurer
6. Prof. S.L. Srivastava, D.Phil.,F.I.E.T.E., F.N.A.Sc., Allahabad.

Foreign Secretary
7. Dr. S.E. Hasnain, Ph.D., F.N.A., F.A.Sc., F.N.A.Sc., F.T.W.A.S., Hyderabad.

General Secretaries
8. Prof. H.C. Khare, M.Sc., Ph.D.(McGill), F.N.A.Sc., Allahabad.
9. Prof. Pramod Tandon, Ph.D., F.N.A.Sc., Shillong.

Members
10. Dr. Samir Bhattacharya, Ph.D., F.N.A., F.A.Sc., F.N.A.Sc., Kolkata.
11. Prof. Suresh Chandra, D.Phil., Grad.Brit.I.R.E., F.N.A.Sc., Varanasi.
12. Prof. Virander Singh Chauhan, Ph.D., D.Phil.(Oxford), F.N.A., F.N.A.Sc., New Delhi.
13. Prof. Asis Datta, Ph.D., D.Sc., F.N.A., F.A.Sc., F.N.A.Sc., F.T.W.A.S.,New Delhi.
14. Prof. Kasturi Datta, Ph.D., F.N.A., F.A.Sc., F.N.A.Sc., F.T.W.A.S., New Delhi.
15. Prof. Sushanta Dattagupta, Ph.D., F.N.A., F.A.Sc., F.N.A.Sc., F.T.W.A.S., Kolkata.
16. Dr. Amit Ghosh, Ph.D., F.A.Sc., F.N.A.Sc., Chandigarh.
17. Prof. H.S. Mani, Ph.D.(Columbia), F.A.Sc., F.N.A.Sc., Chennai.
18. Prof. G.K. Mehta, Ph.D., F.N.A.Sc., Allahabad.
19. Dr. G.C. Mishra, Ph.D., F.N.A.Sc., Pune.
20. Dr. Ashok Misra, M.S.(Chem.Engg.), M.S.(Polymer Sc.), Ph.D., F.N.A.Sc.,Mumbai.
21. Prof. Kambadur Muralidhar, Ph.D., F.N.A., F.A.Sc., F.N.A.Sc.,Delhi.
22. Dr. Vijayalakshmi Ravindranath, Ph.D.,F.N.A.Sc., F.T.W.A.S., Manesar.
23. Prof. Ajay Kumar Sood, Ph.D., F.N.A., F.A.Sc., F.N.A.Sc., F.T.W.A.S., Bangalore.

Special Invitees
1. Prof. M.G.K. Menon, Ph.D.(Bristol), D.Sc.(h.c.), F.N.A., F.A.Sc., F.N.A.Sc., F.T.W.A.S., F.R.S., Mem.Pontifical Acad.Sc., New Delhi.
2. Dr.(Mrs.) Manju Sharma, Ph.D., F.N.A.A.S., F.A.M.I., F.I.S.A.B., F.N.A.Sc., F.T.W.A.S., New Delhi.
3. Prof. P.N. Tandon, M.S., D.Sc(h.c.), F.R.C.S., F.A.M.S., F.N.A., F.A.Sc., F.N.A.Sc., F.T.W.A.S., Delhi.

CONTENTS

Westward electric field in the low latitude ionosphere during the main phase of magnetic storms occurring around local midday hours

Academy News

Forthcoming Symposia/Seminars/Miscellaneous Announcements

Cover page photograph : Superposition of our model (original colours) with the experimental crystal structure (blue) of EGFR kinase domain.

EDITORS' PAGE

Happy New Year! It has been our pleasure to reach you through this journal in the year 2003 and we look forward to working with and for you in the ensuing year 2004. We thank you for encouraging us through your appreciative words for whatever little improvement we could achieve in respect to this journal. However, we most humbly admit that a lot more remains to be done.

Education and research in India has many interesting facets. Both these sectors are under tremendous pressure. One curious (and possibly controversial) facet is the following : Whatever you do to bring about improvement in these sectors (Education and Research), the standards go down. We must remind you that this *statement is only a partial truth and must be considered with due caution.* Research activity of an individual or group should be monitored rigorously. A measure of the research activity comes from the various publications emanating out of their effort. "Effort" could be a genuine concern or the result of a feeling of "competitiveness" amongst fellow scientists. In the case of latter, all concerned start *"publishing to avoid perishing"* with utter disregard for the quality. Does it not call for caution? Please think! Another method adopted for improvement in research and in making it more relevant socially is *"to increase funding in focussed areas".* If you do this, many of us have seen in the past that the "resourceful and/or ambitious" scientists quickly *"de-tune and re-tune"* their research proposals to snatch the funding and go on an equipment buying spree. If you cut funds, the "haves" continue to breathe normally as ever but the earlier "have-nots" are made to starve more. Such depressing talks often take place amongst scientists as if they themselves are in no way responsible for this state of affairs. Does it not call for introspection?

Assured promotional avenues in research organizations and educational institutions to ease tension of scientists have led to disastrous results. Who is to be blamed? Who is to be answerable? We leave you to draw your own conclusions since our remarks may hurt many.

Now we come to our journal. The Council of the Academy and we in the Editorial Board thought that inclusion of "Lead Articles" by newly elected Fellows/Senior Scientists would increase the visibility (and citation index) and usefulness of the journal. Yes, it did so. Prof. U.R. Rao in his Inaugural Address delivered at the Annual Conference of the Academy held at Ahmedabad in October 2003 also recommended publishing of authoritative reviews in Academy's journal (this address is published in this issue of the journal). We are gratified to have received his support and affirmation of journal's policy. However, we ourselves are not satisfied. Only a few newly elected Fellows/Senior Fellows are contributing. We request their indulgence to give credence to the effort of the Academy to improve this journal.

Once again, A VERY HAPPY NEW YEAR!!

Girjesh Govil
Jai Pal Mittal
Suresh Chandra

Homology modelling in protein structure prediction : Epidermal growth factor receptor kinase domain

Sunil K. Panigrahi AND Gautam R. Desiraju*

School of Chemistry, University of Hyderabad, Hyderabad 500 046, India

*To whom correspondence should be addressed. Tel: 040 23010510 (extn. 4828) Fax: 040 23010567.

e-mail: desiraju@uohyd.ernet.in

Abstract

The importance of homology modelling in predicting the three dimensional structures of proteins has been discussed. Efforts in improving the predictive quality are outlined. Successful implementation of homology modelling has been demonstrated in predicting the structure of the kinase domain of Epidermal Growth Factor Receptor (EGFR). A comparison between the modelled and experimental X-ray crystal structure (C_α RMSD 1.96 Å) shows the accuracy of the modelling methods used.

Keywords : Biomolecular structure/ computer simulation/ cancer/ drug design/ crystallography

Introduction

Proteins are among the most important biological macromolecules and they are extremely versatile in their functions. These functions are generally determined by the three dimensional structures. Till date, the experimental structure of perhaps only 1% of all proteins whose sequence is known has been determined. This is due to practical difficulties inherent to the experimental methods (X-ray diffraction, synchrotron X-ray diffraction, NMR, electron diffraction, electron microscopy, fibre diffraction, neutron diffraction, fluorescence transfer) that are used to elucidate the structure. Predicting the structure of an unknown protein to a near enough accuracy through modelling is an alternative approach to structure determination. Protein structure prediction relies on a knowledge of experimentally determined structures and is an amalgamation of a number of strategies. (Fig. 1). The effectiveness of such predictive methods depends on the recent rapid increase in the size of the Protein
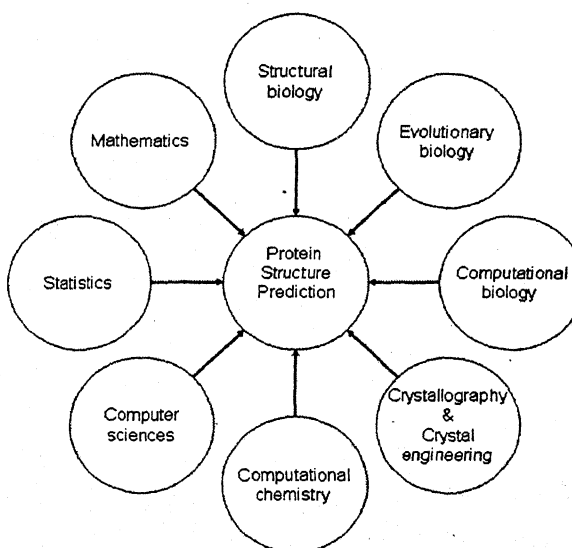

Fig. 1- Protein structure prediction as an amalgamation of various disciplines.

Data Bank (PBD).[1] Fortunately, there has
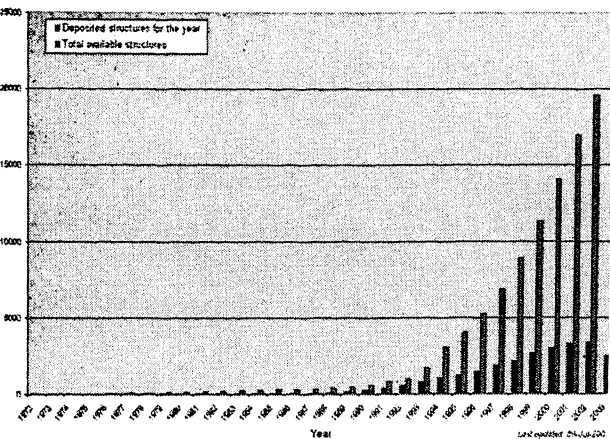
also been a concomitant decrease in the

Fig. 2-Total available structures (green) and annually deposited structures (red) of proteins in the PDB.

number of new folds deposited in the PDB, making structure prediction easier. (Fig. 3). Lastly, improved hardware and software have greatly facilitated this exercise.

Fig. 3- Total number of unique folds (red) available in the PDB with annually deposited new folds
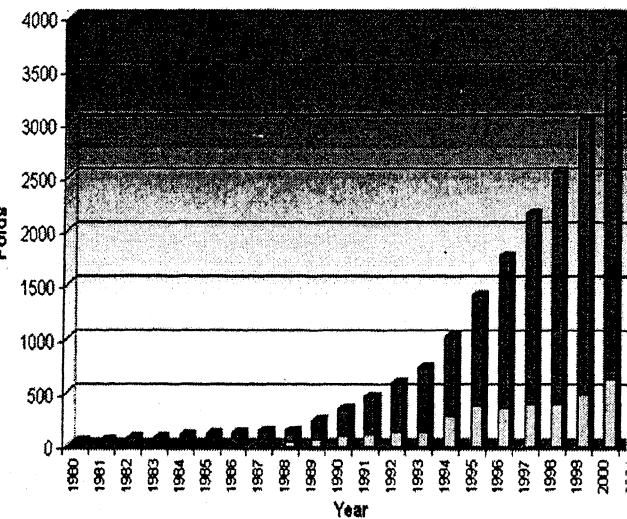
(blue).

There is now a novel platform to assess the strength of modelling methods for protein structure prediction. The Critical Assessment of Structure Prediction (CASP)[2] and the Critical Assessment of

Fully Automated Structure Prediction (CAFASP)[3] exercises are carried out to assess the capability of modern predictive methods. CASP is organised every two years and evaluates and compares predicted structures with crystallographically determined ones. The results are discussed in an online forum called FORCASP. CASP experiments were run in 1994, 1996, 1998, and 2000, and 2002. Similarly CAFASP runs a parallel program solely for automated servers and metaservers using same targets as those in CASP. All CAFASP predictions are part of the CASP exercise. These results every two years provide an estimate of progress by attempting to measure in a quantitative way the success of many groups on a predefined set of structures. Comparative modelling results at CASP 5 have been recently summarised.[4] The results show that protein structure prediction is becoming more reliable, but that there still lie greater challenges.[5] A number of methods are available (Fig. 4). Among these, comparative modelling or homology modelling has achieved success.

Fig. 4- Classification of computational approaches in protein structure prediction.

The present article attempts to explain the technical details of this method and illustrates these with respect to the

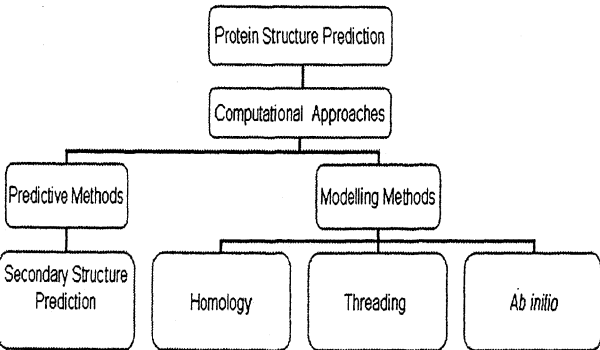modelling of the Epidermal growth factor receptor (EGFR) kinase domain. EGFR has attracted attention because of the findings that deregulation of this receptor system is a significant factor in the genesis or progression of several human cancers.[6] Shortly after we completed our modelling study, the experimental crystal structure of EGFR was published.[7] This gave us an opportunity to compare our model with the experimental structure.

A review of homology modelling

In homology (comparative) modelling the three dimensional structure of a protein (target) is built based on its alignment to proteins of known structure (templates). The method has been reviewed extensively in the literature.[8] The basic assumptions and steps are as follows:

- Related members of a family have evolved divergently with respect to sequence and structure.

- Two evolutionary related neighbours with a similar primary sequence will have similar three dimensional structures.

- Two sequences are evolutionary related if the similarity between the sequences is greater than 30%. The model is best when they are >50% identical, and not very useful when <30%.

- The target sequence is used in a sequence similarity search of the PDB to determine if it has recognizable similarity to sequences for which a structure is known.

- Sequence alignments are then constructed between the sequence to be modelled and the template sequences.

- Multiple domain containing proteins are modelled by considering individual domains separately.

Steps involved in homology modelling

The various steps involved in homology modelling are illustrated in Fig. 5. These are now detailed.

Fig. 5–Flow chart showing the steps involved in homology modelling.
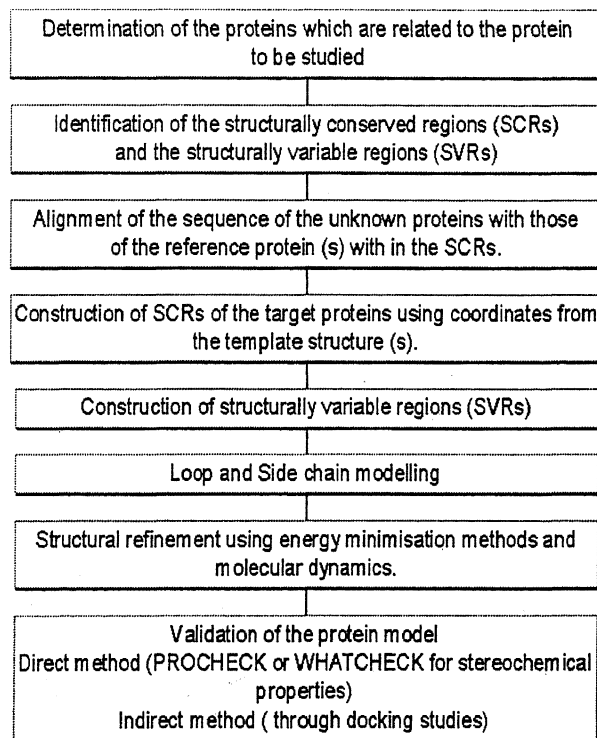
1. *Selection of the template*

This exercise uses various search methods and database mining tools to identify templates in databases such as PDB,[1] SCOP,[9] DALI,[10] and CATH.[11] Broadly protein comparison methods can be classified into three main classes.

a. Pairwise sequence-sequence comparison. These methods compare the target sequence with each of the

database sequences independently, using pairwise sequence–sequence comparison (FASTA[12] and BLAST[13]).

b. Multiple sequence comparison methods. These rely on multiple sequence comparisons to improve the sensitivity of the search.[14] For a given sequence, an initial set of homologues from a sequence database is collected, a weighted multiple alignment is made from the query sequence and its homologues, a position-specific scoring matrix is constructed from the alignment, and the matrix is used to search the database for new homologues. These steps are repeated until no new homologues are found (PSI-BLAST[14]).

c. Threading or 3D template matching.[15] These methods rely on pairwise comparison of a protein sequence and a protein of known structure. The target sequence is threaded through a library of 3D folds. For each sequence-structure pair, independently, structure-dependent scoring functions are used to judge whether or not a given target sequence adopts any one of the many known 3D folds as predicted by an optimization of the alignment.

2. Alignment of target and template

The next step in comparative modelling is the alignment between the target sequence and the template structure. Alignment means a rearrangement of subsets (of a sequence) to find maximum similarities between the target sequence and the template structure.[16] It consists of establishing equivalences between the

residues in two different proteins, as is the case with conventional sequence alignment. The alignment is done on the basis of the three-dimensional coordinates corresponding to each residue, and not on the basis of the amino acid type of the residue.

The procedure involves the alignment of potential templates, which are prepared by superposing their structures. Next, the sequences that are clearly related to the templates and are easily aligned with them are added to the alignment. The same is done for the target sequence. Finally, the two profiles are aligned with each other, taking structural information into account as much as possible.[17] In principle, most sequence alignment and structure comparison methods can be used for these tasks. Widely used is the alignment based on dynamic programming. Their success depends on the degree of sequence identity between the target and template. For closely related protein sequences with identity over 40%, alignment is almost always correct. Regions of low local sequence similarity become common when the overall sequence identity is under 40%.[18] Alignment becomes difficult in the "twilight zone" of less than 30% sequence identity.[19] As the sequence similarity decreases, alignments contain an increasingly large number of gaps and alignment errors, regardless of whether they are prepared automatically or manually. Because insertion and deletion occur at the loop regions of the protein between secondary structures, improvements can be made by introducing penalties for insertions/deletions of α-helices or β-sheets. Phylogenetic inference and motif comparison in the alignment step are vital for correct modelling.

3. Model building

After alignment the model is built using various model building methods. The test of any modelling method lies in its accuracy when the sequence similarity is less than 40%. Most important of all is the selection of the template and proper alignment, which is crucial for model quality irrespective of the modelling methods chosen. Three model building methods are generally used:

(a) Model building by rigid body assembly method.[20] The method dissects the overall protein folds into structurally conserved regions, variable loops, and side chains followed by model building with a small number of rigid bodies obtained from aligned protein structures.

(b) Segment matching method,[21, 22] relies on the approximate positions of conserved atoms in the templates. Comparative models are constructed by using a subset of atomic positions from template structures as "guiding" positions, and by identifying and assembling short, all-atom segments that fit these guiding positions. The segment matching method is based on the idea that most hexapeptide segments in proteins can be clustered into approximately 100 structural classes.[23] Therefore, by transferring the coordinates from the template segment-wise, it is possible to generate a model which has a segment structure very close to the actual one.

(c) Model building by spatial restrain satisfaction,[24,25] uses either distance geometry or optimization techniques to satisfy spatial restraints obtained from the alignment. These methods generate many constraints or restraints on the structure of the target sequence, based on its alignment to related protein structures. The restraints are generally obtained by assuming that the corresponding distances and angles between aligned residues in the template and the target structures are similar. These homology derived restraints are usually supplemented by stereochemical restraints on bond lengths, bond angles, dihedral angles, and nonbonded atom-atom contacts obtained from a molecular mechanics force field. The model is then derived by minimizing the violations of all the restraints.

In the process of model building the loop as well as the side chain is built. Further improvement in the quality of the loop and the side chains may be obtained through specialised modelling tools.

4. Loop building

Loop modelling methods can be categorized into *ab initio*, database search and combinations of both methods.

a. Ab initio methods :

De novo design of the loops is carried out based on the conformational analysis guided by a scoring or energy function in a particular environment.[46, 47] Many methods exploit different protein representations, energy function terms, and optimization or enumeration algorithms. All methods follow basic steps of conformation generation, sampling of the conformation

and selection of the appropriate confor-mation.

b. Database search techniques[26-29]

Loop prediction by a database approach finds a segment of the main chain that fits the two stem regions of a loop. The stems are defined as the main chain atoms that precede and follow the loop but are not part of it. The database approaches are best suited for proteins where loops have a small conformational space. The exponential increase in the number of geometrically possible conformations as a function of loop length limits the database approach. Another approach of loop modelling follows a combination of both *ab initio* and database search methods implemented simultaneously.

5. Side chain modelling

The side chains play a major role in the overall packing quality, interactions types and stability of the protein. Side chain modeling is a daunting task. Some methods

use energy functions to predict side chain conformations.[30] Prediction of side chain conformations are done along with backbone prediction. Side chain prediction at the structurally conserved region is easier than in the structurally variable regions. Inclusion of solvation and hydrogen bonding terms improves the success of side chain prediction markedly.[31] There is a rapid decrease in the conservation of side chain packing as the sequence identity falls below 30%.[32] Although the fold is maintained, the pattern of side chain interactions is generally lost in this twilight range. Various approaches to side chain modelling have been reviewed elsewhere.[33]

6. Model evaluation

Quality control is foremost in model building. The built model should satisfy (a) Stereochemical accuracy, (b) Packing quality and (c) Folding reliability. Various quality checks are listed in Fig. 5. Protein quality check tools like PROCHECK,[34] WHATCHECK,[35] AQUA,[36] SQUID[37] are available to judge protein quality.

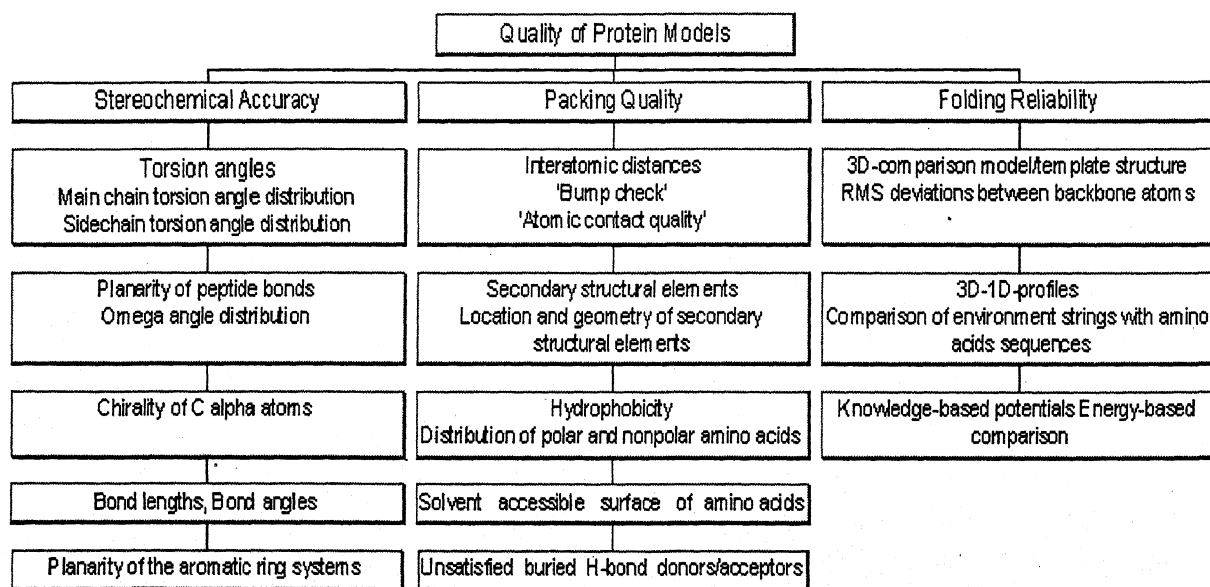| Quality of Protein Models		
Stereochemical Accuracy	Packing Quality	Folding Reliability
Torsion angles Main chain torsion angle distribution Sidechain torsion angle distribution	Interatomic distances 'Bump check' 'Atomic contact quality'	3D-comparison model/template structure RMS deviations between backbone atoms
Planarity of peptide bonds Omega angle distribution	Secondary structural elements Location and geometry of secondary structural elements	3D-1D-profiles Comparison of environment strings with amino acids sequences
Chirality of C alpha atoms	Hydrophobicity Distribution of polar and nonpolar amino acids	Knowledge-based potentials Energy-based comparison
Bond lengths, Bond angles	Solvent accessible surface of amino acids	
Planarity of the aromatic ring systems	Unsatisfied buried H-bond donors/acceptors	

Fig. 6- Protein quality check parameters.

7. Model Refinement

Refinement is done by further minimisation to eliminate bad contacts. Sometimes the model is subjected to molecular dynamics simulations to find out the lowest energy conformation. A manual adjustment of the packing quality of side chain improves model quality.

Errors in homology modelling

A model quality falls with the decrease in the similarity between the target and the templates. Frequently a model may go wrong if (a) Incorrect templates are selected, especially when distantly related proteins are used as templates (i.e., less than 25% sequence identity). (b) The alignment is not proper. If the target-template sequence identity decreases below 30% then the model accuracy depend solely on alignment quality. Alignment errors can be reduced by constructing a multiple alignment taking a large number of sequences. Multiple alignments are generally more reliable than pairwise alignments. However in cases where the sequence identity is greater, the pairwise alignment also performs well.

Strengths and lacunae of homology modelling

A model may attain a structure close to the experimental one when the template selection is good (family, similarity, tertiary structure). Then, methods to construct conserved and variable regions and the side chain work properly. Model prediction fails when the target and templates have a large number of insertions and deletions so that the alignment results

in improper coordinate transfer, when the target and template have sequence homology less than 30% resulting in improper alignment, and when templates having poor resolutions are chosen. When the prediction is not so good, the final model may possess more of template character than target character. To summarise, the different methods in predicting three dimensional structure are illustrated in Fig. 7.

Recognition	Alignment	Modelling	Challenges
Trivial	Trivial	Simple	Loop modelling
Trivial	Easy	Simple	Loop modelling
Simple	Challenging	Challenging	Alignment backbone shift
Difficult	Very difficult	Significant errors	Alignment backbone shift

Fig. 7–Overview of the method as a function of sequence similarity to template (expressed as a percentage).

Results and Discussion

EGFR belongs to the larger class of trans-membrane growth factor receptor tyrosine kinases (RTKs).[38] It consists of 1186 amino acid residues out of which the catalytic domain contains 310 residues.[39] The receptor is divided into three main regions: an extracellular domain ligand binding part, a hydrophobic membrane spanning region, and a cytoplasmic portion containing the kinase domain.(Fig. 8). EGFR and its ligands (EGF, TGF-α) have been implicated in numerous tumours of epithelial origin (e.g. squamous cell carcinoma; breast, ovarian, NSC lung cancer etc) and proliferative disorders of the epidermis such as psoriasis.[6]

A number of competitive inhibitors targeting the ATP binding site are in various phases of clinical trials. In an ongoing research in our group in Hyderabad we wanted to study the nature of the interaction between 4-anilinoquinazolines, an important class of inhibitor, and the kinase domain.[40] Because the crystal structure was not available at the time when we carried out this study, we built the homology model of the kinase domain. Modelling was carried out using a Silicon Graphics O2 workstation and the 'Homology' module of MOE (Molecular Operating Environment, Chemical Computation Inc).[41] While our study was nearing completion, the crystal structure of the protein was published.[7] Thus a comparison of structure quality was performed between our model and the experimental crystal structure.

Methodology

1. Template selectipon

A total of 263 amino acids (688 to 950 of the original receptor) out of 310 residues of the kinase domain ware taken from SWISS-PROT, accession no P00533. Modelling was carried out selecting IR3A.pdb[42] as the primary template. Both share a sequence similarity of 35%. To enhance the quality of proteins in terms of the structurally conserved regions and structurally variable regions we selected 3LCK.pdb,[43] 1IRK.pdb,[44] 1FPU.pdb,[45] 1CDK.pdb[46] as secondary templates. The criteria of selecting IR3 as the primary template are as follows:

a. It is a membrane receptor having architecture similar to that of EGFR.

b. The signal transduction pathway for insulin receptor is quite similar to EGFR.

c. The activated form of the insulin receptor has the same type of conformation in the catalytic domain of the activated form of EGFR.

2. Alignment

The target and the templates were aligned using MOE-Align module which is a modified version of the Needleman and Wunsch[47] method. Alignment was computed by optimising the function based on residue similarity score obtained from the Gonnet[48] matrix method using a gap of one and gap extension of one. Four automated steps, namely initial pairwise build-up (Progressive/Tree-based), round-robin realignment, randomised iterative refinement, and structure-based realignment of MOE-Align module were used for the alignment of target and templates.

3. Model building

Model building was carried using the following steps:

(a) Initial partial geometry specification. Initial geometry from regions of all template chains were copied. All coordinates were copied where residue identity was conserved.

(b) Intermediate model construction. Using a Boltzmann-weighted randomized modelling procedure[22] combined with specialized logic for proper handling of insertion and deletions,[49] independent models of the target proteins were built. Models were evaluated for residue packing quality. Automated loop and side chains modelling was selected.
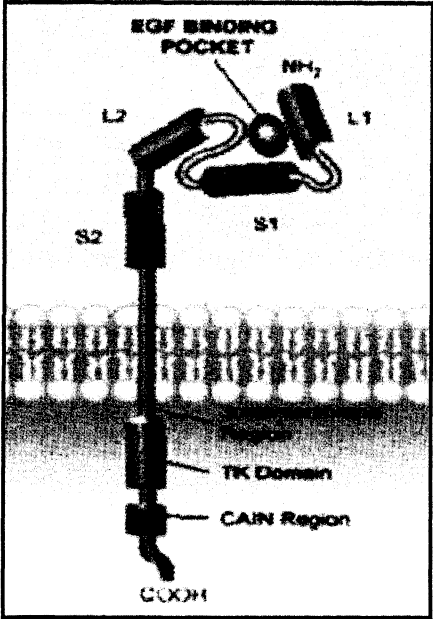
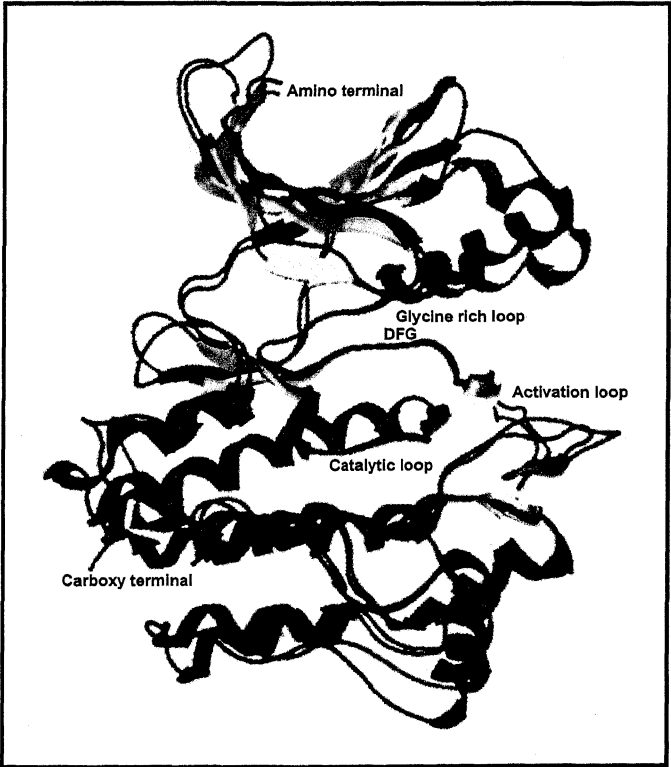Fig. 8- Overall architecture of **EGFR** (adapted from ref. 39).

Fig. 9- Superposition of our modle (or⁣iginal colours) with the experimental crystal structure (blue) of **EGFR** kinase domain.

(c) The final model was built and minimized. Coordinates were generated as the average of the atom coordinates of the intermediate models. After the final model was built, a rotamer exploration was carried out for important residues in the catalytic domain. The lowest energy conformation was chosen for the final model.

4. Quality check (evaluation, refinement and validation)

The final model was subjected to quality check. MOE stereochemical quality evaluation tools were applied to confirm that the stereochemistry of the model is reasonably consistent with typical values found in crystal structures. Tools like PROCHECK and Ramachandran plot were used to evaluate the model quality from a stereochemical viewpoint. Further energy minimisation was carried out to reduce bad contacts. The catalytic domain was treated with special care. Docking studies were performed with one of the potent inhibitors to validate the quality of the model.

Comparison with the crystal structure

The superposition of the homology built model and the experimental crystal structure M14.pdb is shown in Fig. 9. The RMSD with respect to the C_α atoms was 1.96 Å. Both show the bilobate nature like other kinases. The amino terminal lobe consists mostly of β-strands and one α-helix (αC) whereas the carboxy terminal lobe consists mostly of α-helices. The binding site of ATP, ATP analogues and ATP-competitive inhibitor is a cleft created by the amino and carboxy terminal lobe. This cleft consists of five important regions, the glycine-rich nucleotide phosphate-binding loop (Gly695–Gly700)

of the amino terminal lobe, the DGF motif (Asp831–Gly833), the presumptive catalytic (general base) Asp813, the catalytic loop (Arg812–Asn818) and the A-loop (Asp831–Val852) of the carboxy terminal lobe. These regions are indicated in Fig. 9. A comparative look at different regions of the model and the crystal structure gave us greater confidence on the accuracy of the model quality.

Conclusions

Homology modelling is a successful means of protein structure prediction. We have successfully implemented this method to build the three dimensional structure of epidermal growth factor receptor kinase domain. The model quality is as good as the reported crystal structure of the protein. However homology modelling is not the only method to predict the structure of a protein. Threading and *ab initio* methods have shown promising results in model building when the percentage similarity is less than 30% between template and target. In threading or fold recognition, a library of unique or representative structures is searched for structure analogues to the target sequence, and is based on the theory that there may be only a limited number of distinct protein folds.[50] Modelling of the protein when there is no structural template is existence is quite difficult. However *ab initio* approaches or *de novo* design based on biophysical principles have gained some success in this regard. *Ab initio* methods attempt to predict the structure from sequence alone, without relying on similarity at the fold level between the modeled sequence and any known structure.[51] It attempts to find the global free energy minimum by an exploration of many conceivable protein conformations. These methods assume that the native

structure corresponds to the global free energy minimum accessible.

All in all, modelling methods have achieved some success in predicting the structures of unknown proteins but there still remain many challenges to overcome.

Acknowledgments

References

1. Berman, H.M., Westbrook, J., Feng, Z., Gilliland, G., Bhat, T.N., Weissig, H., Shindyalov, I.N. & Bourne, P.E. (2000) *Nucleic Acids Res.* **28** : 235.

2. Veclovas, Z.A., Fidelis, K., & Moult, J. (2001) *Proteins 45 Suppl* **5** : 163.

3. Fischer, D., Elofsson, A., Rychlewski, L., Pazos, F., Valencia, A., Rost, B., Ortiz, A.R. & Dunbrack, R.L., Jr (2001) *Proteins 45 Suppl* **5** : 171.

4. Tramontano, A. (2003) *Nat. Struct. Biol.* **10** : 87.

5. Tramontano, A., D'Alfonso, G., & Morea., V. (2002) *Nat. Acad. Sci. Lett.* (India), **7** : 202.

6. Levitzki, A. and Gazit, A. (1995) *Science* **267** : 1782.

7. Stamos, J., Sliwkowski, M.X., & Eigenbrot, C. (2002) *J. Biol. Chem.* **277** : 46265.

8. Martí-Renom, M.A., Stuart, A.C., Fiser, A., Sánchez, R. Melo, F. & Šali, A. (2000) *Annu. Rev. Biophys. Biomol. Struct.* **29** : 291.

9. Hubbard, T.J.P., Ailey, B., Brenner, S.E., Murzin, A.G., & Chothia, C. (1999) *Nucleic Acids Res.* **27** : 254.

10. Holm, L. & Sander, C. (1999) *Nucleic Acids Res.* **27** : 244.

11. Orengo, C.A., Pearl, F.M.G., Bray. J.E., Todd, A.E., Martin, A.C., Conte, L.Lo., & Thornton, J.M. (1999) *Nucleic Acids Res.* **27** : 275.

12. Pearson, W.R. (1998) *J. Mol. Biol.* **276** : 71.

13. Altschul, S.F., Gish. W., Miller, W., Myers, E.W. & Lipman, D.J. (1990) *J. Mol. Biol.* **215** : 403.

14. Altschul, S.F., Madden, T.L., Schaffer, A.A., Zhang, Z.J., Miller, W. & Lipman, D.J. (1997) *Nucleic Acids Res.* **25** : 3389.

15. Jones, D.T. (1997) *Curr. Opin. Struct. Biol.* **7** : 377.

16. Smith, T.F. (1999) *Structure* **7** : R7.

17. Jeanmougin, F., Thompson, J.D., Gouy, M., Gibson, D.G. & Higgins, T.J. (1998) *Trends Biochem. Sci.* **23** : 403.

18. Saqi, M.A.S., Russell, R.B. & Sternberg, M.J.E. (1999) *Protein Eng.* **11** : 627.

19. Rost, B. (1999) *Protein Eng.* **12** : 85.

20. Blundell, T.L., Sibanda, B.L., Sternberg, M.J.E., & Thornton, J.M. (1987) *Nature* **326** : 347.

21. Jones, T.H. & Thirup, S. (1986) *EMBO J.* **5** : 819.

22. Levitt, M. (1992) *J. Mol. Biol.* **226** : 507.

23. Unger, R., Harel, D., Wherland, S., Sussman, J.L. (1989) *Proteins* **5** : 355.

24. Aszódi, A. & Taylor, W.R. (1996) *Folding Design* **1** : 325.

25. Šali, A. & Blundell, T.L. (1993) *J. Mol. Biol.* **234** : 779.

26. Oliva, B., Bates, P.A., Querol, E., Aviles, F.X. & Sternberg, M.J.E. (1997). *J. Mol. Biol.* **266** : 814.

27. Rufino, S.D., Donate, L.E., Canard, L.H.J. & Blundell, T.L. (1997) *J. Mol. Biol.* **267** : 352.

28. Wojcik, J., Mornon, J-P. & Chomilier, J. (1999) *J. Mol. Biol.* **289** : 1469.

29. Vlijmen, H.W.T. & Karplus, M. (1997) *J. Mol. Biol.* **267** : 975.

30. Petrella, R.J., Lazardis, T. & Karplus, M. (1998).*Folding Design* **3** : 353.

31. Dunbrack, R.L. & Karplus, M. (1993) *J. Mol. Biol.* **230** : 543.

32. Chung, S.Y. & Subbiah, S. (1996) *Structure* **4** : 1123.

33. Vásquez, M. (1996) *Curr. Opin. Struct. Biol.* **6** : 217.

34. Laskowski, R.A., McArthur, M.W., Moss, D.S. & Thornton, J.M. (1993) *J. Appl. Crystalogr.* **26** : 283.

35. Hooft, R.W.W., Sander, C. & Vriend, G. (1996) *J. Appl. Crystallogr.* **29** : 714.

36. Laskowski, R.A., Rullmann, J.A.C., MacArthur, M.W., Kaptein, R. & Thornton, J.M. (1996) *J. Biomol. NMR* **8** : 477.

37. Oldfield, T.J. (1992) *J. Mol. Graphics* **10** : 247.

38. Schlessinger, J. (2000) *Cell* **103** : 211.

39. Pedersen, M.W.& Poulsen, H. S. (2002) *Sci. Med.* **8** : 206.

40. Bridges, A.J. (2001) *Chem. Rev.* **101** : 2541.

41. MOE 2002.03, Chemical Computing Group Inc.: Montreal H3A 2R7, Canada.

42. Hubbard, S.R. (1997) *EMBO J* **16** : 5572.

43. Yamaguchi, H. & Hendrickson, W.A. (1996) *Nature* **384** : 484.

44. Hubbard, S.R., Wei, L., Ellis, L. & Hendrickson, W.A. (1994) **372** : 746.

45. Schindler, T., Bornmann, W., Pellicena, P., Miller, W.T., Clarkson, B. & Kuriyan, J. (2000) *Science* **289** : 1938.

46. Bossemeyer, D., Engh, R.A., Kinzel, V., Ponstingl, H. & Huber, R. (1993) *EMBO J.* **12** : 849.

47. Needleman, S.B. & Wunsch, C.D., (1970) *J. Mol. Biol.* **48** : 443.

48. Gonnet, G.H, Cohen, M.A. & Benner, S.A. (1992) *Science* **256** : 1443.

49. Fechteler, T., Dengler, U. & Schomberg. D. (1995) *J. Mol. Biol.* **253** : 114.

50. Jones, D.T. & Hadley C. (2001) *Bioinformatics: Sequence, Structure and Databanks: A Practical Approach,* ed. Higgins D., and Taylor W., Oxford University Press, Oxford.

51. Bonneau, R. & Baker, D. (2001) *Annu. Rev. Biophys. Biomol. Struct.* **30** : 173.

Bivariate geometric distributions revisited

M. Sreehari

Department of Statistics, Faculty of Science, M.S. University of Baroda, Vadodara-390 002, India.

e-mail : msreehari03@yahoo.co.uk

Abstract

An overview of various bivariate geometric distributions is given. The focus is on characterization results. The role of bivariate distributions in reliability and Statistical Quality Control is illustrated, with examples, in detail.

(Keywords : characterization/survival function/ failure rate function/mean residual life function/ lack of memory property).

Introduction

The extension of univariate probability distributions to two or more dimensions is not an easy task. Very often investigations in this regard result in more than one distribution. Researchers generally believe that certain basic properties associated with a univariate distribution must be preserved (in an appropriate form) by their counter parts in higher dimensions. One of the main problems confronted in pursuing this approach is the fact that there may not be a unique formulation of such a basic property of a univariate distribution in higher dimensions. Also, researchers consider in higher dimension, real life situations similar to those in one dimension for which a univariate distribution is known to be a suitable stochastic model and investigate stochastic models appropriate for those situations. Naturally there will be several candidate probability distributions in higher dimensions which could be considered as extensions of a univariate probability distribution.

The literature concerning bivariate and multivariate exponential distributions is very rich (see, for example, Galambos and Kotz[1]). The investigations were motivated by consideration of appropriate stochastic models as well as by consideration of appropriate versions of characterizing properties of univariate exponential distribution. However, comparatively less is known about multivariate version of the geometric distribution, even though it plays an important role as the discrete counterpart of the exponential distribution in stochastic modelling. It will be seen that different ways of looking at a problem resulted in different versions of geometric distributions in higher dimensions, even in the modest literature concerning this. Interestingly, some researchers have formulated a bivariate geometric distribution whose marginals are *not geometric*.

Bivariate geometric model was initially discussed by Downton[2] in connection with consideration of shock models in reliability that lead to bivariate exponential distribution. Commenting on Downton's

model, Hawkes[3] formulated a bivariate geometric distribution through bivariate Bernoulli distribution. Around the same time, Paulson and Uppuluri[4], Esary and Marshall[5] and Arnold[6] discussed the bivariate and multivariate geometric distributions from the point of view of compounding models.

Block et $al.$[7] gave a very general definition of a bivariate geometric distribution as one for which the marginals are geometric and gave several examples. They constructed some auto regressive processes with bivariate geometric marginals.

Another approach adopted in the literature concerning bivariate geometric distribution is by consideration of characterizing properties.

The aim of this paper is to review the literature concerning characterization results for several bivariate geometric distributions. We shall also mention relevant results concerning a multivariate geometric distribution. No proofs are given but adequate references are provided.

The outline of this paper is as follows. We first list various bivariate geometric distributions. We then discuss some definitions and concepts that play important role in characterizing univariate geometric distribution. Finally we discuss, without proofs, the characterization results concerning the various bivariate geometric distributions listed earlier.

Various bivariate geometric distributions.

(a) The bivariate geometric distribution introduced by Hawkes[3], henceforth referred to as BGD(H) is given by its joint survival function

$R(m,n) =$

$$\begin{cases} p^n \ p_1^{m-n} & 0 \le n < m \\ p^m \ p_2^{n-m} & 0 \le m < n \end{cases}, \ m,n = 0,1,2,..$$

where $0 < p < p_i < 1$, $i=1,2$, $p_1+p_2 \le 1+p$,

or equivalently by its probability mass function (pmf)

$f(m,n) =$

$$\begin{cases} p^n \ p_1^{m-n-1} \ (p_1 - p)(1 - p_1) & \text{if } 0 \le n < m \\ p^m(1 + p - p_1 - p_2) & \text{if } 0 \le m = n \\ p^m \ p_2^{n-m-1} \ (p_2 - p)(1 - p_2) & \text{if } 0 \le m < n \end{cases}$$

$$m,n = 0,1,2,\dots$$

where $0 < p < p_i$, $i=1,2$ and $p_1 + p_2 \le 1+p$.

$Remark$: If $p_1 + p_2 = 1+p$ then the distribution has no mass at the points (m,m), $m=0,1,2,,\dots$

(b) The BGD introduced by Phatak and Sreehari[8], henceforth referred to as BGD(P & S), is given by the pmf

$f(m,n) =$

$$\binom{m+n}{n} p_1^m \ p_2^n \ (1 - p_1 - p_2), \ m,n = 0,1,2,\dots$$

where $0 < p_1, p_2 < p_1 + p_2 < 1$.

(c) Nair and Nair[9] introduced a BGD, henceforth referred to as BGD(N & N), by its joint survival function

$$R(m,n) = p_1^m \ p_2^n \ \theta^{mn} \ , \ m, \ n = 0,1,2,\dots$$

where

$$0 < p_1, p_2 < 1, 0 < \theta < 1, 1 - \theta \le (1 - p_1\theta)(1 - p_2\theta)$$

Corresponding pmf is given by

$$f(m,n) = p_1^m \, p_2^n \, \theta^{mn-1}[(1 - p_1\theta^{n+1})(1 - p_2 \, \theta^{m+1}) + \theta - 1]$$

where p_1, p_2 and θ satisfy the above inequalities.

(d) Nair and Asha[10] considered a BGD, henceforth referred to as BGD(N&A), which is given by the joint survival function

$$R(m,n)= \begin{cases} p_1^m & if \ \ p_1^m \le p_2^n \\ p_2^n & if \ \ p_2^n < p_1^m \end{cases}, \ \ m,n = 0,1,2,...$$

where $0 < p_i < 1$, $i=1,2....$

(e) Asha and Sankaran[11] introduced a BGD, henceforth referred to as BGD(A & S), which is given by its pmf

$$f(m,n)=$$

$$\begin{cases} (p_1p_2)^m (p_2^*)^{n-m-1} \, p_2(1-p_1)(1-p_2^*) \ if \ 0 \le m < n \\ (p_1p_2)^m \, (1-p_1)(1-p_2) & if \ 0 \le m = n \\ (p_1p_2)^n \, (p_1^*)^{m-n-1} \, p_1(1-p_2)(1-p_1^*) \ if \ 0 \le n < m \end{cases}$$

$$m,n = 0,1,2,...$$

where $0 < p_i, p_i^* < 1$, $p_i^* \ne p_1p_2$, $i=1,2$.

Remark : All the bivariate geometric distributions except the *last* have geometric marginal distributions.

Univariate geometric distribution

We shall now state some definitions and discuss related basic properties of a univariate geometric distribution with support $N = \{0,1,2...\}$. We mention a real life situation for which a geometric distribution is an appropriate stochastic model. Unless stated otherwise all random variables $(r.v.s)$ are nondegenerate nonnegative integer valued.

Definition 1 : A r.v. X is said to have a geometric distribution if

$$P \ (X = n) = p \ (1-p)^n \qquad (1)$$

$n = 0,1,2,..., \ 0 < p < 1$.

We shall then write $X \sim G(p)$.

Definition 2 : The failure rate function of a r.v. X is given by

$$h(n) = P(X = n \mid X \ge n) = P(X = n) \, / \, R(n)$$

where $R(n)$ is the survival function, $P(X \ge n)$.

Whenever $P(A|B)$ or $E(Z|B)$ is considered for events A,B and r.v. Z, it is assumed that $P(B) > 0$.

Definition 3 : Residual life of a r.v. X after an elapsed time x is denoted by

$\{X\text{-}x \mid X \ge x\}$ and the mean residual life function $\mu(x)$ is given by

$$\mu \ (x) = E \ [X\text{-}x \mid X \ge x].$$

Definition 4 : A r.v. X is said to possess the lack of memory property (LMP) at t if

$P[X \geq t+s \mid X \geq t] = P(X \geq s), s \geq 0.$

We need the following results concerning a geometric r.v. for later developments and they are easily checked.

If $X \sim G(p)$ then

$$R(n) = (1-p)^n, n = 0,1,2,\ldots \qquad (2)$$

$$h(n) = 1-p, n = 0,1,2,\ldots \qquad (3)$$

$$\mu(n) = 1+E(X), n = 0,1,2\ldots \qquad (4)$$

and

X has LMP at all $t = 1,2,\ldots \qquad (5)$

It is well known that each of the results (2) – (5) uniquely determines the geometric distribution in the class of discrete distributions. In fact, if X has LMP at $t = 1$, then also X has a geometric distribution. It is of interest to note that X need not have geometric distribution if X has LMP at *only* one point $t > 1$. (see Phatak and Sreehari [8], Sreehari [12] and Srivastava and Bagchi [13]). However, if X has LMP at two points m and n which are relatively prime then X has geometric distribution (Sreehari [12] and Srivastava and Bagchi [13]). In fact, Srivastava and Bagchi proved a slightly more general result.

We shall now discuss some properties of a geometric distributuion whose analogues in higher dimensions will be discussed later in the paper.

Property 1

In the class of power series distributions given by $P(X = n) \propto a_n \theta^n$, $n = 0,1,2,\ldots$,

geometric is the only one with $E(X) = \theta/(1-\theta)$.

Property 2

If X and Y are independent identically distributed r.v.s then

$$P(X+Y = k) \propto (k+1) P(X = k), k = 0,1,2,\ldots (6)$$

if and only if their common distribution is geometric.

Property 3

For some r.v. Y

$$P(Y \leq n) - P(X+Y \leq n) \propto P(X+Y = n),$$
$$n = 0,1,2,\ldots \qquad (7)$$

if and only if X is a geometric r.v.

If $X \sim G(p)$, $Y = X+1$ takes values $1,2,\ldots$ and is called a modified or truncated (at zero) geometric r.v.

Example.

Consider a system which is subjected to a series of shocks each of which has a probability p of making the system 'nonworking'. Suppose that the shocks occur independent of each other and that no damage to the life of the system occurs by a shock which is not 'fatal'. Then the number X of non-fatal shocks received by the system before it received a shock that is 'fatal', has the geometric distribution given at (1).

Bivariate geometric distribution, BGD(H).

In this section we shall discuss an example which leads to BGD(H) and give a number of characterization results concerning this distribution. In this and later sections all bivariate random vectors have support $N \times N$ where $N = \{0,1,2,...\}$, unless otherwise stated.

Example :

Suppose two components C_1 and C_2 of a system receive shocks which occur in independent Poisson streams of rates λ_1 and λ_2. Suppose further that each shock may not necessarily be fatal resulting in the failure of the component. Let X_i be the number of shocks received by the component C_i before its failure. Suppose the joint probability generating function $G(s_1, s_2)$ of (X_1, X_2) is

$$G(s_1, s_2) = s_1 s_2 / (1+\alpha+\beta+\gamma - \alpha s_1 - \beta s_2 - \gamma s_1 s_2)$$

where $0 < \alpha, \beta, \gamma < 1$.

We note that the marginal distributions of X_1 and X_2 are geometric distribution over $\{1,2,...\}$. Using the bivariate geometric distribution given by $G(s_1,s_2)$, Downton[2] discussed the joint distribution of the life times of the two components C_1 and C_2 involving the five parameters λ_1, λ_2, α, β and γ. Commenting on Downton's work, Hawkes[3] introduced a bivariate geometric distribution, through a bivariate Bernoulli distribution, with support $\{1,2,3,...\} \times \{1,2,3,...\}$. This distribution is one of the widely discussed bivariate geometric distributions and is a reformulation of BGD(H).

The illustration given in the previous section can be reformulated in terms of observation of a sequence of independent Bernoulli r.v.s $\{X_n\}$, for which $P(X_n = 1) = p$ and $P(X_n = 0) = 1-p$, till a 'one' is observed. Our example of BGD(H) is given in terms of a bivariate Bernoulli distribution.

Definition 5 : Vector (X,Y) is said to have a bivariate Bernoulli distribution with parameters (p_{00}, p_{01}, p_{10}) if

$$P(X=0, Y=0) = p_{00}$$

$$P(X=0, Y=1) = p_{01}$$

$$P(X=1, Y=0) = p_{10}$$

$$P(X=1, Y=1) = 1 - p_{00} - p_{01} - p_{10} = p_{11} .$$

For convenience, let us denote

$$p_{i0} + p_{i1} = p_{i+} \text{ and } p_{0j} + p_{1j} = p_{+j}, \ i,j = 0,1.$$

Consider a sequence $\{(X_n, Y_n)\}$ of independent identically distributed bivariate Bernoulli random vectors. Let U denote the number of 0's before the first 1 in the sequence $X_1, X_2,...$, and let V denote the number of 0's before the first 1 in the sequence $Y_1, Y_2,...$ Then the joint distribution of U and V is given by

$$P(U=m, V=n) =$$

$$\begin{cases} p_{00}^m \ p_{+0}^{n-m-1} \ p_{10} \ p_{+1} & \text{if } m < n \\ p_{00}^m \ p_{11} & \text{if } m = n \\ p_{00}^n \ p_{0+}^{m-n-1} \ p_{01} \ p_{1+} & \text{if } n < m \end{cases}$$

Reparameterizing this distribution we note that (U,V) has the BGD(H). To see this, take $p = p_{00}$, $p_1 = p_{0+}$ and $p_2 = p_{+0}$.

Marshall and Olkin[14] observed that $-\frac{1}{4} \leq \text{corr}(U,V) \leq 1$.

Further, the marginal distributions of U and V are geometric $(1-p_1)$ and geometric $(1-p_2)$ respectively.

A natural extension of the failure rate function to two dimensions is the bivariate failure rate function

$$h(m,n) = \frac{P(U=m, V=n)}{P(U \geq m, V \geq n)}.$$

This was also called Scalar failure rate function by Asha and Nair[15]. It is easily seen that $h(m,n)$ is *not a constant* for the BGD(H). In fact, it is constant in each of the regions $0 \leq m < n$, $0 \leq m = n$ and $0 \leq n < m$. Asha and Nair proved the following result which gives a characterization of the BGD(H).

Theorem 1 : A random vector (U,V) has the BGD with survival function

$$R(m,n) = \begin{cases} p^n\, p_1^{m-n} & n \leq m \\ p^m\, p_2^{n-m} & m \leq n \end{cases} \qquad (8)$$

$0 < p < p_i < 1$, $j = 1,2$, $p_1 + p_2 < 1 + p$ if and only if the Scalar failure rate function is of the form

$$h(m,n) = \begin{cases} C_1 & if \ n < m \\ C_2 & if \ m = n \\ C_3 & if \ m < n \end{cases}$$

where $0 < C_i < 1$, $i = 1,2,3$ and the marginal distributions of U and V are geometric with parameters $1-p_1$ and $1-p_2$ respectively.

Remark : It is noted that the proof given by Asha and Nair is not consistent with their notation for the survival function.

Another extension of the failure (hazard) rate function to two dimensions is by considering the vector failure rate function $(h_1(m,n), h_2(m,n))$ where

$h_1(m,n) = P(U=m, V \geq n)/R(m,n)$ and

$h_2(m,n) = P(U \geq m, V=n)/R(m,n)$,

whenever $R(m,n) > 0$. In terms of this Nair and Asha[16] obtained the following.

Theorem 2 : A random vector (U,V) has the BGD(H) if and only if the components of the vector failure rate function are of the forms

$$h_1(m,n) = \begin{cases} a_1 & for \ n \leq m \\ a_2 & for \ m < n \end{cases}$$

$$h_2(m,n) = \begin{cases} b_1 & for \ n < m \\ b_2 & for \ m \leq n \end{cases}$$

for all $m,n = 0,1,2,\ldots$ and some constants $0 < a_i$, $b_i < 1$, $i = 1,2$ satisfying $(1-a_1)(1-b_1) = (1-a_2)(1-b_2)$ and $b_1(1-a_1) \leq b_2$. Here $p_1 = 1-a_1$, $p_2 = 1-b_2$ and $p = (1-a_1)(1-b_1)$.

Remark : The above result can be reformulated in terms of vector mean residual life time, as was done by Nair and Asha.

If (U,V) has the BGD(H) it is easily verified that the conditional distribution of U given $V=n$ is given by its pmf $g(m \mid n) = P(U=m \mid V=n)$ where

$g(m \mid n) =$

$$\begin{cases} p_1^{m-1} (p/p_1 p_2)^n \; [(1-p_1)(p_1-p)/(1-p_2)] \\ \qquad\qquad\qquad\qquad\qquad\quad \text{if } n < m \\ [(1+p-p_1-p_2)/(1-p_2)] \, (p/p_2)^m \quad \text{if } m = n \\ p^m \; p_2^{-(m+1)} \, [p_2 - p] \qquad\qquad\qquad \text{if } m < n \end{cases}$$

It is well known that if the conditional distribution $f(x_1 \mid x_2)$ of X_1 given $X_2=x_2$, and the marginal distribution of X_2 are known then the joint distribution of (X_1, X_2) is determined. But knowledge of $f(x_1 \mid x_2)$ and that of the marginal distribution of X_1 is not adequate to determine the joint distribution of (X_1, X_2). In this context Nair and Asha[16] proved an interesting characterization result based on a distributional property. Similar results for BGD(P&S) and BGD(N&N) are given in Theorems 12 and 15.

Theorem 3 : If a random vector (U,V) has $P(U=m \mid V=n)$ given as above then U is geometric $(1-p_1)$ if and only if V is geometric $(1-p_2)$. Consequently, (U,V) is BGD(H).

It is well known that if $X_1, X_2,\dots,X_n$ are independent geometric r.v.s then $\min(X_1, X_2,\dots,X_n)$ is a geometric r.v. Similarly, if (X_1,Y_1), $(X_2,Y_2)\dots,(X_n,Y_n)$ are independent random vectors having bivariate geometric distributions of the form given by (8) then

$$\left(\min_{1 \le i \le n} X_i, \; \min_{1 \le i \le n} Y_i \right)$$

has a BGD(H).

An interesting result connecting the BGD(H) with minima of independent geometric r.v.s is the following.

Let Y_1, Y_2, Y_3 be independent geometric r.v.s with parameters $(1-\alpha)$, $(1-\beta)$ and $(1-\gamma)$ respectively. Then (U,V) where $U=\min(Y_1,Y_3)$ and $V=\min(Y_2,Y_3)$ has BGD(H) given at (8) with $p_1 = \alpha\gamma$, $p_2=\beta\gamma$ and $p=\alpha\beta\gamma$. This interesting result noted by Block et al.[7] is a part of Theorem 5.1 in Nair and Asha[16] and is useful in generating random vectors having BGD(H) given at (8) for which $p_1 p_2 < p$.

Remark : Nair and Asha[16] claim a converse to this result in Theorem 5.1 of their paper which appears to be incorrect.

Nair and Asha considered the bivariate no-aging property

$$P[X_1 \ge m+k, X_2 \ge n+k \mid X_1 \ge k, X_2 \ge k] = P[X_1 \ge m, X_2 \ge n] \qquad (9)$$

for $m,n,k=0,1,2,\dots$ to investigate the behaviour of the joint distribution of (X_1, X_2). It is noted that this is a kind of bivariate LMP. They proved the following:

Theorem 4. A random vector (U,V) has the bivariate no-aging property given at (9) and the marginal distributions are geometric if and only if the joint distribution of (U,V) is BGD with survival function $R(m,n)$ given in Theorem 1 for some p_1, p_2 and p.

Failure of a two-component parallel system can be considered to consist of two stages: first one of the two component fails and later the remaining one fails. Working

on this, Sun and Basu[17] introduced total failure rate for the discrete r.v.s set up.

Definition 6 : For a random vector(U,V) the vector $(r(t), r_1(m \mid n), r_2(n \mid m))$ is called the *total failure rate* where

$$r(t) = P [\min(U,V) = t \mid U \ge t, V \ge t] \qquad (10)$$

$$r_1(m \mid n) = P [U=m, V=n]/P (U \ge m, V=n) \text{ for } m > n \qquad (11)$$

$$r_2(n \mid m) = P [U=m, V=n]/P (U=m, V \ge n) \text{ for } n > m. \qquad (12)$$

Note that $r(t)$ is the failure rate of $\min(U,V)$ whereas $r_1(m \mid n)$ is the conditional failure rate of U given U>V and $V= n$. Similar meaning is conveyed by $r_2(n \mid m)$.

Sun and Basu obtained the following characterization result of BGD(H) in terms of total failure rate.

Theorem 5. A random vector (U,V) has the BGD(H) if and only if it has geometric marginals and a constant total failure rate. In this case, $r(t)=1-p$, $r_1(m \mid n) =1- p_1$ for $m > n$ and $r_2(n \mid m) = 1- p_2$ for $n > m$.

Asha and Nair[15] also considered the conditional failure rate functions $r_1(m \mid n)$ and $r_2(n \mid m)$ and studied their behaviour in the context of BGD(H).

Remarks : Suppose that a random vector (U,V) has the BGD(H) given by (8). Let $N_1=U+1$ and $N_2=V+1$. The random vector (N_1, N_2) takes values in $\{1,2,...\} \times \{1,2,...\}$ and its distribution may be called modified BGD. This distribution has been considered by Downton[2], Paulson and Uppuluri[4], Esary and Marshall[5], Arnold[6], Block and Paulson[18], Marshall and Olkin[14,19], Block et al.[7], Nair and Nair[20], Wu[21], Nair and Asha[10] and Abraham and Balakrishnan[22] among others.

Block and Paulson[18] and Block et al.[7] considered bivariate geometric compounding, namely $(\xi, \eta) = \left(\sum_1^{N_1} X_i, \sum_1^{N_2} Y_i \right)$ where (X_1,Y_1), (X_2,Y_2),... are independent identically distributed random vectors, (N_1,N_2) has the BGD discussed above and (N_1, N_2) is independent of $\{(X_n, Y_n)\}$. Block and Paulson investigated the infinite divisibility of the distribution of (ξ, η) .

Marshall and Olkin[19] considered the stability of geometric maximum and geometric minimum. Wu[21] also considered bivariate geometric summation and studied the limiting distributional properties. Wu called the modified BGD of (N_1, N_2) as the general BGD. Wu called the same as ordinary BGD in case $P(N_1 = N_2)=0$, which holds if $1+p = p_1 + p_2$. For a discussion on a general multivariate geometric distribution we refer to Arnold[6].

Block et al.[7] constructed bivariate exponential (geometric) auto regressive and auto regressive moving average models and investigated the stationarity of BEAR and BGAR.

Abraham and Balakrishnan[22] considered Bivariate exponential auto regressive (BEAR(1)) process using the modified BGD in the context of a repairable system.

Bivariate geometric distribution, BGD (P & S).

Phatak and Sreehari[8] introduced the BGD with pmf $g(.,.)$ of a random vector (X_1,X_2) given by

$$g(m,n) = \binom{m+n}{n} p_1^m p_2^n p_0 \ , m,n=0,1,2,..,(13)$$

$$0 < p_1, p_2 < 1, \ 0 < p_0 = 1 - p_1 - p_2 < 1.$$

The marginal distributions are geometric with $EX_1 = p_1/p_0$ and $EX_2 = p_2/p_0$.

We give an illustration of this BGD in Statistical Quality Control.

Example :

In the three-class attributes inspection, a unit which meets all the specifications (important as well as less important) laid down by a quality control engineer is called a good unit. A unit is called a bad unit if it fails to meet one or more important specifications. A unit which is neither good nor bad is called marginal. Let p_0, p_1 and p_2 (=1- p_0- p_1) be the probabilities of a unit inspected being bad, marginal and good unit respectively. Suppose that during the unit by unit inspection process, the number X_1 of marginal units and the number X_2 of good units that pass the inspection before the first bad unit is encountered are recorded. Then the probability mass function of (X_1, X_2) is given by (13).

Phatak and Sreehari proved two characterization results concerning the BGD at (13) based on properties 1 and 2.

Definition 7 : A random vector (X_1, X_2) has a bivariate power series distribution if its pmf is given by

$$f(m,n) = \frac{a_{m,n}\, p_1^m\, p_2^n}{A(p_1,p_2)} \ , m,n=0,1,2,... \quad (14)$$

where

$$A(p_1,p_2) = \sum_{m=0}^{\infty}\sum_{n=0}^{\infty} a_{m,n} p_1^m p_2^n, p_1, p_2, a_{m,n} > 0.$$

Theorem 6 : Let (X_1, X_2) have the bivariate power series distribution given at (14). Then (X_1, X_2) has BGD(P & S) given at (13) if and only if

$$E(X_i) = p_i / (1 - p_1 - p_2), \ i=1,2. \quad (15)$$

Remark : This result is an extension of the property 1 of the geometric distribution. The next result is an extension of the convolution property 2 of geometric distribution.

Theorem 7. Let (X_1,X_2) and (Y_1,Y_2) be independent identically distributed random vectors with pmf g(.,.). Then g(.,.) satisfies the relation at (13) if and only if

$$P[X_1+Y_1 = m, X_2+Y_2=n] = C(m+n+1)g(m,n) \quad (16)$$

for all $m,n=0,1,2...$ where C is a constant.

Phatak and Sreehari proved the Theorem 7 by the method of induction. They mentioned that (16) is equivalent to a partial differential equation satisfied by the probability generating function corresponding to g(.,.) and that by solving that partial differential equation one might get a simpler proof which can be extended to obtain a characterization of multivariate geometric distribution given below.

Definition 8 : A random vector $X = (X_1,...,X_k)$ has a multivariate geometric distribution (MGD) if

$P(X_j = n_j, j=1,...,k) =$

$$\frac{(\sum_{1}^{k} n_j)!}{\prod_{j=1}^{k}(n_j!)} \prod_{j=1}^{k} p_j^{n_j} \cdot p_0, \quad n_1,..,n_k = 0,1,2,...$$

where $0< p_j <1, j=0,1,2...,k, \sum_{j=0}^{k} p_j = 1.$

Srivastava and Bagchi[13] proved a characterization result concerning the above MGD based on the convolution property (extension of Theorem 7) solving a partial differential equation satisfied by the probability generating function of the MGD as conjectured by Phatak and Sreehari.

Phatak and Sreehari considered certain bivariate versions of the LMP at 1 and the property 3 of the univariate geometric distribution.

Extension of LMP at 1 to two dimensions

One may consider

$P[X_1 = m+1, X_2=n+1 \mid X_1 \geq 1, X_2 \geq 1] =$

$P[X_1=m, X_2=n], \quad m,n= 0,1,2...$ (17)

as an extension of the LMP at 1.

The BGD(P & S) *does not* satisfy (17). Nagaraja[23] proposed a different extension of LMP at 1 to the bivariate case which indeed characterizes the BGD(P & S). Nagaraja proved the following :

Theorem 8. A random vector (X_1, X_2) has BGD(P & S) if and only if its pmf $g(.,.)$ satisfies the property

$g(m,n) = c_1 g(m-1,n) + c_2 g(m,n-1), \quad m,n$
$= 0,1,2,..., (m,n) \neq (0,0)$ (18)

and $g(m,n) = 0$ if $m<0$ or $n<0$,

where $0 < c_1, c_2 < c_1 + c_2 < 1.$ In this case $g(0,0)=1-c_1-c_2.$

Nagaraja also proved the following to strengthen a result of Phatak and Sreehari.

Theorem 9. For a random vector (X_1, X_2) any two of the following statements together imply the remaining.

(a) Condition (17) holds

(b) X_1 and X_2 are independent.

(c) X_1 and X_2 are geometric r.v.s with $P(X_1 =0, X_2=0) = P(X_1=0) P(X_2=0).$

Remark : It may be mentioned that Result 3 of Nagaraja in this context is incorrect.

Srivastava and Bagchi[13] obtained a different characterization result for the BGD(P & S) using a bivariate power series distribution and a random version of condition (17). Their result is a generalization of a result of Zijlstra[24], and makes use of the previous theorem of Nagaraja.

Theorem 10. Let $X = (X_1, X_2)$ and $Y = (Y_1, Y_2)$ be independent random vectors and let Y have the bivariate power series distribution given at (14). Then X is BGD(P & S) if and only if

$P[X= Y, Y \neq 0] = c_1 P[X_1= Y_1 -1, X_2=Y_2]$
$+ c_2 P[X_1=Y_1, X_2=Y_2 -1]$

for all p_1, p_2 such that $0 \leq p_1, p_2 \leq M$ where M, c_1, c_2 are positive and $c_1 + c_2 < 1.$

Phatak and Sreehari considered the following extension of Property 3 of univariate geometric distribution due to Puri[25] discussed earlier.

For some random vector Y

$$P(Y \leq n) - P(X + Y \leq n) = \beta P(X + Y = n)$$

holds for all $n = (n_1, n_2)$, $n_1, n_2 = 0,1,2,\ldots$ where β is a constant.

It turns out that there is no Y which satisfies the above condition when X has BGD(P & S). Nagaraja considered an alternative bivariate extension of the condition at (6) and proved the following.

Theorem 11 : A random vector $X = (X_1, X_2)$ has BGD(P & S) if and only if for some random vector $Y = (Y_1, Y_2)$

$$P(Y = n) = (1+\beta) P (X + Y = n) - \theta\beta P(X + Y = B - I_1) - (1-\theta) \beta P(X + Y = n - I_2)$$

where $I_1 = (1,0)$, $I_2 = (0,1)$, θ and β satisfy $p_0 = (1+\beta)^{-1}$, $p_1 = \theta\beta \ p_0$ and $p_2 = (1-\theta)\beta \ p_0$.

Nair and Nair[20] proved interesting results similar to Theorem 3 for the BGD(P & S) and BGD(N & N).

Theorem 12. Let X_1 and X_2 be two r.v.s for which the conditional distribution of X_1 given $X_2 = n$ is given by

$$P(X_1 = m \mid X_2 = n) = \binom{m+n}{m} p_1^m (1 - p_1)^{n+1},$$

$$m = 0,1,2,\ldots$$

and the marginal distribution of X_1 is given by

$$P(X_1 = m) = \frac{p_0}{1 - p_2} \left(\frac{p_1}{1 - p_2} \right)^m , \ m = 0,1,2\ldots$$

where $0 < p_0, p_1, p_2 < 1$, $p_0 + p_1 + p_2 = 1$. Then the joint distribution of (X_1, X_2) is given by (13). That is, (X_1, X_2) is BGD(P & S).

The proof appears to be incomplete and as such the problem considered is open.

A similar result in the case of BGD(N & N) will be discussed later.

Bivariate geometric distribution BGD (N & N).

Nair and Nair[9] considered the following extension of mean residual life function μ (t) given in definition 3.

$$\mu \ (m,n) = (\mu_1(m \mid n), \mu_2(n \mid m))$$

where

$$\mu_1 \ (m \mid n) = E \ [X_1 - m \mid X_1 \geq m, X_2 \geq n] \quad (19)$$

and

$$\mu_2 \ (n \mid m) = E \ [X_2 - n \mid X_1 \geq m, X_2 \geq n] \quad (20)$$

$$m, n = 0,1,2,\ldots$$

Recall that the property that $\mu(n)$ is a constant for all $n = 0,1,2\ldots$, characterizes a geometric distribution. Nair and Nair proposed that if $\mu_1(m \mid n)$ and $\mu_2(n \mid m)$ are independent of m and n then the joint distribution of (X_1, X_2) may turn out to be a bivariate version of geometric distribution. But it turns out that X_1 and X_2 are *independent* geometric r.v.s. They modified the constancy of $\mu_i(m \mid n)$ conditions which led to the BGD(N&N). Suppose

$\mu_1(m \mid n) = a_1(n)$ is independent of m (21)

and

$\mu_2(n \mid m) = a_2(m)$ is independent of n.   (22)

They proved the following result.

Theorem 13 : A random vector (X_1, X_2) has the BGD given by the joint survival function

$$R(m,n) = \quad p_1^m \ p_2^n \ \theta^{mn} \ , m,n=0,1,2\ldots (23)$$

where $0 \leq p_1 \leq p_2 \leq 1$, $0 \leq \theta \leq 1$, $1-\theta \leq (1-p_1\theta)(1-p_2\theta)$ if and only if $\mu_1(m \mid n)$ and $\mu_2(n \mid m)$ satisfy (21) and (22) where $a_1(n)$ and $a_2(m)$ are non-increasing and $a_i(0) = p_i / (1-p_i)$, $i=1,2$.

In view of the equality of conditions (4) and (5) for a geometric r.v. one looks for a bivariate version of the LMP which might also characterize the BGD given at (23). Such a result is proved by Nair and Nair[9] in the following theorem.

Theorem 14 : A random vector (X_1, X_2) has the BGD given at (23) if and only if the following conditional lack of memory properties

$$P[X_1 \geq m+k \mid X_1 \geq m, X_2 \geq n] = P[X_1 \geq k \mid X_2 \geq n](24)$$

and

$$P[X_2 \geq n+k \mid X_1 \geq m, X_2 \geq n] = P[X_2 \geq k \mid X_1 \geq m](25)$$

hold for all non-negative integers m, n and k.

Analogous to Theorem 3 and Theorem 12 we have the following distributional

property characterizing BGD(N & N) proved by Nair and Nair[20].

Theorem 15 : Suppose

$P(X_1=m \mid X_2=n)=$

$p_1^m \ \theta^{mn-1} \ (1-p_2)^{-1} [(1-p_1\theta^{n+1})(1-p_2\theta^{m+1})$

$+ \theta - 1]$, $m = 0,1,2,\ldots$

and

$P(X_1=m) = (1-p_1) \ p_1^m$, $m=0,1,2,\ldots$

where

$0 < p_1, p_2 < 1, \ 0 < \theta < 1, \ 1 - \theta \leq (1 - p_1\theta)(1 - p_2\theta)$.

Then (X_1, X_2) has the BGD given at (23).

Nair and Asha[10] discussed the IFR (and DFR) properties of BGD(H), BGD(N & N) and BGD(N& A).

Bivariate geometric distribution, BGD (A & S)

We now discuss a reliability problem which leads to the BGD considered by Asha and Sankaran.

Example :

Let X_1 and X_2 be the r.v.s representing the lifetimes (measured in the number of cycles of survival) of two components A and B in a two component system. Suppose that the two components are subject to shocks S_1 and S_2 respectively. The shocks occur independent of each other at most once in a cycle. Suppose Z_1 and Z_2 are the numbers of the cycles in which shocks S_1 and S_2 occur causing failure of components

A and B respectively. Clearly component A fails first in cycle m if $Z_1=m$ and $Z_2>Z_1$ and similar is the case with component B. After the failure of either component, the system will continue to operate till a further shock (to the other component) occurs. Let Z_1^* (and Z_2^*) be the number of the cycles in which shock S_1 (S_2) occurs causing failure of component A (and B) if $Z_1<Z_2$ ($Z_1>Z_2$). Then the component lifetimes are

$$X_1 = \begin{cases} Z_1 & \text{if } Z_1 \le Z_2 \\ Z_2 + Z_1^* & \text{if } Z_1 > Z_2 \end{cases}$$

and

$$X_2 = \begin{cases} Z_2 & \text{if } Z_1 \ge Z_2 \\ Z_1 + Z_2^* & \text{if } Z_1 < Z_2. \end{cases}$$

Under the assumption that Z_1, Z_2, Z_1^* and Z_2^* are independent geometric r.v.s with expectations p_1, p_2, p_1^* and p_2^* , the joint distribution of (X_1, X_2) is given by

$$P(X_1=m, X_2=n) =$$

$$\begin{cases} (p_1 p_2)^n (p_1^*)^{m-n-1} p_1(1-p_2)(1-p_1^*) & \text{if } m > n \\ (p_1 p_2)^m (p_2^*)^{n-m-1} p_2(1-p_1)(1-p_2^*) & \text{if } m < n \\ (p_1 p_2)^m (1-p_1)(1-p_2) & \text{if } m = n \end{cases}$$

$$(26)$$

$m,n = 0,1,2,..$

where

$$p_1^*, p_2^* \ne p_1 p_2 , 0 < p_1, p_2, p_1^*, p_2^* < 1.$$

Asha and Sankaran observed that $\min(X_1, X_2)$ is geometrically distributed with mean $p_1 p_2$. The distribution satisfies the

bivariate LMP considered at (9). Further, the BLMP, under certain additional assumptions concerning the marginal distributions, characterizes the above BGD.

The marginal distribution of X_j is a mixture of two geometric distributions and is given by

$$P(X_j=m) =$$

$$\frac{p_j(1-p_{3-j})(1-p_j^*)(p_j^*)^m}{p_j^* - p_1 p_2} - (p_1 p_2)^m$$

$$\left[\frac{p_j(1-p_{3-j})(1-p_j^*) - (p_j^* - p_1 p_2)(1-p_j)}{p_j^* - p_1 p_2} \right] \quad (27)$$

$m = 0,1,2,\ldots$

They obtained a characterization result for the BGD given at (26) through bivariate mean residual functions defined as follows:

Definition 9 : For two r.v.s X_1 and X_2 the bivariate mean residual life is the vector $(\theta\,(t), \theta_1(n \mid m), \theta_2(m \mid n))$ where

$$\theta\,(t) = E[\min(X_1, X_2) - t \mid X_1 \ge t, X_2 \ge t]$$

$$\theta_1(n \mid m) = E[X_1 - n \mid X_1 \ge m, X_2 = n] \text{ for } m > n$$

$$\theta_2(m \mid n) = E[X_2 - m \mid X_1 = m, X_2 \ge n] \text{ for } n > m.$$

Since failure rate and mean residual life times are related it is natural to expect that $\theta\,(t)$, $\theta_1(n \mid m)$ and $\theta_2(m \mid n)$ are related to $r(t)$, $r_1(m \mid n)$ and $r_2(n \mid m)$ defined by Sun and Basu[17]. Asha and Sankaran established the relationship. Further, they proved the following characterization result concerning the BGD given at (26).

Theorem 16. Let (X_1, X_2) be a random vector with marginals given at (27). If $P[X_1 > X_2 \mid \min(X_1, X_2) = z]$ and $P[X_1 < X_2 \mid \min(X_1, X_2) = z]$ are constants, then the bivariate mean residual life $(\theta(t), \theta_1(n \mid m), \theta_2(m \mid n))$ is a constant vector if and only if (X_1, X_2) has the BGD given at (26).

Concluding Remarks

There are several more characterizing properties of univariate geometric distribution. It will be interesting to formulate their analogues in two dimensions and examine whether they lead to any of the bivariate geometric distributions considered here or lead to some new distributions which may have a useful role in stochastic modelling.

References

1. Galambos, J. & Kotz, S.(1978) *Characterizations of Probability Distributions*, Springer Verlag, Berlin.

2. Downton, F.(1970) *J.R. Statist .Soc. B* 32 : 408.

3. Hawkes, A.G.(1972) *J.R. Statist. Soc. B* 34 :129.

4. Paulson, A.S. & Uppuluri, Y.R.R. (1972) *Sankhya Ser. A.* 34 : 297.

5. Esary, J.D. & Marshall, A.W.(1973). *Multivariate geometric distributions generated by a cumulative damage process* , Naval Postgraduate School Report NP555 E Y 73041A, Monterey, California.

6. Arnold, B.C.(1975) *Sankhya Ser.A.* 37 : 164.

7. Block, H.W., Langberg, N.A. & Stoffer, D.S.(1988) *Adv. Appl. Probab* 20 : 798.

8. Phatak, A.G. & Sreehari, M.(1981) *J. Ind. Statist. Assn.* 19 : 141.

9. Nair, K.R.M. & Nair, N.U.(1988) *J. Ind. Statist. Assn.* 26:45.

10. Nair, N.U. & Asha, G.(1997) *J.Mult. Anal.*62:181.

11. Asha, G. & Sankaran, P.G.(2002) *J.Ind. Statist. Assn.* 40 : 1.

12. Sreehari, M. (1981). *J .M.S. University of Baroda(Science, Tech. & Medicine)* 30 : 7.

13. Srivastava, R.C. & Bagchi, K.S.N. (1985) *J. Ind .Statist. Assn* 23 : 27.

14. Marshall, A.W. & Olkin, I.(1985) *J. Amer. Statist. Assn.* 80 : 332.

15. Asha, G. & Nair, N.U. (1998) *Quality Improvement through Statistical Methods.* Ed.by B.Abraham, Brikhauser Publications p.339.

16. Nair, N.U. & Asha, G. (1994) *J. Ind. Statist. Assn.* 32 : 111.

17. Sun, K. & Basu, A.P. (1995) *Statist & Probab. Letters,* 23 : 307.

18. Block, H.W. & Paulson, A.S.(1984). *Sankhya, Ser.A* 46:102.

19. Marshall, A.W. & Olkin, I.(1997) *Biometrika* 84 : 641.

20. Nair, N.U. & Nair, K.R.M. (1990) *Statistica* 50 : 247.

21. Wu, C. (1997) *Statist. & Probab. Letters* 34 : 171.

22. Abraham, B. & Balakrishnan N.(2000). *J. Appl. Probab.* 37 : 696.

23. Nagaraja, H.N. (1983) *J. Ind. Statist. Assn.* 21 : 27.

24. Zijlstra, M. (1983) *J. Appl. Probab.* 20 : 843.

25. Puri, P.S.(1973). *Sankhya Ser. A.* 35 : 61.

Supercapacitor : An emerging power source

S. A. Hashmi

Department of Physics, North Eastern Regional Institute of Science & Technology, Nirjuli (Itanagar) – 791 109, Arunachal Pradesh

E-mail : sah@nerist.ernet.in

Abstract

Fundamentals and recent advances in electro-chemical Supercapacitors, which are recently emerged as an alternative power sources, have been discussed. A general discussion on different types of Supercapacitors namely: electrical double layer capacitors (EDLCs) and electrochemical redox Supercapacitors has been presented in view of their configuration, materials and charge storage mechanisms. Particular attention and emphasis are given to the conducting polymers based redox capacitors and their different types (I, II and III) of the configuration according to three different possible combinations of p- and n-doped conducting polymers. Recent investigations in our laboratory on the development of different Supercapacitors have been briefly given. Various possible applications of Supercapacitors as a power source have also been briefly described.

(Keywords : Supercapacitor/ Polymer Electrolytes/ Gel electrolytes/conducting polymers.

Introduction

Capacitors are important electrical storage devices, which are useful electronic components in high frequency circuit applications such as electronic commu-nication, telephone exchanger etc. and medium frequency circuits like power filters, etc. In general, the existing capacitors can be grouped into three categories: (a) conventional capacitors (ceramic, paper, thin film), (b) electrolytic capacitors, and (c) electrochemical capa-citors. The configuration of the conven-tional capacitors are simple in which a mica /paper/ ceramic film is sandwiched between two metallic electrodes. The configurations of other two types of capacitors are described as follows. The characteristics and possible applications of different types of conventional and electrolytic capacitors are summarised in Table 1.

There exist two types of electrolytic capacitors, which are commonly available in market namely:

(i) Aluminium electrolytic capacitors, and

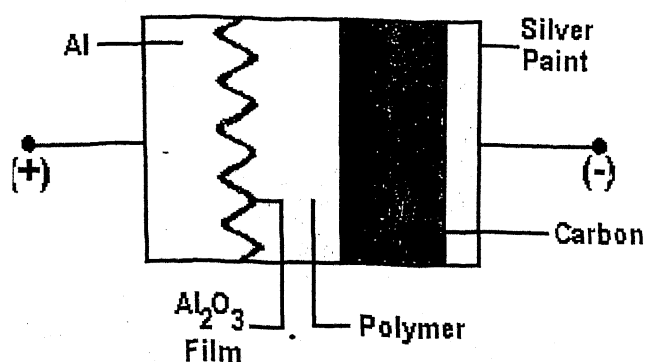(ii) Tantalum electrolytic capacitors

These capacitors use liquid as well as solid electrolytes. Due to various advantages of solid electrolytes over the liquid electrolytes such as no leakage, improvement in temperature and frequency response, heat resistance and possibility of sleek design for miniaturisation, the solid electrolytes based electrolytic capacitors are more popular. The sketch diagrams of tantalum and aluminium solid electrolyte capacitors are shown in Fig.1.

Table 1– Specification and possible applications of conventional and electrolytic capacitors

Capacitor types	Specification	Application
Paper	~ 400 V, <0.1 μF	High frequency electronic circuits
Mica	~ 100 V, <1 μF	High frequency electronic circuits
Ceramic	~ 50 V, <0.1 μF	High frequency electronic circuits
Thin film	~ 50 V, <0.01 μF	High frequency electronic circuits
Aluminum Electrolytic (Liquid)	~ 50 V, >1 μF	Medium frequency electronic circuits, Power supply filters, etc.
Tantalum Electrolytic (Liquid)	~ 50 V, >1 μF	Medium frequency electronic circuits, Power supply filters, etc.
Aluminum Electrolytic (Solid)	~ 25 V, >1 μF	Medium frequency electronic circuits, Power supply filters, etc.
Tantalum Electrolytic (Liquid)	~ 25 V, >10 μF	Medium frequency electronic circuits, Power supply filters, etc.
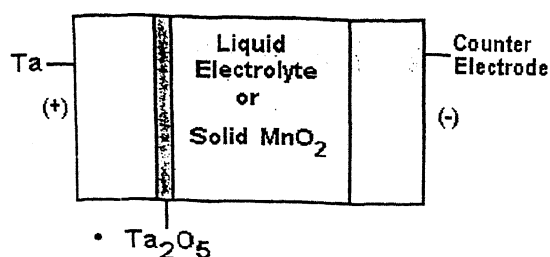
(A) Tantalum Electrolytic Capacitor

(B) Aluminium Electrolyte Capacitor

Fig. 1– The configuration of tantalum and aluminium electrolytic capacitors.

Electrochemical Supercapacitors :

Over the past one decade, a great interest in 'Supercapacitors', commonly referred as 'Electrochemical Capacitors' has been stimulated worldwide due to the growing demand for power sources of transient high power density.[1] These are potential devices to work as an alternative power source for low energy density applications e.g. electronic and medical equipment, whereas due to their high rate capability, they are also considered to be excellent candidates for use in high power applications particularly for load levelling in electrical vehicles. Electrochemical Capacitors, are unique energy storage devices which have the following specific characteristics:
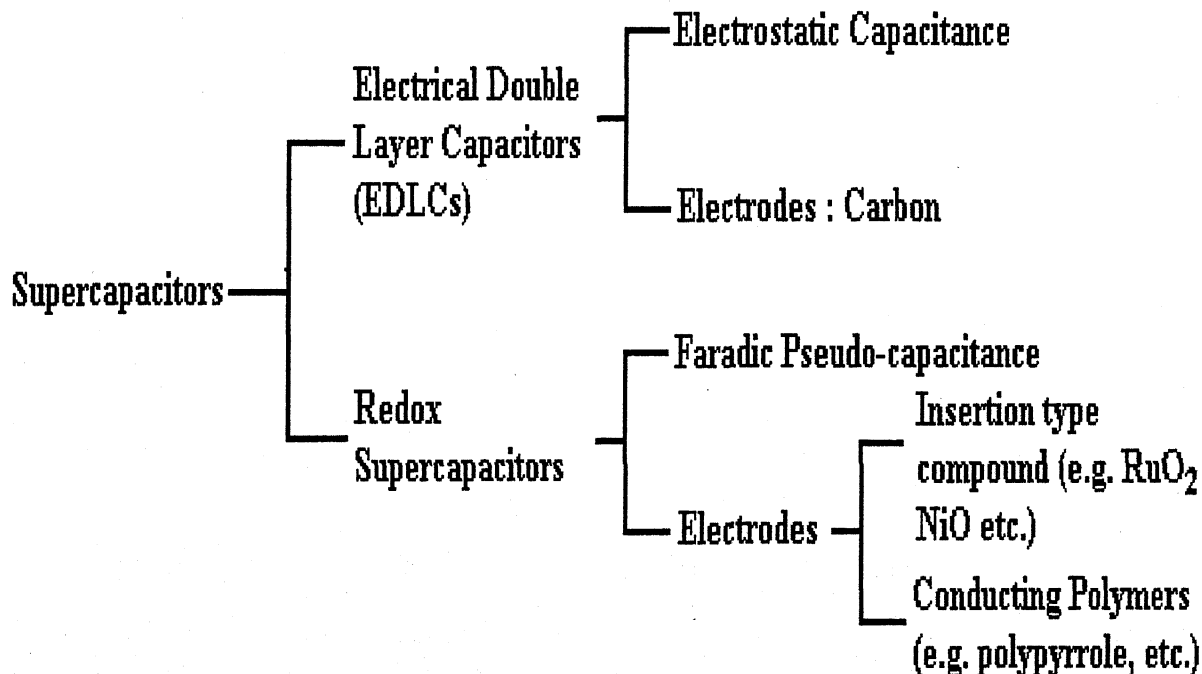
• Large value of capacitance (~20-2000 times per gram or per cm^2 of electroactive materials).

• High power storage/delivering ability.

Historically, Helmoltz in 1879 first considered the storage of charge at electrode-electrolyte interface and regarded the double layer as equivalent to a parallel plate capacitor. The formation of Helmoltz double layer, which acts as a parallel plate capacitor is shown schematically in Fig. 2. Typical values are in the range of 20-40 μF cm^{-2} for electrode-liquid electrolyte interfaces. Rayleigh (1966) reported a substantially higher capacitance of 200 μF cm^{-2} for the interface of platinum and AgBr. This higher value was explained in terms of the adsorption of a layer of ions on the electrode surface. In 1980, NEC Corporation (Japan) reported and commercialised the Electrical Double Layer Supercapacitors, giving hundreds of mF cm^{-2} specific capacitance, composed of large surface area activated carbon electrodes and sulfuric acid electrolyte with a brand name 'SUPERCAPs.' Thereafter the Supercapacitors of various types employing different electrodes and electrolytes have been reported in literature. For details, readers are referred to the reviews / books.[1-5]

The configuration of Supercapacitors is almost similar to that of batteries, the difference being that the former consists of electrolytes sandwiched between two blocking / active electrodes with translation of charge only, whereas a battery employs asymmetrical different electrode materials (anode and cathode) involved in interfacial reactions leading to an overall electro-chemical process for the cell.

In recent developments, two types of electrochemical capacitors have been investigated which are based on two fundamental charge storage mechanisms. These are classified as follows:
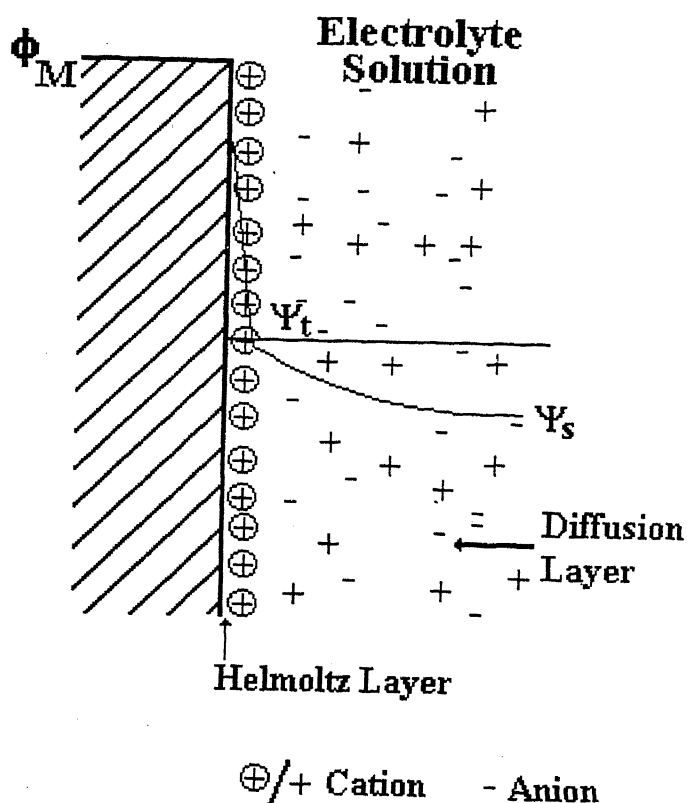
Supercapacitors
- Electrical Double Layer Capacitors (EDLCs)
  - Electrostatic Capacitance
  - Electrodes : Carbon
- Redox Supercapacitors
  - Faradic Pseudo-capacitance
  - Electrodes
    - Insertion type compound (e.g. RuO_2 NiO etc.)
    - Conducting Polymers (e.g. polypyrrole, etc.)

Fig. 2– General representation of Helmoltz double layer and its potential profile.

Electrical Double Layer Capacitors (EDLCs) :

The capacitors, which employ the carbon or other similar materials as blocking electrodes are referred as "electrical double layer capacitors (EDLCs)." Electrodes, which do not participate in any electrochemical reaction including charge transfer at the electrode-electrolyte interface (within the voltage limit of electrochemical stability range of electrolyte), are able to accumulate (store) charges under the application of electric potential. These electrodes are regarded as polarisable or blocking. In general, large surface area carbon electrodes are being used in EDLCs. Several electric double

layer capacitors using large surface area electrodes with different types of carbons have been developed with liquid and polymer / gel electrolytes.[6-11] In particular, activated carbon powders / fibres / fabrics, which can be produced with large surface area up to 2000-2500 m^2 g^{-1}, have attracted much attention for the fabrication of double layer capacitors due to their corresponding very high capacitance values of 400-500 Fg^{-1}. The charge storage mechanism in EDLCs is electrostatic resulting from the separation of charged species at the interfacial double layers. The charge storage mechanism and the operational principle of EDLCs are shown schematically in Fig. 3.

The capacitance, C and the charge, Q, accumulated in the electrical double layer formed at the interface between the blocking (polarisable) electrodes and electrolyte is expressed as [4] :

$$\text{Capacitance } C = \left[\int \varepsilon / 4\pi\sigma\right] dS \qquad (1)$$

Accumulated charge

$$Q = \left[\int \varepsilon / (4\pi\sigma) dS\right] (2\psi_1) \qquad (2)$$

where ε is dielectric constant of the electrolyte, σ is distance from the electrode interface to the centre of ions and S is electrode surface area.

Redox Supercapacitors

Capacitors, which employ the electroactive materials such as insertion type compounds (noble metal oxides e.g. RuO_2, NiO etc.)[12-14] or conducting polymers (e.g. polypyrrole, polythiophene etc.)[15-25] as
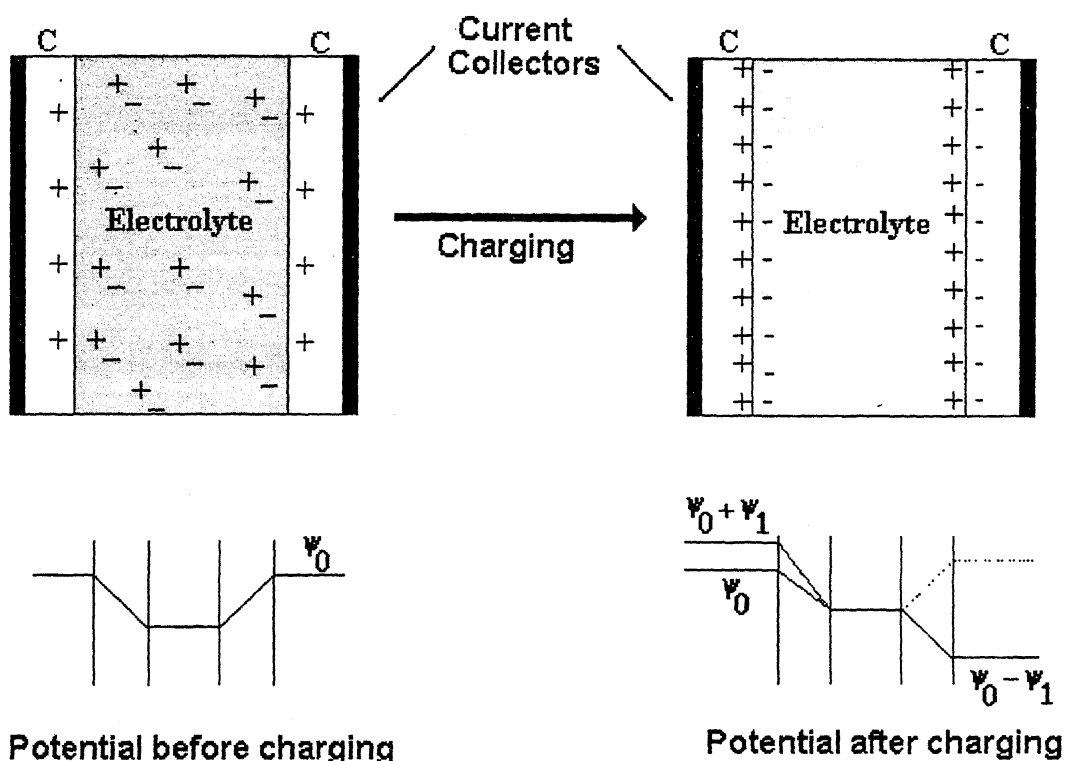
Fig. 3– Schematic structure of electrical double layer capacitor and its potential profile.

active electrodes are referred as 'redox supercapacitors.' In redox supercapacitors a fast faradic charge transfer process takes place which gives rise to a 'pseudoca-pacitance.' Recently a new class of supra-molecular materials (e.g. 1,5 Diamino-anthraquinone oligomer, etc.) have been introduced as promising electrodes for redox supercapacitors, which exhibit high specific capacity with aquous and non-aquous liquid electrolytes. [26, 27]

Particularly, conducting polymers have been shown to be potential electrode materials for redox supercapacitors because they offer several advantageous properties over the other noble metal oxide/carbon electrode materials. These include their low cost, easy chemical or electrochemical preparation in desired extended area thin films and large capability of charge storage

(~ 500 Cg^{-1}) throughout their volume. Particularly for electrochemical capacitors, the ability to charge (or discharge) through the whole volume is most attractive aspect of conducting polymers compared to the large area carbon materials. It is well known that conducting polymers exist in p-doped (oxidised) and n-doped (reduced) states. In view of this fact, Rudge et al [15] proposed three schemes of configuration of conducting polymers based redox capacitors, classified namely as types I, II and III. Two identical p-dopable polymers are employed as active electrodes in type I capacitors, whereas type II capacitors are comprised of two different p-dopable conducting polymers sandwiching the electrolyte materials. In type III capacitors, a configuration of n- and p- doped forms of the same polymers can be used. The

classification of different types of redox capacitors under these three categories is based on the difference in potential range in **which the** conducting polymers become doped or dedoped, resulting in an increase of voltage of the charged capacitors. The type I capacitors are typically limited to ~ 1 volt whereas the type III can be charged to ~ 3 V.

Electrolytes

In most of the studies on the double layer or redox supercapacitors, liquid electrolytes have been used as separators. These include acetonitrile (ACN)-$(CH_3)_4NBF_4$, ACN-$(C_2H_5)_4NBF_4$, ACN-$(C_4H_7)_4NPF_6$, ACN-$LiClO_4$, propylene carbonate PC-$LiClO_4$, PC-$(C_2H_5)_4NBF_4$ etc. Liquid electrolytes based supercapacitors are similar to liquid electrolytes based batteries in that they are associated with the well known disadvantages of corrosion, self discharge, low energy density and bulky design. A limited number of solid-state capacitors have been studied with polymer / gel electrolytes e.g. poly (ethylene oxide) (PEO)-PC-$(C_2H_5)_4NBF_4$, Poly (ethylene glycol) (PEG)- $(C_2H_5)_4NBF_4$, poly (methyl methacrylate) (PMMA)-PC-ethylene carbonate (EC)-$LiClO_4$, polyvinyl alcohol (PVA)-H_3PO_4, PEO – PEG – $LiCF_3SO_3$ etc. All solid-state supercapacitors are in the early stage of development and require improvements in their capacitance values, reduction of internal resistance and enhancement in the electrochemical stability range of potential. Solid electrolytes (polymer / gel electrolytes) as separators possess some limitations in terms of lower conductivity, which leads to the higher internal resistance and hence lower power density. The electrochemical potential ranges of solid electrolytes are also

relatively lower as compared to particularly organic liquid electrolytes, which results the lower energy density of the capacitors. Some important examples of electrical double layer and redox supercapacitors which employ different liquid / polymer / gel electrolytes are listed in Table 2.

Physical Techniques for Supercapacitor's Characterisation

Most of the experimental techniques, which are commonly employed for the charcterisation of electrochemical cells (including batteries, sensors, electrochromic devices, etc.) are equally suitable for the supercapacitors. These include a. c. impedance spectroscopy, linear sweep voltammetry, charge-discharge methods, self discharge, prolonged cyclic tests etc. The performance parameters associated with the supercapacitors can generally be obtained by discharging a fully charged device through a load resistance. The parameters along with their expressions and units are listed as in Table 3.

A. C. Impedance Spectroscopy

An electrochemical capacitor cell, as described previously, is generally fabricated from two identical electrode systems with a liquid or a solid electrolyte separating them. Impedance spectroscopy is an attractive method for characterising the electrochemical behaviour of such cells because of the direct connection between the real system and its idealised equivalent circuit consisting of discrete electrical components (R, C and L) in their series and parallel combinations. As described earlier, the real systems in the present context are electrochemical capacitor cell which

employ either blocking / polarisable electrodes (called double layer capacitors) or electroactive electrode materials (called redox supercapacitors). The blocking electrodes used in the capacitors have either planar geometry (e.g. high density graphite sheets, glassy carbon sheets, etc.) or large surface area porous electrodes (activated carbon powder/ fabrics/ fibre etc.).

Table 2– Characteristics of some important EDLCs and redox supercapacitors

Capacitor Cells	Capacitance (C)		Energy Density (Wh Kg^{-1})	Power Density (kW Kg^{-1})	Ref.
	(Fg^{-1})	(mF cm^{-2})			
Electrical Double Layer Capacitors					
ACF | Nylon 6-10 + 2 H$_3$PO$_4$ | ACF	70	-	1.4	-	7
Ni-ACF | PC-LiClO$_4$ | Ni-ACF	95	-	-	-	8
ACF | PMMA-PEO-(C$_2$H$_5$)$_4$NBF$_4$ – PC | ACF	20	570	16.2	-	6a
ACF | PAN - (C$_2$H$_5$)$_4$NBF$_4$ – PC | ACF	16	370	-	-	6b
ACF | PEO+PEG+LiCF$_3$SO$_3$ | ACF	4	20	-	-	10
ACF | PVA + H$_3$PO$_4$ | ACF	70-90	360-470	14-18	-	10
AC | PVdF-HFP-EC-PC-(C$_2$H$_5$)$_4$NBF$_4$ |AC	123	-	-	-	9
HD-ACF | Aqueous KCl | HD-ACF	28	-	-	-	11
Redox Supercapacitors					
RuO$_2$.xH$_2$O |H$_2$SO$_4$ (aq.) | RuO$_2$.xH$_2$O	720	-	26.7		12
Ni-NiO | 1M KOH (aq.)| Ni-NiO	50-64	-	7.2-11.0	4.0-17.0	13
PPy | PMMA-EC-PC-LiClO$_4$ | PANI	13	-	4.0	0.7	21
PPy | PVA + H$_3$PO$_4$ | PPy	39-84	1.5-5.0	12.0	-	23
PMeT | PEO-PEG-LiCF$_3$SO$_3$ | PPy	25-30	3.0-3.5	10.0-12.0	-	22
pDTT | PEO-PC-(C$_2$H$_5$)$_4$NBF$_4$ | pDTT	25-35	5.0-7.0	3.0-7.0	0.2	19
PEDOT | ACN-LiClO$_4$ | PEDOT	-	-	1.0-4.0	2.5	20
PPy / graphite | KCl (aq.) | PPy/ graphite	400	-	-	-	28
Li-PANI | ACN-(C$_2$H$_5$)$_4$NBF$_4$ | Li-PANI	60-100	-	-	-	29
pDAAQ | PC-(C$_2$H$_5$)$_4$NClO$_4$ | pDAAQ	-	-	25.0-46.0	10.2-30.5	26
pDAAQ| PMMA-EC-PC-(C$_2$H$_5$)$_4$NClO$_4$| pDAAQ	3.7-5.4	125-184	92-135	-	30

ACF : Activated Carbon Fabrics, Ni-ACF : Nickel loaded ACF, HD-ACF : High Density ACF, AC : Activated Carbon Powder, PPy : Polypyrrole, PANI : Polyaniline, Li-PANI : Lithium doped PANI, PMeT : Poly (3-methyl thiophene), pDTT : Poly (thieno [3,4-b : 3',4'-d] thiophene, PEDOT : Poly (3,4 ethylene -dioxythiophene), pDAAQ : poly (1,5-diaminoanthraquinone).

Table 3– Performance parameters of Supercapacitors.

Parameters	Expression	Unit
Capacitance	$C = q/V$	Farad 'F'
Specific Capacitance	$C' = C/M$	Fg^{-1}
	$C'' = C/A$	$F\ cm^{-2}$
Stored Charge	$q = \int \left(\dfrac{V}{R_L}\right) dt$	Coulomb
Energy Density	$E = \dfrac{1}{M} \int \left(\dfrac{V^2}{R_L}\right) dt$ $= \dfrac{1}{2M} CV^2$	$J\ g^{-1}$ or $Wh\ Kg^{-1}$
Power Density	$P = \dfrac{V^2}{MR_L}$	$J\ g^{-1}\ s^{-1}$ or $W\ Kg^{-1}$

A schematic representation of the impedance behaviour of an ideal capacitor cell is illustrated in Fig. 4(a). The impedance pattern shows a steep rising dispersion line overlapping with imaginary axis of the impedance plot. The impedance pattern of a real capacitor (Fig.4 b) shows a perfect semicircle representing a parallel combination of a bulk resistance R_b (resistive component owing to the ion migration owing to the bulk of electrolytes) and geometrical capacitance C_g (due to dielectric polarisation of electrolyte under the influence of an electric field). The interfacial polarisation leads to the formation of double layer capacitor at the two identical interfaces, which is represented by a steeply rising spike in the low frequency region of the impedance spectra (Fig. 4 b).

The equivalent circuit of capacitor cells with either rough or porous electrode in contact with the electrolytes can be represented in the form of a transmission line type distributed circuit which gives variable time constant. Conducting polymer electrodes (e.g. polypyrrole, polytiophene and its derivatives etc.) also show a similar pattern of impedance behaviour as the porous electrodes. The region of the impedance spectrum associated with high capacitance at low frequencies is often interpreted in terms of a distributed R and C network due to ionic penetration throughout the polymer films or the porous electrodes.

The overall capacitance of the cell can be evaluated from the relationship :

$$C = \frac{1}{\omega Z''} \tag{3}$$

where Z'' is the imaginary part of the total impedance measured in low frequency range (100 mHz-1 mHz).
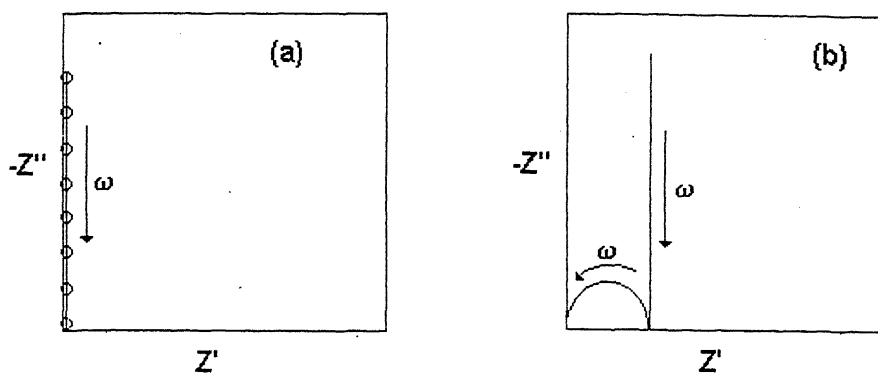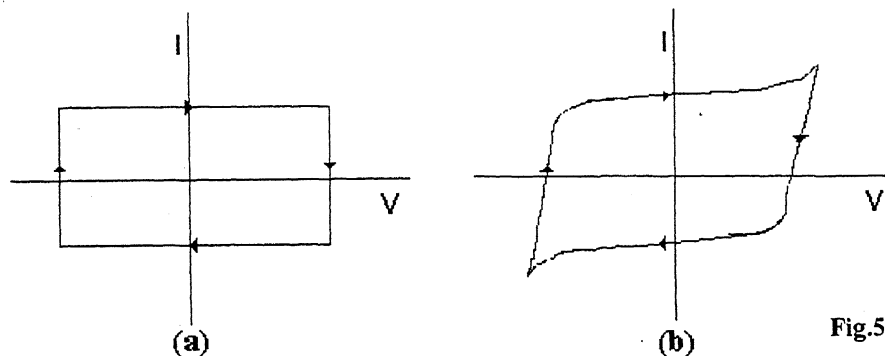
34

Fig.4.

Fig.5.

Fig. 4– Schematic representation of complex impedance plots for (a) ideal capacitor and (b) real capacitor.

Fig. 5– Schematic representation of linear sweep voltammograms for (a) ideal capacitor and (b) real capacitor.

Linear Sweep Voltammetry

The linear sweep voltammetry is another important experimental probe to characterise the capacitors. The cyclic voltammogram of an ideal capacitor (having negligible internal resistance) shows a perfect rectangular shape (Fig. 5a) and it is scan rate dependent. The deviation from the rectangular shape is observed (Fig. 5b) for real capacitors which is represented as a series combination of internal resistance R and ideal capacitance C. The value of capacitance can be evaluated from the expression :

$$C = \frac{i}{s} \qquad (4)$$

where 'i' is the voltammetric current and 's' is scan rate.

Charge-Discharge Methods

Information about an electrochemical system is generally gained by applying an electrical perturbation to the system and by observing the resulting changes in the characteristic behaviour of the system. In impedance spectroscopic measurements an a.c. perturbation is applied, whereas a voltage ramp is applied in the case of linear sweep voltammetry. These methods have already been described earlier. In the charge-discharge technique for characterisation of a capacitor, it is necessary to consider the behaviour of a real capacitor system represented by an ideal capacitor C_e connected with the

internal resistance R_i in series. The perturbation can be either by potential step (called the potentiostatic method) or by current step (called the galvanostatic method).

(a) Potentiostatic method (Voltage step)

When a potential step is applied across the capacitor cell, the capacitor charges and an exponentially decaying current is obtained. The behaviour of the current 'i' with respect to time, on application of the potential step V_0, can be expressed as :

$$i = \frac{V_0}{R} \exp\left(-\frac{t}{\tau}\right) \tag{5}$$

where 'τ ($=RC$)' is the time constant. The capacitor cells start discharging when the operation is reversed and the pattern of discharge curve is similar to the charging curve but with the reverse polarity of the current.

The charge-discharge curves can be integrated numerically to obtain the total charge stored or released from the cell. The capacitance 'C' can be evaluated by dividing the total charge by the applied voltage V_0 i.e.

$$C = \frac{\int i.dt}{V_0} \tag{6}$$

(b) *Galvanostatic method (Current step)*

When a capacitor cell is charged by a constant current 'i', the total voltage 'V' developed across the cell can be expressed as :

$$V = iR_i + \frac{\int i.dt}{C} \tag{7}$$

As the current is constant :

$$V = i\left(R_i + \frac{t}{C_e}\right) \tag{8}$$

Thus, for a current step, the voltage across an ideal capacitor cell, whose capacitance value, C_e, is expected to be constant, increases linearly with time. A schematic V-t curve showing the linear variation is shown in Fig. 6(a). After the full charging of the capacitor at the maximum permissible or desired voltage level, it can be discharged galvanostatically. The voltage decrease across the cell is also linear with respect to time (Fig. 6a). In the real capacitors, The initial sharp jump in voltage while charging or discharging of the capacitor is observed (Fig. 6b), which is owing to an ohmic (iR) loss due to internal resistance of the cell.
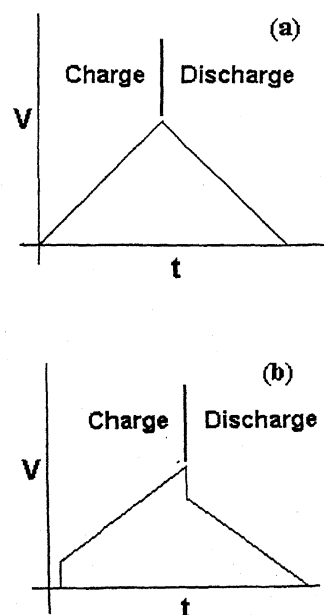

Fig. 6– Schematic representation of galvanostatic charge-discharge curves for (a) ideal capacitor and (b) real capacitor.

The capacitance of the cell can be evaluated from the linear region of the curve following the relation :

$$C_e = i \frac{\Delta t}{\Delta V} \qquad (9)$$

where ΔV is the change in voltage for Δt interval of time. The charge-discharge experiment can be carried out for several cycles (10^3 to 10^5 cycles) to test the cyclic efficiency of the cell. It may be noted that the cyclic efficiency of supercapacitors is 100-1000 times larger than that of the rechargeable (e.g. Ni-Cd, Ni-metal hydride etc.) batteries. This aspect makes the supercapacitors more attractive as power source over the rechargeable batteries.

The coulombic efficiency can also be calculated easily from the results of galvanostatic charge-discharge experiment. When constant current is used in charging and discharging the coulombic efficiency 'η' can be described by :

$$\eta = \frac{\Delta t_D}{\Delta t_C} x100\% \qquad (10)$$

where Δt_C and Δt_D are time intervals for charging and discharging, respectively.

Some Experimental Studies

Some important results recently obtained in our laboratory on different types of double layer and redox supercapacitors have been discussed. Particular emphasis on all solid state supercapacitors based on polymer / gel electrolytes have been given.

Polymer / Gel Electrolytes

Various polymer / gel electrolytes have been synthesised and used to fabricate different types of solid-state supercapacitors. These include polymer electrolytes, PVA-H$_3$PO$_4$ aqueous blend, PEO$_{15}$.NaClO$_4$ + PEG and polymeric gel electrolytes, PMMA-EC-PC-NaClO$_4$ and Polyvinylidene fluoride-co-hexafluoropropylene (PVdF-HFP)-EC-PC-alkyl ammonium salts. Films (~200-300 μm thick) of the polymer/gel electrolytes were prepared using standard 'Solution Cast' technique. Details of the preparation methods of these films have been described by us elsewhere.[24, 25]

Fig. 7 shows the typical electrical conductivity profile of polymer and gel electrolytes with respect to temperature for the temperature range 0^{0}C to 150^{0}C. The polymer electrolytes based on PVA and PEO are generally obtained in the form of free standing thin films. The polymeric gel electrolytes based on PMMA and PVdF-HFP, used in the present work, have also been observed in the form of free standing mechanically stable thin films. The electrolytes show the conductivity of the order of 10^{-4}-10^{-3} S cm^{-1} at room temperature (25^{0}C). This order of conductivity of the polymer/gel electrolytes is acceptable because it offers low resistance (say 100 ohm cm^2) when the electrolytes are used in the form of thin film of smaller thickness (say ~200 μm).

The electrochemical potential window i.e. the working voltage range, which is the measure of electrochemical stability of the electrolytes, is another important parameter to be evaluated, which limits the working voltage of the capacitors. The electrochemical potential window of the aqueous based polymer electrolytes like

PVA-H_3PO_4 blend is limited to 1.2 V, whereas the PEO, PMMA and PVdF based organic polymer / gel electrolytes, used in the present studies, offer the potential range more than 2.5 V.
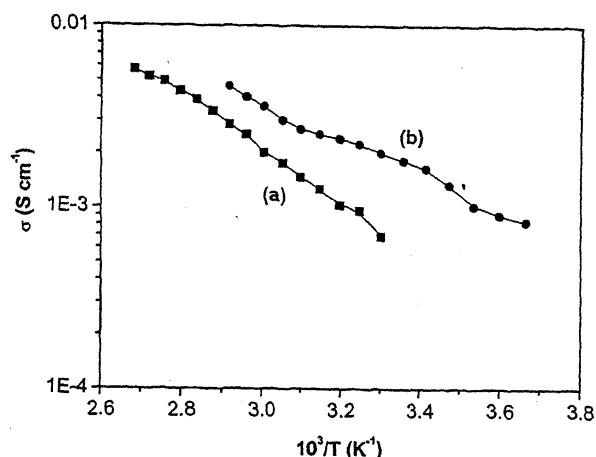

Fig. 7– Temperature dependence of the electrical conductivity of (a) PEO_{15}. $NaClO_4$ + 50 wt% PEG polymer electrolyte and (b) PMMA-EC/PC-$NaClO_4$ gel electrolyte.

All-Solid-State Electrical Double Layer Supercapacitors

The electrical double layer capacitors have been constructed from large area activated carbon fabric (ACF, large surface area ~ 2500 m^2 g^{-1}, Spectracorp, USA) electrodes with the polymeric gel electrolytes. The gel electrolytes were based on (PVdF-HFP)-EC–PC–tetraethyl ammonium tetra fluoroborate ($TEABF_4$). Following three different model capacitor cells have been constructed using ACF electrodes and gel electrolytes of different compositions :

Cell A :   ACF | PVdF-HFP (30 wt %) – EC:PC (1:1 V/V)-1.0 M $TEABF_4$ | ACF

Cell B :   ACF | PVdF-HFP (25 wt %) – EC:PC (1:1 V/V)-1.0 M $TEABF_4$ | ACF

Cell C :   ACF | PVdF-HFP (20 wt %) – EC:PC (1:1 V/V)-1.0 M $TEABF_4$ | ACF

The performance characteristics of the capacitors have been characterised using a.c. impedance spectroscopy, linear sweep voltammetry and prolonged cyclic tests.

Impedance Studies

Fig. 8 shows a typical complex-impedance spectrum of a capacitor cell C. As discussed earlier that the behaviour of an ideal capacitor is shown as a straight line parallel to the imaginary axis of the impedance plots. The impedance response of all the cells, in the present studies, shows a small semicircular spur in the high frequency region followed by steep rising portion in the lower frequency region up to 10 mHz. This steep rising behaviour indicates the capacitive character of the cells at lower frequency range, whereas the high frequency semicircle shows the bulk properties of the electrolytes and interfacial charge transfer processes. Various electrical parameters i.e. charge transfer resistance R_{ct}, the total resistance R and capacitance values (evaluated using eqn. 3) at frequencies 100 mHz and 10 mHz for all the cells A-C are listed in Table 4. A comparison indicates that ACF shows a highest capacitance value of ~28.0 mF cm^{-2} (equivalent to single electrode specific capacitance ~ 4 Fg^{-1}) at 10 mHz with the PVdF-HFP (20 wt. %) – EC:PC (1:1 V/V)-1.0 M $TEABF_4$ gel electrolytes. The gel electrolyte containing 20 wt.% of PVdF-HFP also offers the least value of charge-transfer resistance R_{ct} of about 5.0 ohm cm^2. The high value of C and low value of R_{ct} is the combined effect of large surface

Table 4– Electrical parameters of different EDLCs evaluated from impedance analysis.

Capacitor Cells	R_{ct} (ohm cm^2)	100mHz			10mHz		
		R (ohm cm^2)	C (mF cm^{-2})*	(F g^{-1})**	R (ohm cm^2)	C (mF cm^{-2})*	(F g^{-1})**
A	88	455	2.3	0.34	1800	4.4	0.7
B	15	170	5.0	0.74	1170	7.5	1.1
C	5	61	16.4	2.4	325	28.0	4.1

* Overall capacitance of the cells

** Single Electrode Capacitance

area (~ 2500 m^2 g^{-1}) of ACF electrode and highly conducting and mechanically flexible gel electrolytes. The capacitance value based on 2000 m^2 g^{-1} of ACF and sulphuric acid liquid electrolyte has been reported in literature to be a larger value of 100 Fg^{-1}.[31] The lower value observed in the present studies of all-solid state capacitor is possibly due to inaccessibility of all of the surface area of ACF to form capacitive interface with the solid-like gel electrolytes.

Linear Sweep Voltammetry

A typical linear sweep voltammograms of the capacitor cell C at different scan rates between –800 mV and 800 mV is shown in Fig. 9. At lower scan rates (say 10-20 mV sec^{-1}), the votammograms of all the cells A-C show an almost featureless square shape, which is the basic characteristic of a capacitor. The deviation from the shape at higher scan rates is owing to the equivalent series resistance (ESR), which is practically present in series in the real capacitors. Further, the response of each capacitors cells have been found to be scan rate dependent, which is also expected for a capacitor cell.[24]
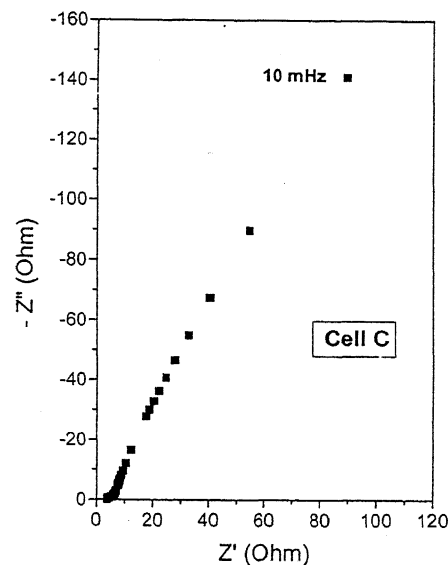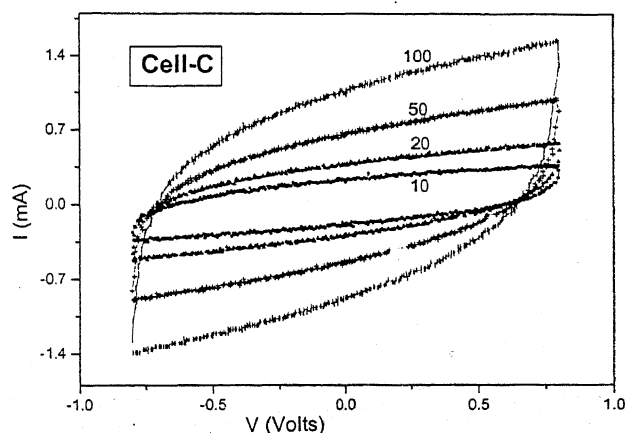

Fig. 8– The typical complex-impedance plot of the capacitors cell C: ACF | PVdF-HFP (20 wt

Fig. 9– Cyclic voltammogram of the capacitor cell C at different scan rates. The scan rates (in mV sec^{-1}) are marked on the figures.

The values of capacitance have been calculated using the eqn. 4 and found to be in almost good agreement with the values obtained from impedance analysis, described above. The cyclic behaviour i.e. the stability of the supercapacitors for large number of charge-discharge cycles has also been evaluated. Fig. 10 shows the variation of capacitance of the typical capacitor cell C as a function of voltammetric cycles between –800 mV and 800 mV at scan rate 100 mV sec⁻¹. After a slight decrease for initial few cycles, the values of capacitance become almost constant up to 1000 cycles even more. The initial decrease in capacitance is possibly attributed to the charge consumption in some possible irreversible faradic reaction(s) associated with loosely bound surface groups at the electrode-electrolyte interfaces.
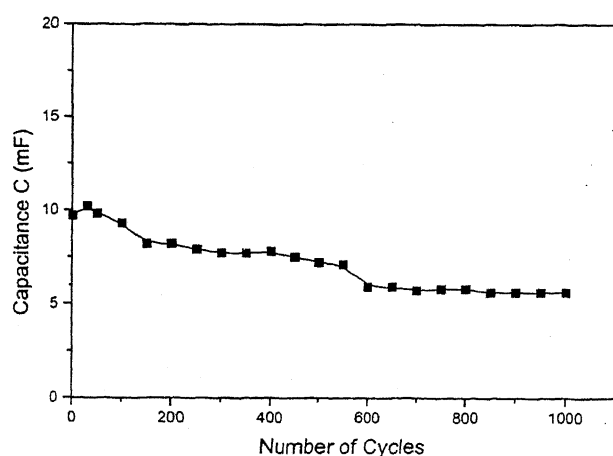

Fig. 10– Capacitance of the capacitor cell C : ACF | PVdF-HFP (20 wt %) – EC:PC (1:1 V/V)-1.0 M TEABF₄ | ACF as a function of voltammetric cycles at the scan rate 100 mV sec⁻¹ (Cell area : 2.0 x 1.8 cm²).

Polypyrrole and poly(3-methyl thiophene) based solid-state redox supercapacitors

Polypyrrole (pPy) and poly (3-methyl thiophene) (pMeT) based type I and type-II solid state redox supercapacitors have been constructed by us using polymeric electrolytes, PVA-H₃PO₄ blend and PEO-NaClO₄ complex plasticised with PEG and gel electrolyte, PMMA-EC-PC-NaClO₄. A comparative study on the capacitors with symmetical type-I and asymmetrical type-II cell configurations have been carried out. Results based on galvanostatic charge-discharge method have been discussed.

The polypyrrole and poly (3-methyl thiophene) were electrochemically deposited on indium tin oxide (ITO, Balzers, sheet resistance ~80 ohm cm²) coated glass substrates in a one compartment three electrode cell, following the procedure described by us elsewhere.[24] Different model capacitor cells have been constructed using p-doped polypyrrole and poly (3-methyl thiophene) with different polymer / gel electrolytes. Their configurations are reported in Table 5.

Charge-Discharge studies

The galvanostatic charge-discharge experiments have been carried out for all the capacitor cells. The typical charge-discharge characteristics of the PMMA-gel electrolyte based capacitor cells are illustrated in Fig. 11 (a-d). The discharge capacitance values were calculated from the linear portion of the discharge characteristics of different cells [Fig11 (a-d]. The values of internal resistance R_{in},(evaluated from initial sudden voltage drop in discharge curves), discharge capacitance 'C' (evaluated from eq. 9) and

coulombic efficiency 'η' (evaluated from eq.10) of different capacitor cells are listed in Table 5.

The pPy based symmetrical type-I cells were charged up to 1.0 volt, which was determined by the potential range over
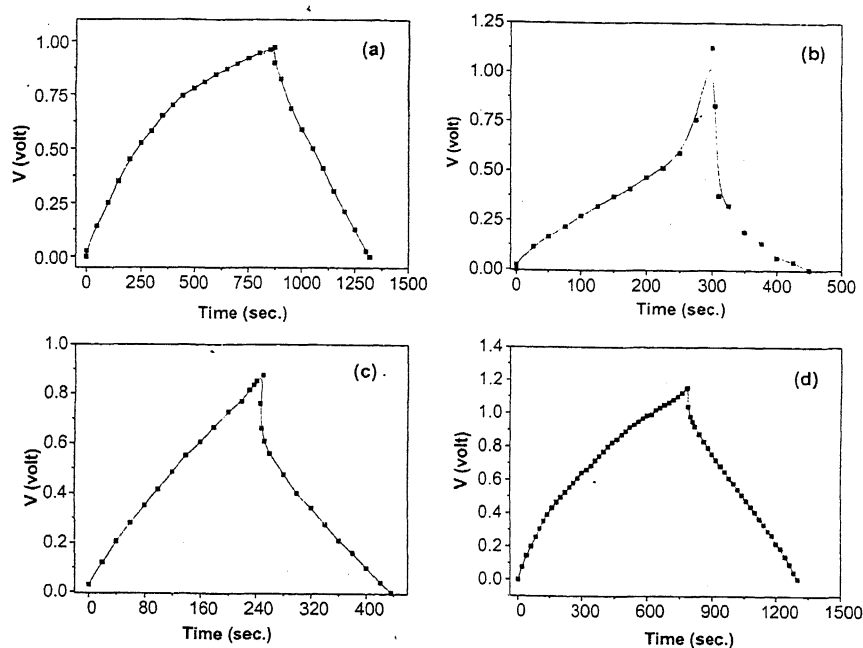

Fig. 11– Galvanostatic charge-discharge characteristics of different capacitor cells; (a) pPy | PMMA-EC/PC-NaClO4 | pPy; and (b) pMeT | PMMA-EC/PC-NaClO4 | pMeT, (c) (-)pPy | PMMA-EC/PC-NaClO4 | pMeT (+) ; and (d) (+) pPy | PMMA-EC/PC-NaClO4 | pMeT (+). (+)/(-) signs show the polarity of the applied current for charging the capacitor cells (charging current = 100 □A and cell area~ 4.0 cm-2).

Table 5– Charge-discharge characteristics of different polypyrrole and poly (3-methyl thiophene) based redox capacitor cells.

Cell configuration	Type	Working voltage (V)	Internal Resistance Ri (Kohm cm^2)	Capacitance mF cm^{-2}	Coul. Eff. η (%)
pPy	PVA-H$_3$PO$_4$	pPy	I	~ 1.0	0.9	10.0	90
pMeT	PVA-H$_3$PO$_4$	pMeT	I	~ 0.8	40.0	2.5	82
pPy	PEO-NaClO$_4$-PEG	pPy	I	~ 1.0	36.0	8.0	84
(-) pPy	PEO-NaClO$_4$-PEG	pMeT (+)	II	~ 1.2	-	10.0	-
(+) pPy	PEO-NaClO$_4$-PEG	pMeT (-)	II	< 1.0	8.0	2.2	-
pPy	PMMA-EC/PC-NaClO$_4$	pPy	I	~ 1.0	1.5	15.0	70
PMeT	PMMA-EC/PC-NaClO$_4$	pMeT	I	~ 0.5	-	10.0	78
(-)pPy	PMMA-EC/PC-NaClO$_4$	pMeT (+)	II	~ 1.1	1.4	12.0	64
(+) pPy	PMMA-EC/PC-NaClO$_4$	pMeT (-)	II	~ 0.6	1.0	8.0	-

which the pPy electrode can be doped and dedoped. These cells show almost symmetrical charge-discharge characteristics [Fig. 10a] which are indicative of identical and symmetrical electrode-electrolyte interfaces. The pMeT based type-I cell with PVA-H₃PO₄ blend also shows the similar behaviour. While charging the pMeT electrode and gel electrolyte based type-I capacitor cell a steep rise in current after about 0.5 V was observed [Fig.10b]. This indicates the limitation of the working voltage of the cell upto 0.5 V.

The relatively higher voltage (>1.0 volt) is expected in the type-II asymmetric pPy/pMeT cells due to different voltage range of doping-dedoping of pPy and pMeT electrodes.[15] The asymmetric type-II cells show peculiar characteristics dependent upon polarity of applied charging current. The cell configuration (+)pPy | PEO-NaClO₄ -PEG | pMeT(-) shows steep rise in voltage after ~ 1.0 volt which limits the range of working voltage <1.0 volt. Also, the linear capacitive region has been observed for a shorter range of voltage. In contrast, the cell with reversed polarity functions for slightly higher voltage (~1.2 volt) and linear capacitive region has been observed for relatively larger voltage range. This asymmetric polarity dependent feature and the capacitance values have distinctly been observed in the gel electrolyte based capacitors [Fig. 10c&d]. It appears from the observed feature that one of the interfaces in the asymmetric configuration of the capacitor cells becomes dominant over the other in terms of charge retention. It further suggests that the redox reactions at the two interfaces are not truly reversible. In order to confirm this aspect, some more electrochemical studies would be required.

Redox Supercapacitors based on MnO₂-Polypyrrole Composite Electrodes

Redox Supercapacitors using electrochemically synthesized MnO₂-polypyrrole composite electrodes have recently been fabricated by us with different electrolytes, namely polymer electrolyte film, PVA-H₃PO₄ aqueous blend, aprotic liquid electrolyte, LiClO₄-PC and polymeric gel electrolyte, PMMA)-EC-PC-NaClO₄.

MnO₂ is well known to be an important material used in primary dry cells as depolariser and in rechargeable lithium batteries as active cathode.[32-34] This aspect of MnO₂ was considered to be exploited as a possible promising electrode material for supercapacitors. However, since MnO₂ exhibits poor conductivity, a conducting network is essentially needed to use it as an electro-active electrode material. Generally activated carbon or acetylene black powder is dispersed in MnO₂ to make it conducting. Recently, S. Kuwabata et al [35] reported a composite MnO₂-polypyrrole (MnO₂-pPy) for its application in lithium secondary batteries as cathode material. The MnO₂-pPy composite works as conducting network of electro-active material in thin film form. Efforts have been made to utilize this conducting network as electro-active electrodes for the fabrication of solid state redox supercapacitors.

Secondly, polypyrrole itself is a potential conducting polymer electrode for secondary batteries and Supercapacitors.[1-3, 15-19, 22] The utilisation of the polypyrrole can be enhanced by preparing the highly porous film which may permit the easy insertion-deinsertion of ions at the electrode-electrolyte interfaces.[36] Consequently, the enhancement in the energy/power density is possible with the porous

polypyrrole films. Many authors reported different ways to enhance the porosity of polypyrrole.[36] The MnO_2-pPy system also acts as a porous composite film, which may have an added advantage for its possible application as electrodes in redox super-capacitors.

In view of the above facts, the MnO_2-pPy composite electrode material has been used to fabricate redox-supercapacitors. A comparative study has been carried out on the supercapacitors with different electroly-tes, solid polymeric electrolyte, PVA-H_3PO_4 blend, aprotic liquid electrolyte $LiClO_4$-PC and sodium ion conducting gel electrolyte, PMMA-EC/PC-$NaClO_4$. The performance characteristics of the capa-citors have been evaluated by galvanostatic charge-discharge tests.

The MnO_2-pPy composite electrodes were electrochemically deposited on ITO coated glass substrates. The electrode-position was carried out at constant current in single compartment three electrodes cell. The procedure of electrosynthesis has been described in detail by us elsewhere.[25] Following three model capacitor cells have been constructed using MnO_2-pPy com-posite electrodes and three different electrolytes :

Cell 1 : MnO_2-pPy | PVA-H_3PO_4 | MnO_2-pPy

Cell 2 : MnO_2-pPy | $LiClO_4$-PC | MnO_2-pPy

Cell 3 : MnO_2-pPy | PMMA-EC/PC-$NaClO_4$ | MnO_2- pPy

Charge-Discharge studies

The galvanostatic charge – discharge characteristics of the capacitor cells 1-3 are shown in Fig. 12. All the cells were charged up to 1.0 volt, which is fixed within the voltage range of electrochemical stability of the electrolytes. The symmetrical polypyrrole based capacitors are usually charged up to a 1.0 volt limit which is determined by the potential range over which the polypyrrole based electrodes can be doped and dedoped.

The typical charge-discharge character-istics (i.e. voltage vs. time plot) of the cell MnO_2-PPy | PVA-H_3PO_4 | MnO_2-pPy shows a non-linear behaviour [Fig.12(a)]. This indicates a non-capacitive behaviour of the cell. The charge-discharge characteristics has been compared with the similar cell with pure polypyrrole electrodes, as shown in Fig.12(b). This shows a typical linear discharge characteristics which is an indication of capacitive behaviour of the cell. The non-linear behaviour of the charge-discharge characteristics confirms the role of MnO_2 present in the composite network of MnO_2-pPy system. This is possibly owing to the following reversible chemical reaction of MnO_2 with water based proton conducting electrolyte, PVA-H_3PO_4 blend.[37]

$$MnO_2 + H_2O + e^- \longrightarrow MnOOH + OH^-$$
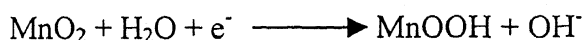
In order to confirm this aspect, a capacitor cell has been constructed with aprotic liquid electrolyte $LiClO_4$-PC to avoid the above aqueous based reaction. The discharge characteristics of the cell (Fig. 12c) is almost linear which indicates its capacitive behaviour. This is possibly owing to the easy insertion and de-insertion of Li^+ ion through the MnO_2 matrix along

with the conventional Faradaic charge-discharge reaction with polypyrrole, leading to the pseudo-capacitance. This comparison indicates that the MnO_2-pPy composite is a suitable electrode system only for aprotic (non-aqueous) electrolytes.

shows the typical variation of discharge capacitance with respect to the varying current density for the cell MnO_2-pPy | Gel Electrolyte | MnO_2-pPy. The stable values of capacitance (10.0-18.0 mF cm^{-2}) for different discharge current densities have been observed. The internal resistance of
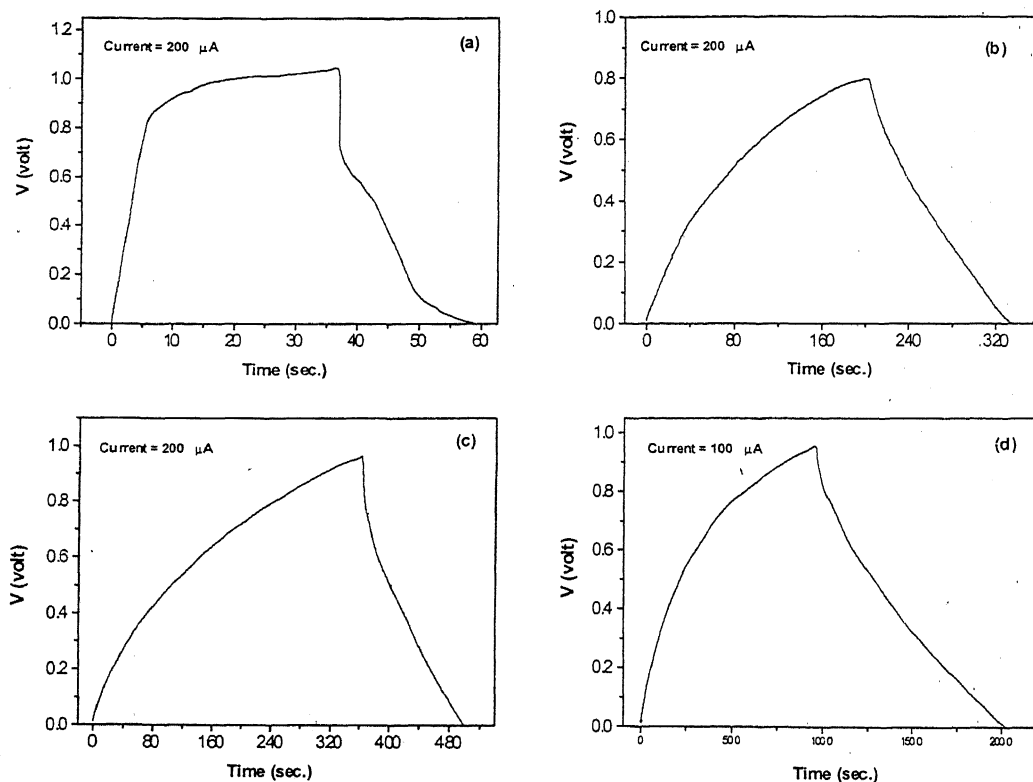

Fig. 12– Galvanostatic charge-discharge characteristics of different capacitor cells; (a) MnO_2-pPy | PVA-H_3PO_4 | MnO_2-pPy, (b) pPy | PVA-H_3PO_4 | pPy, (c) MnO_2-pPy | LiClO$_4$-PC | MnO_2-pPy, and (d) MnO_2-pPy | PMMA-EC/PC-NaClO4 | MnO_2-pPy.

A solid state redox capacitor cell based on Na^+ ion conducting gel electrolyte (PMMA-EC/PC-NaClO$_4$) has also been fabricated which shows a capacitive charge-discharge behaviour, as shown in Fig. 12(d). The values of discharge capacitance (evaluated from eqn. 9), internal resistance R_i (evaluated from initial sudden voltage drop in discharge curves) and the coulombic efficiency, η, (evaluated from eqn. 10) are listed in Table 6. Fig. 13

the cell (observed to be ~1500 ohm cm^2) has been compared to that of the cell with pure polypyrrole electrodes and almost same value of internal resistance has been observed. This indicates that the incorporation of MnO_2 in polypyrrole exhibit no substantial effect on the internal resistance of the capacitor cell. The polypyrrole plays the effective role to form conducting network in the MnO_2-pPy composite system. Finally, it has been concluded that the MnO_2-pPy composite

44

Table 6– Charge-dischargecharacteristics of different MnO_2-polypyrrole based redox capacitor cells.

Cell configuration	Internal Resistance R_i (ohm cm^2)	Discharge Capacitance C (mF cm^{-2})	Coulombic Efficiency η (%)
MnO_2-pPy | PVA-H_3PO_4 | MnO_2-pPy	5×10^4	Non-capacitive	-
MnO_2-pPy | $LiClO_4$-PC | MnO_2-pPy	1.5×10^3	~10.0	44
MnO_2-pPy | PMMA-EC/PC-$NaClO_4$ | MnO_2-pPy	1.5×10^3	10.0-18.0	66

system has been proved to be a potential electrode material for fabrication of redox supercapacitors using aprotic (non-aquous) liquid or polymer/gel electrolytes.
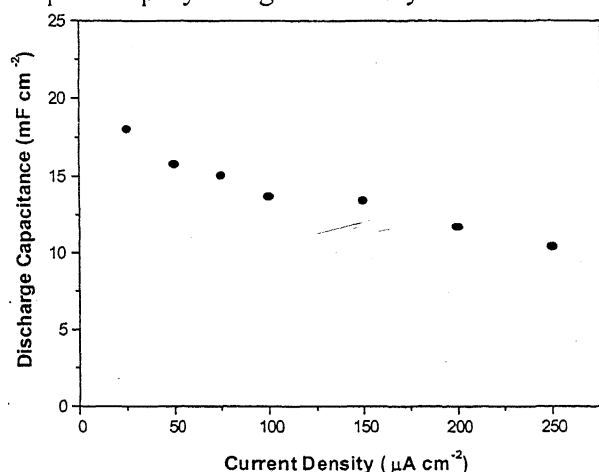

Fig. 13– Variation of discharge capacitance of the cell 3: MnO_2-pPy \| PMMA-EC/PC-$NaClO_4$ \| MnO_2-pPy as a function of current density.

Applications

There has been increasing global interest in the development of 'Supercapacitors' due to their various possible technological applications as power source, mentioned below:

- Portable electronic equipment
- Computer memory back-up
- Medical equipment
- Power supplies
- Load levelling
- Electrical Vehicles

In low energy density applications such as electronic/medical devices, supercapacitors may be used as an alternative power source, whereas it is a complementary power source to the batteries in electrical vehicle like high energy density applications[1-3]. One of the most promising application of Supercapacitors is expected in the hybrid power design for electrical vehicles where they would be used as complementary power system to the main rechargeable batteries. The battery system would provide energy for continuous motion where the Supercapacitors (connected in parallel to the batteries) ensure peak power delivery for acceleration.

Acknowledgement

References

1. Conway, B.E. (1999) *Electrochemical Supercapacitors : Scientific Fundamentals and Technical Applications, Kluwer Academic/Plenum Publishers,*.

2. Delnick, F.M., Intersoll, D., Andriew , X. & Naoi, K. (1997) (eds.), *Electrochemical Capacitors II*, Electrochem. Soc. Proc. Ser. Penington, NJ.

3. Kotz, R. & Carlen, M., (2000) *Electrochim. Acta* 45 : 2483.

4. Nishino. A.. (1996) *J. Power Sources* 60 : 137.

5. Sarangapani, S., Tilak, B.V. & Chen, C. P. (1996) *J. Electrochem. Soc.*, 143 : 3791.

6. (a) Ishikawa, M., Morita, M., Ihara, M. & Matsuda, Y. (1994) *J. Electrochem Soc.*, 141 : 1730. (b) Ishikawa, Y., Ihara, M., Morita, M. & Mabada, Y. (1995) *Electrochim. Acta* 40 : 2217.

7. Lassagues, J.C., Grondin, J., Becker, T., Servant, L. & Hernandez, M. (1995) *Solid State Ionics*, 77 : 311.

8. Shiraishi, S., Kurihara, H., Lan Shi, Nakayama, T. & Oya, A. (2002) *J. Electrochem Soc.*, 149 : A855.

9. Osaka. T.. Liu. X. Nojima M. & Mmomma T. (1999) *J. Electrochem Soc.*, 146 : 1724.

10. Hashmi, S.A., Latham, R.J., Linford, R.G.& Schlindwein, W.S. (1997) *J. Chem. Soc., Faraday Trans.* 93 : 4177.

11. Nagakawa, H., Shudo, A. & Miura, K. (2000) *J. Electrochem. Soc.*, 147 : 38.

12. Zheng, J.P. & Jow, T. R. (1995) *J. Electrochem. Soc.*, 142 : L6.

13. Liu K-C. & Anderson, M. A. (1996) *J. Electrochem Soc.*, 143 : 124.

14. Srinivasan, V. & Weidner, J.W. (2000) *J. Electrochem Soc.*, 147 : 880.

15. Rudge, A., Davey, J., Raistrick, I. & Gottesfeld, S. (1994) *J. Power Sources*, 47 : 89.

16. Rudge, A., Davey, J., Raistrick, I. & Gottesfeld, S. (1994) *Electrochim. Acta.* 39 : 273.

17. Arbizzani, C.. Mastragostino M. & Menegheta, L. (1994) *Electrochim. Acta*, 41, 21.

18. Arbizzani, C., Catellani, M., Mastragostino, M.& Mingazzini, C. (1995) *Electrochim. Acta.* 40 : 1871.

19. Arbizzani, C., Mastragostino, M.& Meneghello, L. (1995) *Electrochim. Acta*, 40 : 2223.

20. Carlberg, J.C.& Inganas, O. (1997) *J. Electrochem. Soc.*, 144 : L61.

21. Clemente, A., Panero, S., Spila, E. & Scrosati, B. (1996) *Solid State Ionics*, 85 : 273.

22. Hashmi, S.A., Latham, R.J.,.Linford R.G & Schlindwein W.S. (1997) *Ionics* 3 : 177.

23. Hashmi, S.A., Latham, R.J., Linford R.G., & Schlindwein, W.S. (1998) *Polymer International* 47 : 28.

24. Hashmi, S. A. & Upadhyaya, H.M. (2002) *Solid State Ionics*, 152 : 883.

25. Hashmi S. A. & Upadhyaya, H.M. (2002) *Ionics*, 8 : 272.

26. Naoi, K., Suematsue S. & Manago, A. (2000) *J. Electrochem Soc.*, 147 : 420.

27. Suematsue, S. & Naoi, K. (2001) *J. Power Sources*, 97 : 816.

28. Park, J. H., Ko, J. M., Ok Park, O. & W.Kim D-, (2002) *J. Power Sources* 105 : 20.

29. Ryu, K.S., Kim, K. M., Park, Y.J., Park, N-G., Kang, M.G. &. Chang, S. H. (2002) *Solid State Ionics*, 152 : 861.

30. Hashmi, S. A., Suematsue S. & Naoi, K. ( ) *J. Power Sources*, to be published.

31. Jow, T. R. (1992) "*Proceedings of Second International Seminar on Double Layer Capacitors and Similar Energy Storage Devices* Vol.-2" eds. S.P. Wolsky and N. Marincic, Florida, USA.

32. Kahraman, E., Binder, L. & Kordesch, K. (1991) *J. Power Sources* 36 : 45.

33. Nohama, T., Yamamoto, Y., Nakane, I. & Furukawa, N. (1992) *J. Power Sources* 39 : 57.

34. Shokoohi, F., Tarascon, J.M., & Wilkens, B.J. (1991) *Appl. Phys. Lett.* 59 : 1260.

35. Kuwabata, S., Kishimoto, A., Tanaka T. & Yoneyama, H. (1994) *J.Electrochem. Soc.* 141 : 11

36. Naoi, K., Oura, Y. & Tsujimoto, H. (1997) *Proc. Symp.Electrochem. Capacitors*, The Electrochem. Soc. Proc., Volume 95-29 : 162.

37. Kozawa, A. & Yeager, J.F. (1965) *J. Electrochem. Soc.* 111 : 954

Present scenario and changing future role of The National Academy of Sciences, India : Some reflections

U.R. Rao

Chairman, PRL Council (Former Chairman, ISRO & Secretary, DOS, Government of India.

Department of Space, Antariksh Bhavan, New BEL Road, Bangalore - 560 094, India.

The National Academy of Sciences, India, founded in 1930 with Prof Meghnad Saha, one of the doyens of Indian Science in the early twentieth century, as its first President, is the oldest science academy in the country. The main objective of the Academy is to provide a national forum for the publication of research work carried out by Indian scientists and to provide opportunities for exchange of views among them. The Academy, starting with 19 fellows and 57 ordinary members grown to its present size of nearly 1012 fellows and 1350 members, is taking a leading role in fostering research in frontier areas of sciences by arranging topical symposiums during its Annual Sessions. The Academy is also trying to mould national consensus on important issues of both scientific and societal interest by holding discussion sessions and symposiums on issues related to science and society that have an important bearing in the national context. An important activity of the academy is to provide opportunity to young scientists to participate in the Annual Sessions and present their research work. This allows the younger generation to interact with peers in their own field and benefit from the discussions with their peers. The peers, in turn, have the opportunity of getting exposed to some radically new ideas, which can only come from the younger scientists, who are not burdened with preconceived ideas. It is indeed a laudable activity that will go a long way in fostering appropriate research culture among the upcoming young scientists.

The lack of effort to impart science education in a manner that will generate curiosity and genuine interest and nourish creativity and innovativeness among the younger generation in the country has been a matter of grave concern. This led the Academy to start a programme of Science Communication during the last decade involving organisation of various activities for school students and refresher courses for college teachers. This programme has now been widened in its scope as a result of the Vision Paper prepared during the current year, to include intensive discussions on topical issues of Science and Technology that have direct societal relevance.

The Current Session

The Annual Session of the Academy is being held at Ahmedabad after nearly a

quarter century and for the first time at PRL. The aim of the Academy to foster relationship with as large an academic community as possible during such a meet is also well served by the fact that the Physical Research Laboratory and the Gujarat University are co-hosting this Session with the University holding the Biological Sciences Session in its premises. The interest shown by the academic community in participating in the deliberations of the scientific sessions is evident from the presentation of nearly 200 papers. The gesture of the Academy and the host institute to provide support to a large number of young students and research scholars from Gujarat and the neighbouring States to participate in the Annual Session is indeed very laudable.

The Physical Research Laboratory has a very strong tradition in the field of astronomy and astrophysics. PRL is unique in that, under one umbrella, it has been studying physical phenomena related to the earth's interior core, upper atmosphere, ionosphere, magnetosphere, interplanetary space, cosmic ray propagation, stellar astronomy and cosmology. It was in 1936 Prof Saha published a paper titled "On a stratospheric astrophysical laboratory" bringing out the advantage of carrying out observations in space. PRL with its pioneering work in the fields of cosmic rays, X-ray astronomy and radio-astronomy realised the importance of space based observations, thanks to Dr Vikram Sarabhai's Vision in the fifties and started building up its space capability. PRL, under the leadership of Dr Sarabhai, thus became the cradle of the Indian Space Programme. Starting with sounding rocket experiments from Thumba for investigating the upper atmosphere, equatorial electrojet, and X-ray astronomy phenomena, PRL was respon-

sible for initiating steps to build a strong space science and technology group. At present PRL has active research programmes in the fields of infra-red and optical astronomy carried out from the Observatories at Mt. Abu and Udaipur respectively. A low energy X-ray payload, designed and developed at PRL, that was launched into space early this year by GSLV, is currently collecting valuable data on solar X-rays which have already yielded interesting results. These can shed new light on our understanding of the solar flare phenomena over a wide scale, from major flares to nano-flares. Laboratory studies that have important bearing on solar system astrophysics are also being pursued actively. Plans are afoot to enter into the new field of sub-millimeter astronomy and enhance the capabilities of the solar observatory at Udaipur. PRL is also taking a lead role in ISRO's ambitious future programme on planetary exploration with the proposed Lunar Polar Orbiter mission in 2008 as its forerunner. Apart from the experimental initiatives, PRL hosts a very strong theoretical group in Astro-particle physics and cosmology that has made very significant contributions, particularly in the field of neutrino astronomy, a very active area of current research in the global context. It is therefore very appropriate that a national symposium on "Astronomy in the New Millennium" is being held as a part of this Annual Session of the Academy.

Observational astronomy has made rapid strides during the last decade both in the global and national context. Space-based platforms, such as the Hubble Telescope, the "Chandra" Observatory, and the recently launched Space Infrared Telescope Facility (SIRTF) offer new vistas in observational astronomy, which have led

to significant refinement in our understanding of the early evolution of the universe and formation and evolution of various stellar objects. Significant improvements in performances of ground-based astronomical Observatories as well as establishment of new facilities across the globe have complimented the space-based observations and consolidated our understanding of astrophysical processes both at small and large spatial and temporal scales.

India has a long-standing tradition in observational astronomy starting with the study of solar phenomena from the Kodaikanal Observatory in the early twentieth century to the recent developments such as the establishment of the Giant Meter Wave Radio Telescope (GMRT) near Pune, the high altitude observatory at Hanley for observations in the optical and infrared regions and the gamma-ray Observatory at Mt. Abu. There are ongoing plans for several new Observatories as well as for upgradation and expansion of existing facilities to venture into new research areas in the field of solar, stellar and extragalactic astronomy. New initiatives for space-borne astronomical observations using indigenous satellite launch capabilities have been successfully implemented and work has been initiated for a dedicated astronomical satellite, the Astrosat. An ambitious programme for the exploration of our own solar system is also being launched.

Research in the field of Astronomy and Astrophysics in India is thus poised for a major advance and the proposed symposium on "Astronomy in the new millennium" is extremely timely. A broad spectrum of subjects (cosmology and early universe, evolution of stars and galaxies, high energy stellar phenomena, neutrino astronomy, X-ray and gamma ray astronomy, Sun and solar system studies) are being covered during the symposium by leading experts from various Institutions and Observatories. It is hoped that the Symposium will review critically the global vs local status in this field of research that will lead to a better definition and focus of the new programmes and at the same time provide an overall perspective of this exciting field of research to the broad spectrum of people from various branches of sciences constituting the fellowship and membership of the Academy.

Role of Academy

I thought I should touch upon some issues, which in my opinion are critical to the future functioning of this Academy as well as other similar Academies. *I believe that the academy should be a think-tank and a pressure group.* It should initiate and encourage open discussions on topical issues of science and technology and on issues of societal importance. A few suggestions are made here for the consideration of the Academy:

1. Induction of young scientists - Only 12 out of 1012 Fellows of the academy are below the age of 45. The proportion of younger scientists in other academies is still worse. This does not auger well for the future growth of science in India. A concerted effort by the fellows is required to identify and induct bright young scientists in India as fellows of the academy.

2. Very little is done in promoting science and technology education in the country, which is in a very bad shape. · Revitalisation of education by providing training to teachers, promoting quality

research and encouraging younger generation to share the excitement of science are some areas in which the Academy can play a positive role. Massive use of distance education is necessary to accomplish these aims.

We have a catch 22 situation in the publication of journals. Good papers are not published in our journals, which results in poor citation. Poor citation does not encourage scientists to publish good papers. *It may be worthwhile to have journals carry only expert review articles on various subjects along with short papers/notes.*

Ethics of Science

Since science and technology deal with people's requirement for better living, it must necessarily be based on ethical principles. Historically two lines of thought emerged, the first derived from Plato and Descartes and the second by Aristotle. The Plato approach (principle based) based on universal principles derived from pure reason without regard to the situation, culture or consequences, was later modified by Barker and Mill to make it consequence oriented. This resulted in the moral choice, if we may call it so, being bestowed on utilitarian yield - the greatest good for the greatest numbers. Aristotle's ideas, (practical wisdom), which were forgotten for a considerable time, have been resurrected by contemporary philosophers such as Dreyfus to take into consideration the variable of specific situations, practices and norms.

Application of ethics, however, have got very complicated in the modern age because of the range and influence of scientific actions, which can have local (building collapse, shuttle explosion), large

area (environmental) or even global effect, (green house emission) and manifest very quickly (over the internet), very slowly (radio-active disposal), temporarily persistent (organic pollutants) or become even irreversible (genetically modified organism and cloning). It is therefore all the more necessary that scientists integrate societal and technical parameters in their thinking not only for the development but also for the survival of humankind.

In order to promote the above objective, *the Academy must become the conscience of scientific community.* Penchant for going to the press without going through peer reviews has caused a lot of damage. Cold fusion, plagiarizing, sensationalisation (recent controversies on pesticide/chemical contamination of cold drinks) are some examples of the above trend. Pseudo self-styled environmental scientists making statements, starting agitations merely for publicity (environment, dams, energy, pollution, etc.), without caring for the consequences can only cause great damage to societal development. On the other hand the habit of scientists and engineers to promote large programs, without studying their consequences, is equally regrettable. Talking on large dams like Hirakund dam and Damodar valley project, Prof Saha, in 1954, chided the scientific community of big dam enthusiasts with these words "we shall make the highest dams in the world, may be a very good slogan, but is very bad from the scientific point of view". Instead of taking our decisions on objective cost-benefit analysis, we often seem to give our advise palatable to the whims of the self seeking politicians.

Academy should consider setting up of an ethics committee of eminent scientists to look into matters, which relate to misuse,

sensationalisation and even general conduct of scientists. Larger issues such as, ethics of xeno-transplantation, cloning, energy, space mines, destablisation of food chain by indiscriminate activities etc., need to be discussed objectively and dispassionately. Multi-national companies with their monopoly of terminator seeds can control world's food supply. Infection of fields of farmers, who have not used this technology, by pollen from crops carrying the terminator gene is a real problem. While the crops in the particular season will not be affected, some of the seeds may become sterile when they are sowed in the next season, affecting the entire food chain. Use of space mines, which is being pushed in the name of security, can itself accidentally wipe out the space assets of many nations. Unless Academies take a proactive role in matters which affect the society as a whole, I believe they will remain as elite clubs at best, far removed

from reality. Intensive subject discussions can and are best held during purely scientific meetings/workshops in particular identified areas. Larger issues can only be discussed and dealt with by the academies.

I wish to conclude with the statement made by the great scientist Peter Kapitza on Soviet Academy, which applies equally to our Academy, and which was often quoted by Prof M N Saha: "The academy of science is the general headquarters of science and should be the idealogical guide of the science of the whole nation. Every individual institute and member of the academy must follow the same policy, strive to become the guiding influence in their particular sphere of science and try to achieve the maximum development". I hope this academy will take greater interest in harmonizing scientific progress with societal aspirations.

Studies on altered characteristics of urease immobilized on reinforced beeswax and on pellicles of garden cress *(Lepidium sativum)*

Kespi A. Pithawala AND A. Bahadur*

Department of Zoology, P.T.S. College of Science, Surat-395001, India.

E-mail : anita26p@rediffmail.com

Abstract

Urease (3,5.1.5) from jack bean meal was immobilized by embedding in dry films of reinforced bees wax and by covalent linkage using ethylene diamine-glutaraldehyde arm onto seed coats (pellicles) of garden cress *(Lepidium sativum)* in aqueous suspension. The Activity of free and immobilized enzyme as a function of pH, temperature, storage stability, kinetic parameters and periodic use were compared. Enzyme bound under mild conditions retained good activity and storage stability during repeated use as compared to the free urease. Kinetic parameters viz K_m and V_{max} are in accordance with Michaelis-Menten rate equation

(Keywords: urease/seed coats/beeswax/immobilized enzyme)

Natural supports offer ideal means for immobilizing enzymes. A number of enzymes have been immobilized using temperate conditions on various natural substances such as seed coats, cellulose etc.[1,2]. These are extremely cheap, eco-friendly and ready to use as compared to synthetic supports. Amongst supports used for immobilization, biological macromole-cules like cellulose and its derivatives through physical adsorption or chemical linkages have been studied most extensively[3,4]. Urease has been immobilized on many supports like calcium alginate paraffin wax, lac and some natural seed coats[5,6]. Immobilization of enzymes on beeswax, a natural animal product is yet not reported. Bees wax is a mixture of myricyl palmitate $[CH_3\text{-}(CH_2)_{14}\text{-}COOC_{30}H_{61}]$ and n-hexacosanyl palmitate $[CH_3\text{-}(CH_2)_{14}\text{-}COO\text{-}C_{26}H_{53}]$. This substance finds enormous applications in food, pharmaceutical, cosmetics, microencapsulation, polishes and leather industries.

When enzymes are bound under mild conditions on polysaccharides activated by various means. mechanical instability is a major problem. Another difficulty that arises is due to their particle size, which makes them readily compact resulting in high pressure drops in packed bed column reactors. To overcome this problem, the use of pellicular catalysts, which consist of enzyme immobilized only on the outer porous shells of carrier particles, is highly recommended[7]. Because of its more exposed outer structure within an inert hard

core, *Ocimum basilicum* seeds have served as efficient natural pellicular support for immobilizing enzymes[1].

Lepidium.sativum seeds are used as diuretic. tonic, aphrodisiac, laxative, rubifacient in poultices for hurts and sprains. Seeds also yield a semidrying oil, used for burning and soap making. The seed mucilage called 'cress seed mucilage' is used as a substitute for tragacanth and arabic gum. It allays irritation of the intestines in diarrhoea and dysentry. The present paper reports the use of alternative *Lepidium sativum* seeds, which are mucilaginous, nontoxic [edible] and offer a cheaper and natural polysaccharide support for enzyme immobilization. Also, same enzyme is immobilized on bees wax, a non-toxic biocompatible substance.

The enzyme urease from jackbean meal (Loba Chem. Pvt. Ltd. India.), -its substrate urea (Loba) and glutaraldehyde (Loba) were used and 1,4- butenediol diglycidyl ether was a Sisco product. Nessler's reagent, Tris buffer and other chemicals used were of Analar grade. Muslin cloth (Tata fabric pure cotton) was used. *Lepidium sativum* seeds were procured from local market and beeswax was extracted from honeycomb as described below.

Dry honey combs of *Apis dorsata* were chopped into smaller pieces and boiled in hot water in an aluminium vessel for 10 – 15 minutes till all the cells of honey combs separated from each other and yellow coloured melted wax started to float on the surface. This was then strained through a strainer made of fine mosquito net cloth. The filtrate contained water plus wax floating on the surface, which cooled to

solid. The wax layer from the top thus collected was again boiled in distilled water and wax, free from insoluble material was collected. The wax thus obtained was further purified by washing in methanol first and then in acetone and was used for further experiments.

(1) *Preparation of immobilized urease on bees wax films:*

To 4g of melted beeswax in thermostated waterbath. 1g of enzyme powder was added and kept on stirring continuously at slow speed. Muslin cloth was previously washed in distilled water and sundried. Of this 1 sq.cm pieces were cut (wt. 5mg.). Each of these pieces was dipped in wax enzyme mixture which was continuously agitated and kept in water bath thermostated at 60°C. After 3-5 seconds these pieces were removed by using pointed B.B. forceps, slightly shaken to remove dripping wax and allowed to dry. In this way 1 cm^2 reinforced film of beeswax with enzyme was made. Films were weighed to find out amount of enzyme immobilized.

(2) *Preparation of immobilized enzyme on seed coats:*

Dry seeds of *Lepidium sativum* were swollen by soaking in distilled water at room temperature for 20-24 hours. These were then epoxy activated by method of Sundbfrg and Porath[8] after slight modification. To 20 ml of swollen seeds 10ml of 1-4 butenediol diglycidyl ether and 10 ml of 0.6 N NaOH was added and kept on stirring for 4 hours and then they were left undisturbed for another 20 hours. After this reaction was stopped by washing the seeds with ample water. These epoxy-

activated seeds were then treated with 10 ml of 0.1M ethylene diamine (pH 11.0), at room temperature for 24 hours with occasional shaking. To this reaction mixture, 10 ml of 2% glutaraldehyde was added and kept for another 24 hours with initial shaking only. These were then washed with excess of water.

A solution of urease (5mg/ml) was added to gluteraldehyde activated seeds and kept in cold with intermittent shaking for 24 hours. The reaction was terminated by washing the seeds with distilled water and then with phosphate buffer pH 7.0. Seeds with immobilized enzyme were stored in phosphate buffer solution in glass stoppered bottles at 4 °C.

Free enzyme in the washings was measured colorimetrically using Lowry's method to obtain the amount of bound enzyme. The amount of enzyme immobilized on the support was calculated later.

Enzyme assays

(1) Assay of native urease : The standard solution was prepared by dissolving 10mg urease in 10ml phosphate butler (pH 7). 1ml of 3% urea solution and 1 mg/ml of enzyme was taken and incubated for 15 minutes at pH 7 and temperature 55°C in a water bath, The reaction was stopped by placing the reaction mixture in ice-bath and 0.66N H_2SO_4 was added. 1ml of Nessler's reagent was then added to develop colour and optical density of the solution. was measured using ESICO colorimeter at 500 nm.

(2) *Assay of urease immobilized on beeswax film :* One film of beeswax was

taken in 1ml buffer solution and reacted with 1ml 3% urea solution for 15 minutes in water bath. The same procedure followed the reaction and measurements were similar to the native enzyme except that the films were taken out from the reaction mixture just before stopping the reaction.

(3) *Assay of enzyme immobilized on seed coats :* To 1ml of seeds containing immobilized enzyme 1 ml of phosphate buffer and 1 ml 3% urea solution was reacted for 15 minutes. The same procedure followed the reaction and measurements were similar to that carried out for native enzyme except that seeds were removed before chilling the solution and adding H_2SO_4.

Determination of enzyme activity

The catalytic activity of native and immobilized enzymes was measured colorimetrically at 500nm. After reaction with the substrate urea, the amount of ammonia liberated was measured using Nessler's reagent method · as described before.

Determination of kinetic parameters

For determination of kinetic parameters substrate concentration was kept on changing keeping enzyme concentration fixed for both native as well as immobilized enzyme system at constant temperature 40°C and pH=7.0. Measurements were made as described before using Nessler's reagent method. Absorbance was read at 500 nm. Velocity was measured in moles of NH_3 produced / min / mg enzyme. K_m and V_{max} were determined using Lineweaver-Burke plot.

Results and Discussion : Due to mild and precise conditions of physical and chemical treatment during the immobilizing procedure the structural integrity and activity of urease was preserved. The entrapment of urease in the beeswax was such that it left some part of enzyme exposed to carry out catalytic function and in such a condition it retained 40% activity. Urease is a thermostable enzyme that is denatured only at 80°C and therefore it could easily be immobilized on beeswax at 60°C. The reinforced films of bees wax were durable.

L. sativum seeds like other mucilaginous seeds swell upon wetting. Seed mucilage known as cress seed mucilage is used as a substitute of tragacanth gum and is used to allay irritation of intestines in dysentery and diarrhoea[9]. This pectinous outer layer substance is termed as amyloid and is a galactosan [polysaccharide] having empirical formulae $[C_6H_{10} O_5]_n$[10]. It has a large capacity for hydration. One gram of dry seeds on soaking result in about 15 ml of swollen seeds. The mucilage consists of thread like microfibrillar structure with a large surface area as observed under a microscope. The seed consisting of a hard core with pectinous porous outer layer can serve as a cheap and ready' to use natural polysaccharide support for immobilizing enzymes. The polysaccharide layer can be modified by epoxy activation for successful binding of urease using covalent attachment via. ethylene diamine-glutaraldehyde arm. Enzyme thus bound (2mg/ml seeds) retained 63% activity.

No leakage of enzyme was observed after continuous washing the preparation with 0.2 M phosphate buffer or distilled water. The column of urease bound seeds maintained high flow rate [10ml column/30 minutes for 10 ml buffer]. Studies were carried out with these preparations and compared with native enzyme to find out utility of urease in hydrolyzing urea.

pH activity profile

The pH dependence of the relative activity of the enzyme urease is compared with that of the enzyme immobilized on various supports. The reaction was carried out in 0.2M phosphate butter for pH range 5.6-7.8. The optimum pH for native and immobilized enzymes on seeds were 6.8 and 7.0, respectively. This shows that immobilization shifts the optimum pH range to basic side by 0.2 units but in the case of enzyme immobilized on bees wax film showed optimum pH at 7.2, a shift of 0.4 units to basic range. This shows urease can be used in narrow basic range than native urease. (Fig. 1)
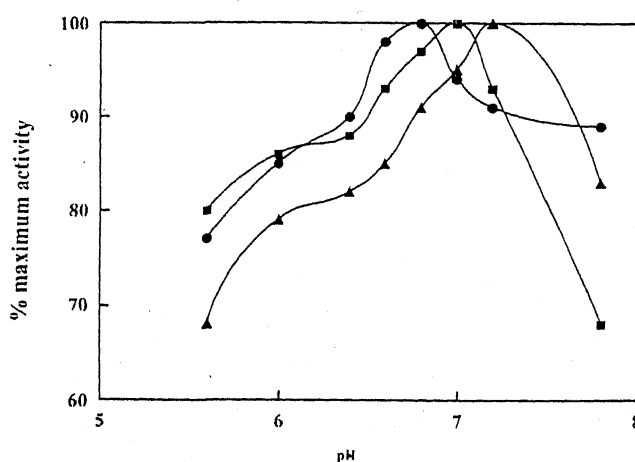

Fig. 1– Plot of percentage maximum activity vs. pH for pH profile of free (●) and immobilized urease on beeswax (▲) and seeds (■).

Thermal stability

The optimum temperature for free as well as immobilized enzyme was around

56

55 °C, when thermal stability studies were noted at different temperatures and at constant pH=7 kept for 15 minutes. Both the native as well as immobilized enzyme were stable upto 75°C. However, the activity of immobilized enzyme on seeds was higher at high temperatures as compared to native enzyme (Fig. 2). Temperature stability studies for enzyme immobilized on bees wax could not be carried out as the melting point of bees wax was around 58°C.
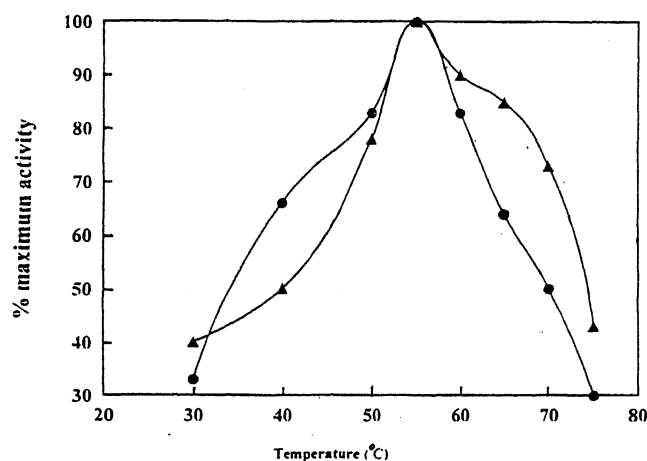

Fig. 2– Plot of percentage maximum activity vs. temperature for thermal stability of free (●) and immobilized urease on seeds (▲).

Storage stability

The native enzyme retained same activity for about 15 days, which slowly decreased and was lost completely after a month. The enzyme immobilized on beeswax retained 98% activity for 15 days and 59% activity even after a month in dry condition. Enzyme immobilized on seeds retained more than 82% activity after about 15 days when stored at 4°C (Fig.3). Moreover no physical change, structural alterations or microbial growth was seen on seeds stored at room temperature for longer periods.
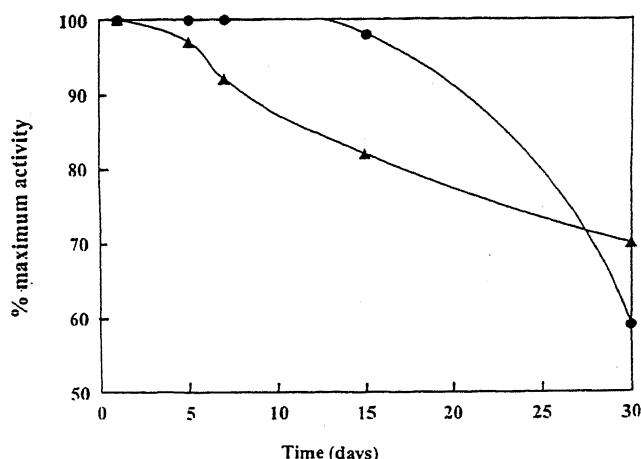

Fig, 3– Plot of percentage maximum activity vs. time (days) for storage stability of urease immobilized on beeswax (●) and seeds (▲).

Retention of activity after reuse

Immobilized enzyme on beeswax film could be used repeatedly upto 13 batches under assay condition retaining 90% activity while immobilized enzyme on seeds retained 60% activity upto 5-6 batches under assay conditions (Fig. 4).
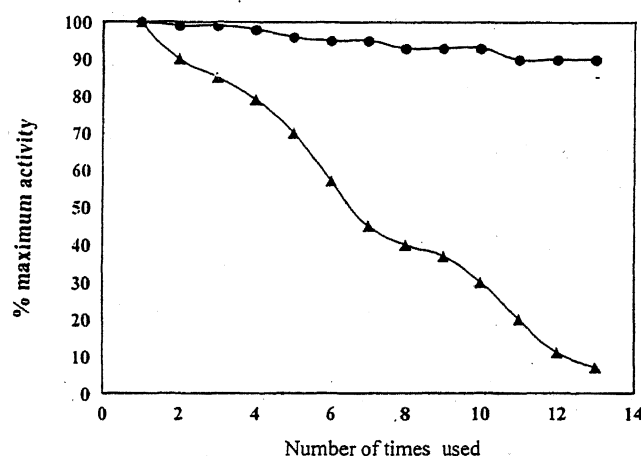

Fig 4– Plot of percentage maximum activity vs. number of times used for reusability of urease immobilized on beeswax (●) and seeds (▲).

Mechanical stability

Beeswax films were mechanically stable when centrifuged or kept on magnetic stirrer at full speeds. Seeds were

also stable and resistant to destruction when stirred continuously for 10-12 hours on magnetic stirrer. When seeds were centrifuged initially they adhered to each other forming a pellet but could be separated easily when resuspended in aqueous medium.

Kinetic studies

The kinetic parameters of K_m and V_{max} were evaluated using Lineweaver and Burke plot (Fig. 5) and are tabulated (Table- 1). The kinetic parameters are in accordance with Michaelis – Menten equation. Immobilization of enzyme leads to a decrease in both K_m and V_{max} values. This shows that active sites of enzyme are masked due to immobilization. Further that in case of immobilization on seeds K_m value is further lowered This can be attributed to the use of chemicals viz. ethylene diamine-glutaraldehyde for covalent linkage and therefore more active sites are blocked.

Fig. 5– Double reciprocal plot of velocity V (moles of NH₃ produced/min/mg enzyme.) vs. concentration of urea for free (●) and immobilized urease on beeswax (▲) and seeds (■).

Table 1– Kinetic parameters of free and immobilized urease on bees wax and seeds

	K_m (moles x 10^{-1})	V_{max} moles/min/ mg.enzyme
Native	0.250	1.54×10^{-4}
Immobilized enzyme on beeswax	0.200	1.11×10^{-4}
Immobilized enzyme on seeds	0.143	1.30×10^{-4}

Acknowledgement

References

1. Melo,D' souza & Nadkarni (1986) Biotechnol. Letters. 8(12) : 885.

2. Paul, C.D., Bahadur, A. & Shah, B.A. (1997) Cellulose. Chem. Technol. 31 : 315.

3. Hajime miyama, Takaomi Kobayashi & Yoshio Nosaka. (1982) Biotechnol, Bioengg. 24 : 2757.

4. Minamoto Y. & Yugari Y. (1980) Biotechmol. Bioengg 22 : 1225.

5. Bahadur. A., Rao, Y. K. & Gosh. S. (1988) Ind. J. Biochem Biophy 25 : 273.

6. Atkinson B. Rort. J., & Rousseau I. (1977) Biotechnol. Bioengg. 19 : 1037.

7. Wayne, H. & Pitcher Jr. (1975) in Immobilized Enzyme for Industrial Reactors, Academic Press. R.A. ed. Messing p. 151.

8. Sundbfrg, L. & Porath, (1974) J. J. Chromato. 90 : 87.

9. (1986) The Useful Plants of India. PID.CSIR. New Delhi p.323

10. Bass, P. & HilL TG. (1921) An Introduction to Chemistry of Useful Plant Products, Longmann Green and Co, Paternester Rom, London. Vol 1, 3rd Edn. p. 39.
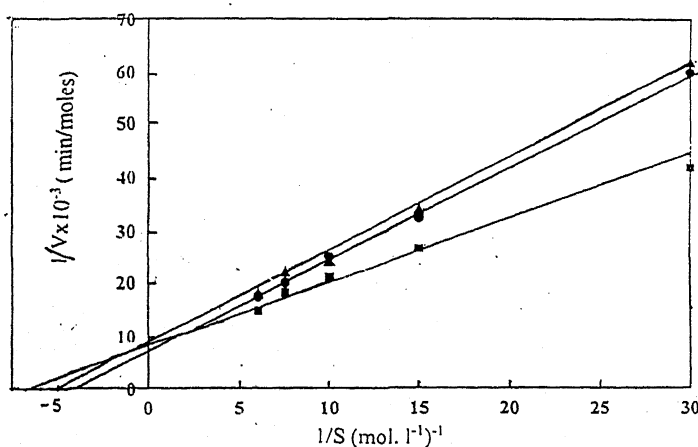
Preparation and characterisation of solid solutions of cadmium-calcium hydroxylapatites containing arsenate

Prema. N. Patel, A.K. Samantaray, Mrs. Shanti Pandey* AND #S.N. Moharana

Department of Chemistry & Research in Applied Chemistry, Government (Autonomous) College, Rourkela-769004, India.

Department of Zoology, Government (Autonomous) College, Rourkela-769004, India.

#*State Forensic Science Laboratory, Bhubaneswar-751010, Orissa, India.*

Abstract

Homogeneous solid solutions of cadmium calcium hydroxylapatite, containing arsenate, $[Ca_{10-n}Cd_n(PO_4)_{6-m}(AsO_4)_m(OH)_2]$ with fixed m = 1 ; n = 1, 2, 3...... have been prepared over the entire compositional range by co-precipitation at $37 \pm .5^0$ C in aqueous media by addition of ammonium dihydrogen phosphate and ammonium arsenate to the solutions of cadmium and calcium nitrate made strongly basic with liquor ammonia. The infrared spectra and lattice parameters of the solid solutions have been measured.
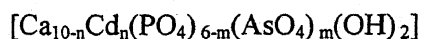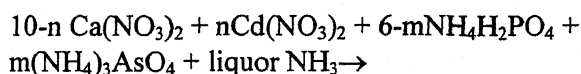
(Keywords : Hydroxylapatite / solid solutions / co-precipitation)

Introduction

In recent years, attention has been directed towards all the basic calcium phosphates for the process of calcification in general and for dentistry in particular. Hydroxylapatite, represented as $[Ca_{10}(PO_4)_6(OH)_2]$, is now recognized as the most important of the inorganic constituents of human bone and teeth[1,2]. It belongs to an isomorphous series of compounds known as apatite which exists in nature as the mineral hydroxylapatite and is similar, if not identical, to bone mineral which can be prepared in aqueous solution[3,4]. Solid solution of cadmium and calcium hydroxylapatites containing arsenate were prepared separately earlier by heating $(\sim 1300^0C)$ mixtures containing various proportions of cadmium and calcium hydroxylapatite with asenate[5]. These samples prepared by the solid state reaction were, however, found to be non-homogeneous.

An attempt has now been made to prepare homogeneous solid solutions of cadmium-calcium hydroxylapatite with arsenate over the entire compositional range by co-precipitation in aqueous media[6,7].

$$10\text{-n } Ca(NO_3)_2 + nCd(NO_3)_2 + 6\text{-m}NH_4H_2PO_4 + m(NH_4)_3AsO_4 + \text{liquor } NH_3 \rightarrow$$

$$[Ca_{10-n}Cd_n(PO_4)_{6-m}(AsO_4)_m(OH)_2]$$

Materials

Chemicals used for the preparation of these samples were of reagent grade. Water used in the preparation and in washing was boiled to remove CO_2 and then used immediately.

Preparation

Stoichiometric quantities of ammonium dihydrogen phosphate (0.25 M) and arsenate (0.25 M) solution A and solution B containing (0.25 M) solution of each of cadmium and calcium nitrate were prepared separately in CO_2 free doubly distilled water. Both solutions were initially more basic than pH 11 by addition of liquor ammonia and this high basicity was maintained during the precipitation reaction and subsequent digestion. Then a part of solution B was put in a flask (2L) fitted with two separating funnels and a delivery tube. For the preparation of pure CaHA, an excess of calcium ion was necessary to prevent the uptake of excess phosphate accordingly considerable cation excess was used throughout. Solutions A and B were taken separately in the separating funnels and added drop wise to the flask simultaneously in a calculated amount. Precipitation was carried out by bubbling CO_2 free air. The whole was heated under reflux for 2 hrs to improve homogeneity and crystallinity of the precipitate. Desired pH during precipitation was maintained by testing the filtrate after separation of the precipitate, since any alteration of pH of the medium during precipitation leads to the formation of cations deficient apatite[8]. The precipitate was allowed to settle overnight and washed repeatedly with doubly distilled water until the wash water reached pH 7. The precipitate was filtered, dried at 110^0C for few hours and was analysed

complexometrically by EDTA[9]. Densities were determined using toluene[10] as a solvent and molar volumes were calculated.

Infrared Absorption Techniques

Samples used for IR studies were washed with acetone and air-dried. All the bands were recorded on a Perkin-Elmer Infrared Spectrophotometer-577 in KBr. A few milligrams of the sample was ground with two drops of Nujol in an agate mortar. About 50 mg of a fine polyethylene powder (VESTOLENA 6016 Chem. Werke Huels Germany) was added. The resulting paste was melted rapidly at about 140°C and lightly pressed between two glass plates to get slightly wedge shaped film of an average thickness of 0.1 mm.

X-Ray Diffraction Techniques

After dying 110^0C and then heating 4 hrs at 950^0C, samples obtained that gave sharp X-ray diffraction patterns of the pure hydroxylapatite phases. The X-ray diffraction patters of the samples were obtained with Siemens powder difractometer with NaCl (TL) counter employing $Cu-k_\alpha$ (nickel filtered) radiation with a scanning speed of $1^0/min$ using tube voltage of 20 Kv and 24 mA.

Lattice Constant Measurements

Cadmium Hydroxylapatite and calcium hydroxylapatite and their solid solutions with arsenate are hexagonal with two lattice constants a_0 and c_0. These were determined for few suitable samples by measuring the diffraction angle, 2θ of the three planes, (312), (213) and (321). Each sample was thoroughly mixed with 25% NaCl (recrystallised from HCl) which served as a standard so that the observed values of $Sin\theta$

for the solid solution lines could be directly corrected for absorption and instrumental errors. The lattice constant of NaCl at 26 °C was taken to be 5.6403Å[11]. A least squares calculation on the corrected values of Sinθ for the three reflection gave the two parameters, a_0 and c_0 for each sample. The average probable error in unit cell parameters is less then $\pm.005$Å.

Results and Discussion

The results of chemical analyses of the sample are given in Table 1. Molecular formula for each of the samples was assigned on the basis of the results of chemical analysis. The molecular formulae of the samples were calculated from the results of Table 1. Observed values of Molar g atomic ratio of Ca/P, Ca/As, Cd/P, Cd/As for end members and (Ca + Cd)/ (P + As) were found to be equal to 1.666 (theoretical 1.67) consistent with the formation of homogeneous solid solutions[10,11]. This was further supported by the closeness of the values of molar volumes of the end members and those of the intermediate samples which lie within the range of end members.

The formation of solid solutions can be confirmed further by the X-ray diffraction analysis[12]. Lattice parameters showed unit cell contraction / dilation consequent upon the introduction of smaller ion Cd^{2+} (0.97Å) and larger ion AsO_4^{3-}(2.48Å) in place of Ca^{2+}(0.99Å) and PO_4^{3-} (2.38Å) respectively in the apatite lattice. This suggests that these are real solid solutions and are not mixtures of two components or one component with adsorbed material.

Infrared spectra of mixed hydroxy-lapatites were studies in the range 4000-400 cm^{-1}. The results of the IR measurements

are collected in Table 2. The general formula of the apatite considered here is $M_{10}(RO_4)_6X_2$ (M=divalent cation like Ca, Cd; RO_4= orthophosphate PO_4, arsenate AsO_4; X = monovalent anion, OH). In this formula, when M or X is replaced by a related ion, the position of the phosphate bands in the IR spectra are changed.

The CaHA and its solid solutions with cadmium and arsenate are interesting examples of solid state of fairly simple molecules of tetrahedral symmetry[13,14]. This is the symmetry imposed by the static field of the surrounding ions. In addition to this field, there is a dynamic interaction between the ions, which has also strong influence on the internal vibration of PO_4^{3-}. Under this ideal symmetrical condition only two infrared active modes are observable[15,16] in regions 1000-1100 cm^{-1} (v_3 the P-O stretch) and 500 – 570cm^{-1} (v_4 and P-O bending).

From the spectra of the samples (Table 2) it is evident that the v_3 and v_4 frequencies corresponding to PO_4^{3-} are v_3 (1075cm^{-1}) and v_4 (570 cm^{-1}) for CaHA, v_3 (1065 cm^{-1}) and v_4 (565 cm^{-1}) for CdHA and frequencies corresponding to AsO_4^{3-} ion are v_3 (800 cm^{-1}) and v_4 (400 cm^{-1}) and for solid solutions containing arsenate, the frequencies lie in the above mentioned region. The shape of the peaks was also effected by the introduction of cadmium and arsenate ions into the samples.

The frequency v_3 corresponding to OH^{1-} ion is observable at 3550 cm^{-1} (Cal. 3578 cm^{-1}) for CaHA. In case of CdHA, the free OH^{1-} stretching mode appears at 3525 cm^{-1} where as in the case of solid solutions containing arsenate, the absorption band of OH^{1-} ion appeared at lower frequencies.

Table 1– Chemical analysis of solid solutions fo cadmium – calcium hydroxylapatites containing arsenate $Ca_{10-n}Cd_n$ $(PO_4)_{6-m}(AsO_4)_m(OH)_2$ where m = 1, n = 1,2,3......etc.

Sl. No.	COMPOUNDS	Wt.%				G. Atom Ratio	Molar Volume
		Ca	Cd	P	As		
0	$Ca_{9.991}(PO_4)_{5.987}(OH)_2$	39.921	-	18.487	-	1.671	337.732
1	$Ca_{9.004}Cd_{0.991}(PO_4)_{5.005}(AsO_4)_{0.991}(OH)_2$	32.241	09.952	13.850	6.633	1.667	351.984
2	$Ca_{7.991}Cd_{1.888}(PO_4)_{5.010}(AsO_4)_{0.989}(OH)_2$	26.892	18.763	13.029	6.221	1.662	355.516
3	$Ca_{6.993}Cd_{2.991}(PO_4)_{5.001}(AsO_4)_{0.993}(OH)_2$	22.184	26.611	12.260	5.888	1.668	356.900
4	$Ca_{5.995}Cd_{4.001}(PO_4)_{4.993}(AsO_4)_{0.995}(OH)_2$	17.978	33.652	11.571	5.577	1.671	352.189
5	$Ca_{5.001}Cd_{4.993}(PO_4)_{5.003}(AsO_4)_{0.998}(OH)_2$	14.220	39.819	10.994	5.304	1.669	367.062
6	$Ca_{3.997}Cd_{6.006}(PO_4)_{4.991}(AsO_4)_{0.990}(OH)_2$	10.817	45.589	10.439	5.008	1.672	369.301
7	$Ca_{2.987}Cd_{6.998}(PO_4)_{4.998}(AsO_4)_{0.991}(OH)_2$	7.710	50.662	09.970	4.781	1.671	370.580
8	$Ca_{2.001}Cd_{7.979}(PO_4)_{4.995}(AsO_4)_{0.987}(OH)_2$	4.940	55.248	09.550	4.518	1.668	372.131
9	$Ca_{1.005}Cd_{8.975}(PO_4)_{5.005}(AsO_4)_{0.979}(OH)_2$	2.377	59.537	09.148	4.328	1.670	366.780
10	$Cd_{9.996}(PO_4)_{5.012}(AsO_4)_{0.986}(OH)_2$		63.459	08.767	4.172	1.668	368.119

Table 2– X-ray and ir spectra of solid solutions of cadmium – calcium hydroxylapatites containing arsenate.

Sample No. of Table-I	Lattice Parameters (Å)			Unit cell volume $\dfrac{\sqrt{3}a^2c}{2}$	Frequency (cm^{-1})				
					PO_4^{3-}		AsO_4^{3-}		OH^-
–	a	c	c/a	–	v_3	v_4	v_3	v_4	v_3
–	–	–	–	–					
0	9.372	6.862	0.732	521.970	1075	572	----	----	3550
2	9.272	6.764	0.730	503.595	1077	575	805	405	3500
4	9.346	6.775	0.725	512.497	1075	575	808	405	3475
6	9.355	6.755	0.724	511.969	1070	570	805	402	3450
8	9.327	6.706	0.719	505.217	1075	580	810	402	3450
10	9.336	6.677	0.715	504.004	1068	572	800	400	3425

References

1. Neuman, W.F. & Neuman, M.W. (1953) *Rev.* **53** : 1.

2. Wallaeys, R. & Chaudron, G. (1950) *Compt. Rend.* **231** : 355.

3. Hayek, E. & St-adlmann, W. (1955) *Angrew Chem.* **67** : 327.

4. Wells, A.F. (1950) *Structural Inorganic Chemistry,* Oxford University Press London, P. 70.

5. Van Wazar, J.R. (1966) *Phosphorus and its compounds,* Interscience Publishers, *New York,* Vol. II P. 1429.

6. Patel, P.N. (1978) *Chem. Ind. London* **20** : 804.

7. Patel, P.N. (1980) *J. Inorg. Nucl. Chem.* **42** : 1129

8. Berry, E.E. (1967) *J. Inorg. Nucl. Chem.* **29** : 1585.

9. Welcher, F.J. (1965) *The Analytical uses of Ethylenediamine Tetra Acetic Acid.* D. Van, Nostrand Company, INC.

10. Partington, J.R. (1952) *An Advanced Treatise on Physical Chemistry,* Longman Green & Co. Vol. III P. 121.

11. Chapman, A.C. & Thirlwell, L.E. *Spectrochim. Acta* **20** : 937.

12. Baddiel, C.B. & Berry, E.E. (1966) *Spectrochim. Acta* **22** : 1407.

13. Klee, W.F. & Engel, G. (1970) *J. Inorg. Nucl. Chem.* **32** : 1837.

14. Nakamato, K. (1960) *IR spectra of Inorganic and Co-ordination compounds,* Wiley, New York. : 103

15. Herzberg, G. (1964) *The Infrared and Raman Spectra of Polyatomic Molecules,* D. Van Nostrand & Co, New York. : 280

16. Busing, W.R. & Morcan, H.W, (1958) *J. Chem. Phys.* **28** : 998.

Controlling chaos by periodic parametric excitation in Froude pendulum

Ila Sahay[*] AND L.M. Saha[+]

*Department of Mathematics, University of Delhi, Delhi-110007, India

+ Zakir Husain College, University of Delhi Delhi-110002, India

Abstract

Chaotic evolution in Froude pendulum driven by a periodic forcing has been investigated in detail. Control of such chaotic motion has been studied by using periodic parametric excitation method. Melnikov's method has also been employed to derive meaningful results. Numerical results have been obtained to support the analytical calculation.

(Keywords : nonlinear / chaos / chaos control)

Introduction

In the past few years' extensive studies have been done on chaotic dynamics of typical nonlinear system. With the results of such studies, it has been observed that the chaotic motion emerging in the system have been suppressed or synchronized .A number of techniques are coming out which are applicable to control chaos. While the dynamics of Duffing equation and Vander Pol oscillator are almost exhaustively investigated[1], there have been few studies in the system called Froude pendulum. Froude pendulum is essentially a pendulum mounted on a rotating shaft. The shaft and the pendulum are coupled through friction, which is nonlinear. Such system can have self-excited oscillation[2], on account of the nature of damping. The objective of the present paper is to search a method to control chaos in Froude pendulum. We have attempted to apply periodic parametric excitation procedure here and obtained some significant results.

Chaos control in Froude Pendulum

The equation governing the dynamics of the pendulum can be written as[3]

$$\ddot{x} + A \sin x + q_1 \dot{x} (q_2 \dot{x}^2 - 1) = 0 \qquad (1)$$

The system represented by equation (1) is found to show limit cycle behavior, typical of the nonlinear damping term. In one study, Thomas and Ambica[4], used an external periodic forcing $f \cos \omega t$ and by writing equation (1) as

$$\ddot{x} + A \sin x = - q_1 \dot{x} (q_2 \dot{x}^2 - 1) + f \cos \omega t \qquad (2)$$

investigated occurrence of chaotic evolution. They have obtained some interesting results on this system. To study "smale horseshoes

dynamics" of the Froude pendulum, Melnikov's technique[5-9] was used. This technique is now considered as a powerful technique to study nonlinear system.

In our work we seek to inquire whether such chaos occurring during evolution of system (2) could be controlled by periodic parametric excitation. Thus we investigate whether;

$$\ddot{x} + \alpha(1 + \cos pt)\sin x = q_1 \dot{x}(q_2\dot{x}^2 - 1) + f\cos \omega t \quad (3)$$

can evolve regularly or not, when A (a constant) is replaced by $\alpha(1+\cos pt)$ (periodic function) in (2)

We consider the equation

$$\ddot{x} = -\alpha(1 + \cos pt)\sin x + q_1\dot{x}(q_2\dot{x}^2 - 1) + f\cos \omega t$$

The system can be equivalently written as

$$\dot{x} = v$$

$$\dot{v} = -\alpha(1 + \cos pt)\sin x + \{q_1\dot{x}(q_2\dot{x}^2 - 1) + f\cos \omega t\} \quad (4)$$

The undamped and undriven system corresponds to

$$\frac{dx}{dt} = v$$

$$\frac{dv}{dt} = -\alpha(1 + \cos pt)\sin x \quad (5)$$

From (5) we derive the Hamiltonian function given by

$$H(x,y) = \frac{v^2}{2} + \alpha(1 + \cos pt)(1 + \cos x)$$

For $H = 0$, we have

$$\frac{v^2}{2} = -\alpha(1 + \cos pt) \, 2\cos^2\frac{x}{2}$$

From which, after some calculation, we obtain

$$x = \pm 2 \tan^{-1} \sin h \{[(2k/p)\sin pt/2\}$$

$$v = \pm 2 \sec h \{(2k/p)\sin pt/2\} \, k. \cos pt/2$$

In this case Melnikov function is given by

$$M(t_0) = \int_{-\infty}^{\infty} v_0 \, (t-t_0)(-q_1v \,(q_2v^2 - 1) + f\cos \omega t)dt$$

Evaluating the above integral we get

$$M(t_0) = 0$$

Numerical Results and Discussion

We have studied the effect of periodic parametric excitation in forced Froude Pendulum.

We have considered the equation

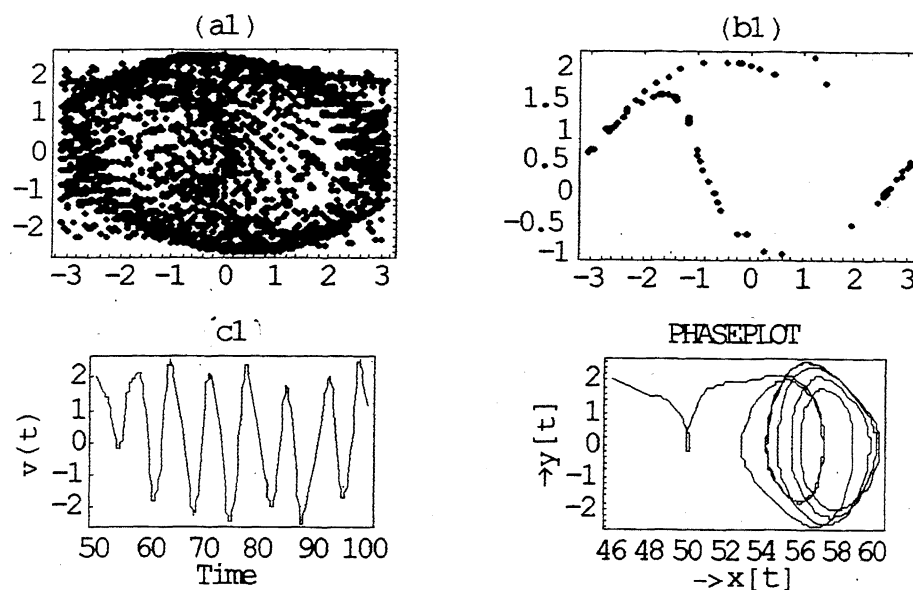$$\ddot{x} + \alpha(1 + \lambda\cos pt)\sin x = q_1\dot{x}(q_2\dot{x}^2 - 1) + f\cos \omega t$$

Fig. 1--Evolutionary behaviour of Froude pendulum when no periodic parametirc excitation is applied (i.e., lamda = 0)
Fig. (a1, (b1), (c1) and phase plot represent surface of section, poincare map, time series plot and phase plot respectively.
The parameter values are $\alpha = 1.0$, $q_1 = 0.3$, $q_2 = 0.5$, $\omega = 0.9$, $f=1.7$, $p = 1.8$, epsilon = 0.0007.

Fig. 2--Evolutionary behaviour of Froude pendulum when periodic parametirc excitation is applied (i.e., lamda = 0.8)
Fig. (a2, (b2), (c2) and phase plot represent surface of section, poincare map, time series plot and phase plot
respectively. The parameter values are $\alpha = 1.0$, $q_1 = 0.3$, $q_2 = 0.5$, $\omega = 0.9$, $f=1.7$, $p = 1.8$, epsilon = 0.0007.

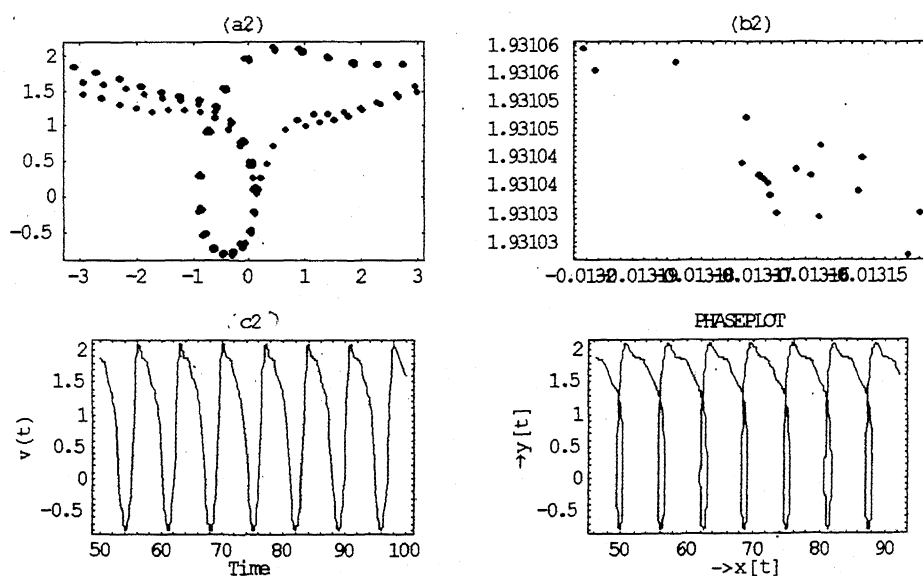for numerical calculation. When this effect is not into consideration (i.e., $\lambda = 0$) the system evolves chaotically which we can observe through surface of section, poincare map, time series and phase plots as shown in Fig. 1. Then we start increasing the value of λ. We observe that for λ upto 0.5, system evolves chaotically. But for $0.6 \leq \lambda \leq 1.0$, chaos in the system is substantially reduced. The best result is obtained at $\lambda = 0.8$. The result has been shown in Fig 2. Our analytical work also shows that Melnikov integral is zero when $\lambda = 1$. But when $\lambda = 1.1$ the system again evolves chaotically. This indicates that chaotic motion in the system can be controlled by suitably selecting the values of λ.

References

1. Guckenheimer.J & Homes.P.J. (1983) *Nonlinear oscillation, dynamical systems and bifurcation of vector fields*, Springer, Berlin

2. Davis.H.T. (1960) *Introduction to Nonlinear differential and integral equation,* Dover Publication Inc., New York

3. Moon.F.C. (1987) *Chaotic vibration.* John Wiley

4. Thomas.K.I & Ambika.G (1994) *Computational Aspect in Chaos and Nonlinear Dynamics,* (ed): Ambica, G & Nandkumaran, V.M, Wiley Eastern Ltd, New Delhi

5. Homes, P.J & Marsden, J.E (1982) *Commn.Math Phys.* **82** : 523

6. Jing, Z.J (1983) SIAM *J.Appl.Math* **43** : 1247

7. Wiggins, S. *Global bifurcation and chaos* Springer, Berlin.

8. Ambika, G & Babu Joseph (1988) *Pramana (J.Phys)*, **31** :1.

9. Rio, E.D, Lozano, A. & Velarde, M.G. (1994) *Chaos, Solitons and Fractals* **4** : 255.

Westward electric field in the low latitude ionosphere during the main phase of magnetic storms occurring around local midday hours

R.G. Rastogi

Physical Research Laboratory, Ahmedabad-380009, India,

Department of Physics, Gujarat University, Ahmedabad--380009, India.

Abstract

Magnetic storms occurring during local midday hours are shown to produce much larger decrease of the geomagnetic H field at equatorial electrojet station, Kodaikanal compared to the decrease of H at off-equatorial low latitude station Alibag situated in the same longitude sector. These storms are associated with the disappearance of equatorial Es configuration on the Kodaikanal ionograms indicating a reversal of ionospheric electric field in the ionosphere during the periods of minimum H field.

The analysis of H data from the chain of stations in India shows that the storm time decrease of H is almost constant with latitude for local night time storms. But for the day time storms the H field decreases progressively with decreasing latitude from Alibag-Annamalainagar- Trivandrum. This clearly indicates the effect of a westward electric field imposed over the low latitude ionosphere during the main phase of the magnetic storm.

The ionospheric current contribution identified by SqH and the ring current contribution identified by Dst-H index are subtracted from the observed hourly values of H on the five ID and five IQ days of each month of the years 1988-1990 for Trivandrum and Alibag. The modified disturbance solar daily variation SD (H) showed usual dawn maximum and dusk minimum at both the stations. But an additional very distinct minimum is observed in ΔH during the forenoon hours at Trivandrum. Difference between SD (H) at Trivandrum and Alibag showed largest forenoon decrease during equinoctial and least effect during June sotstices or during local summer months.

It is concluded, that during the main phase of the storm when the ring current is in the developing phase, an electric field opposite in direction to the atmospheric dynamo electric field is imposed on the equatorial ionosphere.

Introduction

Egedal[1] has shown an abnormally large enhancement of the daily variation of the geomagnetic horizontal field, H, over the magnetic equator, Chapman[2] suggested this phenomenon to be the effect of a band of eastward flowing current in the ionosphere within $\pm$ 3° dip latitudes during the day time hours and named it as Equatorial Electrojet Current (EEJ). Baker and Martyn[3] explained this EEJ as due to enhanced electrical conductivities in the atmospheric E region within $\pm$ 3° over the magnetic equator. In India equatorial

electrojet geomagnetic observatories have been operating at Trivandrum (dip 0.6°S) since 1957, at Ettayiapuram (dip 2.2°N) since 1920, at Kodaikanal (dip 5.0 °N) since 1950 at Annamalainagar (dip 7.8 °N) since 1957, besides other low latitude observatories at Hyderabad (dip 21.8 °N) Alibag (dip 25.4°N), Ujjain (dip 33.9°N), Jaipur (dip 45.4 °N) Sabhawala (dip 49.6 °N) and at Gulmarg (dip 51.6 °N). This chain is supplemented by observatories in former USSR namely at Tashkent, Ashkhabad, Alma Ata, Karaganda, Navosobirsk and others providing a chain of stations from equator to pole within a limited longitude sector, unique anywhere in the world. Rastogi[4] has described the various magnetic and ionospheric effects over a wide latitude and altitude regions due to the interaction of electric and magnetic fields within this relatively narrow region of the electrojet.

Chapman[5] had concluded that the magnetic disturbances do not produce any abnormal effects on the disturbed daily variation of the equatorial electrojet as the quiet day solar daily variations, Sq. It was soon observed that the size of the storm sudden commencements, SSC, are considerably enhanced at Huancayo compound with those at Cheltanham[6,7]. Rastogi et al.[8] showed that the latitude variation of SSC in H was closely related to the latitude variation of the electrojet in any longitude sector. Rastogi showed that the SSC at Huancayo were associated with simultaneous increase of the electric field in the E region of the ionosphere. Rastogi[9] showed that the Disturbance Daily variation of the equatorial electrojet current at Trivandrum has a very clear anti-Sq shape with a minimum around noon, contrary to the earlier results of SD variation at

Huancayo by Chapman[5]. Later, the study of storm time variations of H at the geomagnetic observatories in Indo-Russian chain showed progressive enhancement at the magnetic equator over and above the normally expected decrease of Dst (H) due to the ring current effects corrected for geomagnetic latitudes. The present paper discusses the storm time variations of H at Indian chain of stations due to the magnetic storms with the main phase occurring during the local midnight and midday hours.
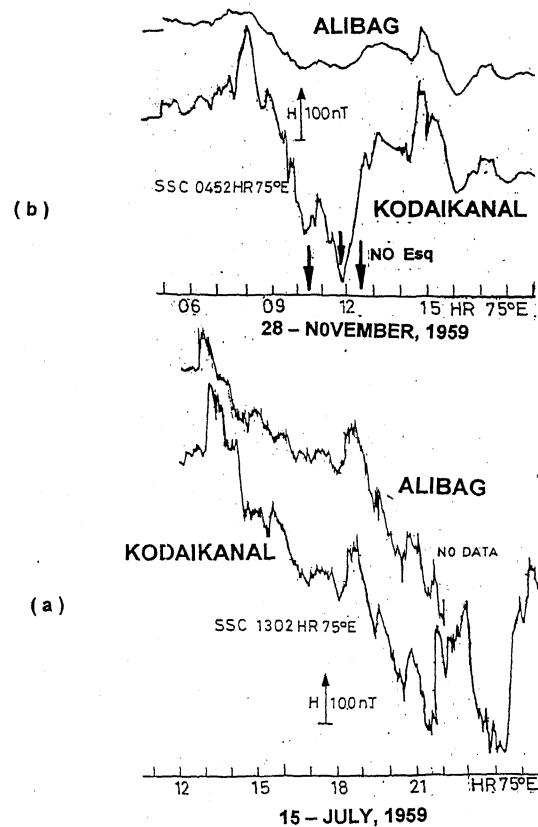

Fig. 1– Storm time magneto grams at Kodaikanal and Alibag for the storms on 06-15 July 1959 and 28 November 1959.

70

Fig. 1(a) reproduces the tracings of H magnetogram at Kodaikanal (dip 5.0° N) and at Alibag (dip 25.4°N) during the SC type of storm starting at 1302 hr 75°E MT on 15 July 1959 with its main phase minimum H occurring during the local midnight hours. The storm has a range of 785 nT at Kodaikanal but the trace during minimum H at Alibag had gone out of the paper and so the data was lost. It is seen the amplitude of SSC occurring during midday hours was 118 nT at KOD and 79 nT at Alibag indicating electrojet enhancement of day time SSC-H. It is to be noted that the short time fluctuations of H are enhanced at KOD during the daytime but the night time fluctuations in H are of the same magnitude at the two stations. The slower component of the H variations at the two stations were also of the same order.

Fig. 1(b) shows the H magnetogram traces at Kodaikanal and Alibag following a SSC at 0452 hr 75°EMT on 28 November 1959. The amplitude of SSC was 28 nT at KOD and 31 nT at Alibag and were of the same order as the SSC had occurred during the night time when the electrojet was absent. The main phase of the storm started at 0900 hr and the minimum of the H field was observed at 1700 hr LT. The fluctuations of H field was much larger at Kodaikanal than at Alibag and even the general decrease of the H field was much larger at Kodaikanal. The storm range of H field was 402 nT at Kodaikanal and only 204 nT at Alibag. The normal midday maximums of ΔH during the noon hours observed at Kodaikanal and Alibag on magnetically quiet days was replaced by a deep minimum at noon hours on 28 November 1959. A counter electrojet event had occurred and the normally observed q-type of sporadic E had disappeared during the maximum phase of the storm indicating

a reversal of the ionospheric electric field due to the storm. This indicates that the magnetic storms cause the imposition of a westward electric field on ionosphere during the main phase causing an additional decrease of the equatorial magnetic field in addition to the decrease due to the westward equatorial ring current in the may magnetosphere.
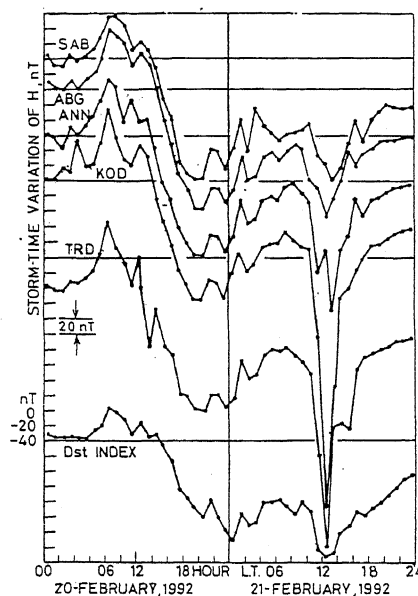

Fig. 2(a)– Storm time variations of the geomagnetic horizontal H field at Indian stations following a SSC storm at 0109UT on 20 February 1992.
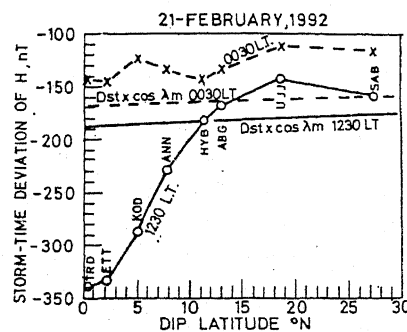

Fig. 2(b)   Latitudinal variation of the storm time $\Delta H = Hd - SqH$ - Dst H at 0030 LT and 1230 LT on 21 February 1992.

Table 1– 21 February 1992 H storm time

Station	Dip Angle	0030 LT	Dst 168 Cos im	1330 LT	Dip Lat.	Dst 187 Cosλm	X_m	Cos X_m ,
TRD	0.6	-143	168	-339	0.3	187	-0.8	
ETT	2.2	-145	168	-333	1.1	187	0.6	
KOD	5.0	-122	168	-267	2.5	187	0.9	
ANN	7° 8'	-133	168	-229	3.6	187	1.9	.999
MUB	21°49'	-149	166	-181	11.3	185	2.0	.990
ABG	25°23'	-133	166	-168	13.4	184	9.7	.986
UJJ	33.9	-111	163	-142	18.6	181	14.0	.920
SAB	45.9	-116	157	-160	27.3	175	20.9	.934
GUL								

Fig. 2(a) shows the storm time variations of the H field at Indian geomagnetic observatories following the SSC at 0609 LT on 20 February 1992. The Dst index indicated significantly positive values during midday hours on 20 February and the main phase decrease started at 1500 hr on 20 Feb. followed by a minimum of Dst around the midnight of 20-21 Feb. Dst index tried to recover but was followed by another energization of the ring current at 09 hr on 21 Feb. followed by another minimum of Dst at 1200 hr (noon) on 21 Feb. The storm time variation of H at Sabhawala (SAB) a station close the Sq focus latitude faithfully followed the variations of Dst index with minimum of H around the midnight and later during the noon of 20-21 Feb. 1992. At Annamalainagar (ANN), station close to the edge of the electrojet belt, the midday decrease on 21 Feb. was significantly larger than the decrease during midnight of 20-21 Feb. 1992. At Kodaikanal the storm time

decrease during the night time was -170 nT but during the following noon the storm time decrease was -390 nT, even though Dst index at these two times were not too different. At Trivandrum too the midday decrease of the H field was much larger than the night time.

In Fig. 2(b) are shown the latitudinal variation of storm time H field at 0000 hr and 1200 hr on 21 Feb. 1992 compared with the latitudinal variation of the corrected Dst index. It is seen that the midnight storm time ΔH showed a small decreasing trend with decreasing latitude. The midday storm time ΔH showed a small decrease from Ujjain (UJJ) to Alibag (ABG) and Hyderabad (HYB) all outside the electrojet belt. There was a strong decreasing trend of storm time ΔH thereafter from Hyderabad – Annamalai-nagar-Kodaikanal - Ettayiapuram to Trivandrum, close to the equator. The observed decrease at TRD was -340 nT

compared to the Dst index of only -170 nT. This clearly indicates that a strong westward electric field was imposed on the eqauatorial electrojet region during the main phase of the storm.
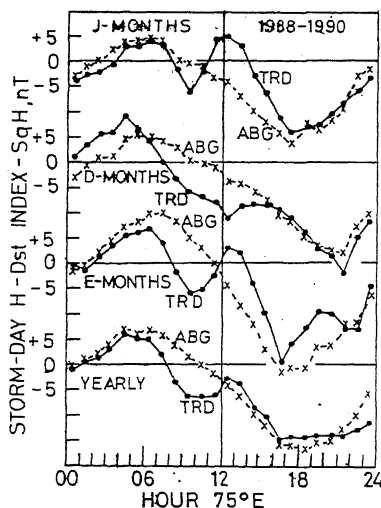

Fig. 3(a)   Modified Disturbance Daily variations of the horizontal magnetic field H, (SDH)* at equatorial electrojet station, Kodaikanal and at off equator low latitude station, Alibag average for there seasons of the years 1988 to 1990.
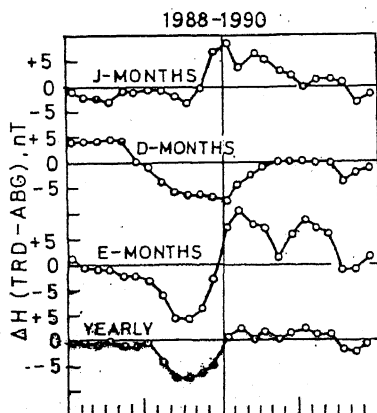

Fig. 3(b)   The difference between (SDH) * variations at Kodaikanal minus the same at Alibag for different seasons of the years 1988-1990.

Next, from the monthly data tables of the observed hourly mean H field at Trivandrum and Alibag, another table was generated giving the hourly values of the observed H field minus the mean H field on five international quiet days (i.e. SqH) minus the corresponding hourly mean value of Dst index. This modified $(\Delta H)^*$ indicates the remenant H field at three stations devoid of the effects due to normal quiet day electrojet current and due to the disturbed day ring current. Next, mean daily variation of this modified $(\Delta H)^*$ on five 1 Q and five 1 D days were computed. Next, mean of the variation on ID minus the same on IQ days were computed giving the modified Disturbance Daily variation (SOD)* of the H field at these stations. Fig. 3(a) shows the modified (SDH)* averaged for the three seasons and for the whole year for the period January 1988 to December 1990. It is to be noted that the yearly average (SDH)* at ABG and TRD show comparable values during the hours midday to next sunrise, with the usual dawn maximum and dusk minimum. During the forenoon period from 0600-1200 LT (SDH)* at ABG shows slow decrease from dawn maximum to dusk minimum. But (SDH)* at TRD shows a very distinct minimum during this period of the day. Examining the seasonal effect on this, it is seen that the forenoon decrease of (SDH)* at TRD is most pronounced during equinoctial months, less during D months (local winter) and least during J months.

In Fig. 3(b) are shown the difference of (SOH)* variations at TRD minus the same at ABG, thus removing the common cause of disturbance daily variation at the time stations namely the dawn-duck magnetospheric electric field effect. A very clear forenoon decrease of the difference curve is seen during the equinoctial and December months.

It is suggested that this additional effect is due to the immediate transfer of the polar electric field during the phase of the magnetic storms when the equatorial ring current is being emergized.

Acknowledgements

References

1. Egedal, J. (1947) *Terr. Magn. Atmos. Electr.* **52** : 449.

2. Chapman, S. (1951) *Arch. Meterol. Geophys. Bioklimatol.*, **A4** : 368.

3. Baker, W.G. & Martyn, D.F. (1952) *Nature London*, **170** : 1090.

4. Rastogi, R.G. (1989) *The equatorial electrojet : magnetic and ionospheric effects in geomagnetism* Vol. 3 p. 462

5. Chapman, S.(1951) *Geofisica Pura. et. Applicata* **14** : 151, Ed. Jacobs, J., Academic Press Ltd.

6. Ferraro, V. C. A. & Unthank, H. W. (1951) *Geofisica Pura. Appl.*, **20** : 3.

7. Suguira, M. (1953) *J. Geophys. Res.* **58** : 585.

8. Rastogi, R.G., Trivedi N.B. & Kaushika N.D. (1964) *J. Atmos. Terr. Phys.* **26** : 771.

9. Rastogi, R.G. (1998) *Current Science* **74** : 457.

10. Rastogi, R.G. (1999) *Annales Geophysical* **17** : Ed. Jacobs, J., Academic Press Ltd. 438.

(I) **AWARDS**

1. **Prof. R.S. Sirohi,** *Ph.D., F.N.A.E.,F.N.A.Sc.,* Director, Indian Institute of Technology, Delhi has been selected for the Hari Om Ashram Trust Award entitled "Sir C.V. Raman Award: Physical Sciences", for the year 2002 by the University Grants Commission. This award includes a sum of Rs.50,000/= and a citation.

2. **Dr. V.P. Sharma,** *D.Phil,D.Sc.,F.N.A.,F.A.Sc.,F.N.A.Sc.,F.A.M.S.,F.R.A.S,* formerly Additional Director-General, ICMR & Director, Malaria Research Centre, Delhi has been conferred 24th G.P. Chatterjee Memorial Award (2003-2004) by Indian Science Congress Association, Kolkata.

3. **Dr. Jayant Vishnu Narlikar,** *Ph.D.(Cantab.),Sc.D.(Cantab.),F.N.A.,F.A.Sc.,F.N.A.Sc., F.T.W.A.S.,* Director, Inter-University Centre for Astronomy and Astrophysics, Pune, has been conferred Padma Vibhushan by the President of India.

(II) **PROGRAMME OF SCIENCE COMMUNICATION ACTIVITIES OF THE ACADEMY**

Popular Lecture	January 27, 2004 by Prof. Govindji at Allahabad.
Science Extension Lectures	February 10-20, 2004, at Allahabad
Outstation Science Extension Lectures	February 10-15, 2004 at Satna & adjoining areas of M.P. February 15-20, 2004 at Jaunpur, U.P.
Local (Allahabad) Level Science Communication Activities	Science Fiction and creative contest on 17th February, 2004
State Level Science Contests (to be held at Allahabad)	Science Quiz February 24, 2004 Science Debate February 25, 2004 Science Oration February 26, 2004 Science Exhibition February 27, 2004
State Level Essay Contest	For Degree Colleges of U.P. on February 27, 2004
State Level Teachers Workshop	From February 25-27, 2004 at Allahabad.
National Science Day	February 28, 2004 being jointly organized with Harish-Chandra Research Institute, Allahabad.

1.   G.D. BIRLA AWARD FOR SCIENTIFIC RESEARCH

Last date for sending Nomination   31st March 2004

For details please contact

   K.K. BIRLA FOUNDATION
   Hindustan Times House,
   10th Floor, 18-20, Kasturba Gandhi Marg,
   New Delhi – 110 001
   Phone : (011) 23718282, 23317735

2.   THE DISABLED CHILDREN ASSOCIATION AWARD FOR SCIENTIFIC RESEARCH (2004)

Last date for sending Nomination   30th November, 2004

For details please contact –

   The Award Secretariat
   Disabled Children Association,
   P.O. Box – 8557,
   Zip Code : Riyadh 11492
   Saudi Arabia.

JOURNAL FORMAT AND GUIDELINES FOR THE AUTHORS/CONTRIBUTORS

[A]   WHAT TO SUBMIT

All papers would pass through a strict "Peer review" to ensure high quality.

The National Academy Science Letters publishes articles under the following categories :

(i)   ***Lead Articles/Overviews of new developments in Science and Technology*** from "recognized experts" to educate, initiate and provocate young scientists for undertaking research in innovative, challenging and cross – disciplinary new research areas. ALL EXPERTS ARE WELCOME TO CONTRIBUTE. These articles are not meant to be Bibliographic or complete literature reviews but are expected to give selected references and future/past trends. Articles may be of 3000 to 5000 words. Special "Academy Award Lectures" and "Presidential Addresses" etc. may occasionally be published under this category.

(ii)   ***News/Views/Comments*** with an aim to bring out recent national/international scientific developments and controversial viewpoints. The number of words in such article should be less than 3000. Short Comments and author's rebuttal on articles published in this category are also welcome (max 500 words).

(iii)   ***Science & Technology Development and Policy Issues*** with an aim to serve as Science-Society interface. Articles should be less than 2000 words.

(iv)   ***Short Research Communications*** with an aim to publish *high quality* and break through *investigations*, which need immediate and rapid attention. Routine research work or data shall not be acceptable which may be submitted to the regular *Proceedings of the National Academy of Sciences, India* for consideration. The maximum number of words for these articles is 2000.

(v)   ***Academy News/Announcements***

(vi)   ***Forthcoming Meetings/Seminars/Conferences*** will serve as an avenue for informing a wide audience of professional scientists about the Meetings/Seminars etc. being organized by different organizations. This would include title and scope of the conference/organizer's address/important dates or deadlines. The maximum number of words is 100.   All scientists/recognized professional organizations can submit such notifications.

(vii)   ***Miscellaneous Special Issues.***

[B]   HOW TO SUBMIT

(a)   Manuscripts may be submitted to either of the following :-

(i)   **Prof. Girjesh Govil** (Member, Board of Editors), Formerly Senior Professor, Tata Institute of Fundamental Research, Colaba, Mumbai – 400 005, **E-mail :** <u>govil@tifr.res.in</u>; Fax No. (022) 22804610.

(ii)   **Prof. Jai Pal Mittal** (Member, Board of Editors), Director, Chemistry and Isotope Group, Bhabha Atomic Research Centre, Trombay, Mumbai – 400 085, E-mail : <u>mittaljp@magnum.barc.ernet.in</u>; Fax No. (022) 25505151, 25519613

(iii)   **Prof. Suresh Chandra** (Member, Board of Editors) Emeritus Scientist, Department of Physics, Banaras Hindu University, Varanasi – 221 005, E-mail : <u>schandra@banaras.ernet.in</u>.; Fax No. (0542) 2317040.

(iv)   **Dr. M.S. Sinha**, Executive Secretary, The National Academy of Sciences, India, 5, Lajpatrai Road, Allahabad – 211 002, E-mail : <u>nasi@sancharnet.in</u>; Fax No. (0532) 2641183.

(v)   **Dr. Niraj Kumar**, Assistant Executive Secretary, The National Academy of Sciences, India, 5, Lajpatrai Road, Allahabad – 211002, E-mail : <u>nasi@sancharnet.in</u>; Fax No. (0532) 2641183.

(b)   Manuscripts should be typewritten in English, double-spaced and should be submitted in triplicate. All mathematical expressions should be typed or written clearly in black ink. <u>For speedy publication, an electronic version in a "Floopy (3.5", IBM PC format only, not Macintosh)" is desirable</u>. The text of the manuscript as per format of the Journal, and preferably with scanned figures, should be supplied as a plain ASC II file (WordStar 5.5 or 7.0 and Microsoft Word for Windows 6.0 are acceptable, but ASC II is preferred).

(c)   The communication should contain a minimum number of tables, figures and photographs. Figures must be drawn in such a way that they can be reduced to one column width (7.5 c.m.). Figures must be original drawings or exceptionally sharp glossy prints of about manuscript size. The space occupied by the figures/tables/photographs will be at the expense of text "word-length" as specified above in [A]. Each Figure will be counted as 200 words, each short table as 150 words and full-page table as 300 words.

(d)   All references should be indicated in the text by superscript Arabic numerals, e.g. 'Mirri[2] while working on ....' The list of references should be arranged in order of their occurrence in the text. Reference should be given in the following style :

2. Mirri, M.A. (1982) <u>J. Chem. Phys</u>, <u>58</u> : 282 (for articles in Journals).
    Author   Year   Journal Vol. I   beginning page
White, M.J.D. (1973) <u>Animal Cytology and Evolution,</u> 3rd Ed., Cambridge University Press, London, p. 320 (for Books)
Osgood, C.F. (1977) in <u>Number Theory and Algebra</u>, ed., Zassenhaus, H., Academic Press, New York, p. 321 (for edited Books).
Abbreviations of the names of periodicals should conform to those given in the World list of Scientific Periodicals.

(e)   Keywords : A maximum of 5 keywords should be supplied. Each of these words will be separated by a slash (/) and printed just below the title of the research paper, e.g. (steroid receptors/protein-DNA interaction/gene regulation).

(f)   Acknowledgements, if any, should appear at the end of the letter but just before the references.

(g)   Proofs will not ordinarily be sent to authors, unless desired.

REPRINTS : 25 free reprints will be given for each paper.

SUBSCRIPTION RATE :

(1)   Annual Subscription for non-members
    Inland (by Book-Post)   Rs. 300.00
    Foreign   U.S. $ 125.00
(2)   Single issue for non-members
    Inland (by Book-Post)   Rs. 40.00
    Foreign   U.S. $ 20.00
(3)   Annual Subscription for members
    (by Book-Post)   Rs. 50.00
    Foreign   U.S. $ 50.00

Note : Registration and Air Mail Charges Extra